SIMULATION-BASED PEDESTRIAN LEVEL-OF-SERVICE FRAMEWORK INCORPORATING PEDESTRIAN INTERACTION

TRICIA MAE MARTINEZ

A DISSERTATION SUBMITTED TO

THE FACULTY OF GRADUATE STUDIES

IN PARTIAL FULFILLMENT OF THE REQUIREMENTS

FOR THE DEGREE OF

MASTER OF APPLIED SCIENCE

GRADUATE PROGRAM IN CIVIL ENGINEERING

YORK UNIVERSITY

TORONTO, ONTARIO

July 2026

© Tricia Mae Martinez, 2026

Abstract

Pedestrian Level-of-Service (PLOS) is commonly used to evaluate sidewalk walking conditions. Traditional frameworks, including the Highway Capacity Manual, primarily use pedestrian space as the main indicator. However, pedestrian space alone does not fully capture how pedestrians interact while walking, especially when pedestrian pair interactions cause changes in speed or direction. This study proposes a PLOS framework that combines pedestrian space and pedestrian interaction to provide a more comprehensive evaluation of sidewalk performance.

Pedestrian interaction is introduced as an indicator that measures the influence pedestrians have on one another based on proximity and walking direction. The framework was applied to York Lanes at York University's Keele campus using PTV Viswalk microsimulation and visualization outputs. Six scenarios were analyzed, including a Base Scenario and five Alternative Scenarios involving advertisements, seating, stairs, construction zones, and hazard tape. Results show that pedestrian interaction identifies changes in walking conditions not captured by traditional single-indicator PLOS models.

Acknowledgements

Thank you, God, for guiding me through this journey.

Thank you to my supervisor, Dr. Peter Park, for seeing potential in me and believing in me. You sparked my passion for transportation engineering and helped shape the path I am on today. I am forever grateful for your guidance, support and encouragement, and the many opportunities you have given me.

Thank you to my mentors, Dr. Ahmad Mohammadi and Dr. Tanvir Chowdhury, for your patience and for taking the time to help me through this process. Your guidance and willingness to answer my questions made this journey so meaningful, and I am grateful to have learned so much from both of you.

To my amazing family and Fadil, this is for you. Thank you for your unwavering love and for being there through every step of my journey. You all have been my motivation and my biggest supporters. This accomplishment means so much more because I get to share it with you.

Table of Contents

Abstract ii

Acknowledgements iii

Table of Contents iv

List of Figures viii

List of Tables x

List of Acronyms and Abbreviations xi

Chapter 1. Introduction 1

1.1 Study Motivation 1

1.1.1 Pedestrian Facilities 1

1.1.2 Pedestrian Level-of-Service 2

1.1.3 Problem and Opportunities Statement 5

1.2 Study Goal and Objectives 8

1.3 Study Scope 9

1.4 Study Structure 10

Chapter 2. Literature Review 11

2.1 Existing PLOS Indicators 11

2.2 Pedestrian Data Collection and Simulation Approaches 22

2.2.1 Real-World Data Collection 22

2.2.2 Simulation Tools 23

2.3 Existing PLOS Models 27

2.3.1 HCM PLOS 28

2.3.2 City of London PLOS 28
2.3.3 Limitations of Existing PLOS Models 30
2.4 Scenario-Based Application of PLOS Models 31
2.5 Chapter Summary 33
Chapter 3. Methodology 35
3.1 Process to Develop Input Indicator 36
3.1.1 Develop and Identify Input Indicators 36
3.1.2 Combine Pedestrian Interaction Sub-Indicators 37
3.1.3 Calculate Aggregated Pedestrian Interaction 45
3.1.4 Develop Heat Map 47
3.2 Process to Design 2D Microsimulation Model and 3D Visualization 48
3.2.1 Case Study Area 48
3.2.2 Develop a 2D Microsimulation Model and 3D Visualization 49
3.3 Process to Develop PLOS Model 51
3.3.1 Develop Three Categories for Each PLOS 51
3.3.2 Identify PLOS Model Thresholds and Boundary Values 54
3.3.3 New PLOS Model 54
3.4 Process to Apply New PLOS Model 55
3.5 Chapter Summary 56
Chapter 4. Develop PLOS Model 58
4.1 Develop Three Categories for Each PLOS 58

4.2 Identify PLOS Model Thresholds and Boundary Values 74
4.3 New PLOS Model 85
4.4 Chapter Summary 87
Chapter 5. Apply the PLOS Model Through Case Studies 89
5.1 Select Base and Alternative Scenarios 89
5.1.1 Base Scenario 90
5.1.2 Alternative Scenario 1: Addition of Advertisements 91
5.1.3 Alternative Scenario 2: Removal of Seats 93
5.1.4 Alternative Scenario 3: Removal of stairs 94
5.1.5 Alternative Scenario 4: Addition of Construction Zone 95
5.1.6 Alternative Scenario 5: Addition of Hazard Tape 96
5.2 Determine the Required Parameters for Scenarios 97
5.2.1 Selecting PLOS C 97
5.2.2 Pedestrian Volume and Speed as Input Parameters 97
5.2.3 Collecting the outputs from PTV Viswalk to input into Unity 98
5.3 Chapter Summary 98
Chapter 6. Results of PLOS Analysis 100
6.1 Results of PLOS Analysis for Case Studies 100
6.1.1 Base Scenario 100
6.1.2 Alternative Scenario 1: Addition of Advertisements 105
6.1.3 Alternative Scenario 2: Removal of Seats 108

6.1.4 Alternative Scenario 3: Removal of stairs 111

6.1.5 Alternative Scenario 4: Addition of Construction Zone 114

6.1.6 Alternative Scenario 5: Addition of Hazard Tape 118

6.2 Heat Map Results 121

6.2.1 Base Scenario versus Alternative Scenario 1 122

6.2.2 Base Scenario versus Alternative Scenario 2 124

6.2.3 Base Scenario versus Alternative Scenario 3 126

6.2.4 Base Scenario versus Alternative Scenario 4 128

6.2.5 Base Scenario versus Alternative Scenario 5 131

6.3 Discussion of Results 133

6.4 Chapter Summary 136

Chapter 7. Summary, Conclusion and Recommendations 138

7.1 Summary 138

7.1.1 Development of Input Indicators to Capture Pedestrian Space and Pedestrian Interaction 139

7.1.2 Proposal of a New PLOS model Incorporating Pedestrian Space and Pedestrian interaction 140

7.1.3 Implementation of New PLOS Model and 3D Visualization of Results 141

7.2 Future Work and Recommendations 142

Chapter 8. References 150

List of Figures

Figure 1.1. Pedestrian Space versus Pedestrian interaction 7

Figure 2.1. Data Collection Approaches 26

Figure 3.1. Study Methodology 35

Figure 3.2. Passing versus Meeting Event for Pedestrian interaction 44

Figure 3.3. Identifying Aggregated Pedestrian interaction 46

Figure 3.4. Study Area 49

Figure 4.1. Data Sampling Process for Model Calibration 60

Figure 4.2. Raw Dataset Calibration Results for the 1st Second (901 seconds) for PLOS C 62

Figure 4.3. Model Development Calibration Results for 901-925 seconds for LOS C 64

Figure 4.4. Normalized histograms with smoothed probability density functions of Pedestrian interaction for PLOS A under (a) uni-directional and (b) bi-directional walking 69

Figure 4.5. Normalized histograms with smoothed probability density functions of Pedestrian interaction for PLOS B under (a) uni-directional and (b) bi-directional walking 70

Figure 4.6. Normalized histograms with smoothed probability density functions of Pedestrian interaction for PLOS C under (a) uni-directional and (b) bi-directional walking 71

Figure 4.7. Normalized histograms with smoothed probability density functions of Pedestrian interaction for PLOS D under (a) uni-directional and (b) bi-directional walking 72

Figure 4.8. Normalized histograms with smoothed probability density functions of Pedestrian interaction for PLOS E under (a) uni-directional and (b) bi-directional walking 73

Figure 4.9. Identification of PLOS Model Thresholds and Boundary Values for PLOS A 77

Figure 4.10. Identification of PLOS Model Thresholds and Boundary Values for PLOS B 79

Figure 4.11. Identification of PLOS Model Thresholds and Boundary Values for PLOS C 81

Figure 4.12. Identification of PLOS Model Thresholds and Boundary Values for LOS D 83

Figure 4.13. Identification of PLOS Model Thresholds and Boundary Values for LOS E 85

Figure 4.14. New PLOS Model 87

Figure 5.1. Base Scenario in 2D Microsimulation versus 3D Visualization 91

Figure 5.2. Addition of Advertisement Scenario 2D Microsimulation versus 3D Visualization . 92

Figure 5.3. Removal of Seats Scenario in 2D Microsimulation versus 3D Visualization 93

Figure 5.4. Removal of Stairs Scenario in 2D Microsimulation versus 3D Visualization 94

Figure 5.5. Addition of A Construction Zone Scenario 2D Microsimulation versus 3D Visualization 95

Figure 5.6. Addition of Hazard Tape Scenario in 2D Microsimulation versus 3D Visualization 96

Figure 6.1. Results for Base Scenario 104

Figure 6.2. Results for Addition of Advertisements (Alternative Scenario 1) 108

Figure 6.3. Results for Removal of Seats (Alternative Scenario 2) 111

Figure 6.4. Results for Removal of Stairs (Alternative Scenario 3) 114

Figure 6.5. Results for Addition of Construction Zone (Alternative Scenario 4) 117

Figure 6.6. Results for Addition of Hazard Tape (Alternative Scenario 5) 120

Figure 6.7. Heat Map for Base Scenario versus Alternative Scenario 1 124

Figure 6.8. Heat Map for Base Scenario versus Alternative Scenario 2 126

Figure 6.9. Heat Map for Base Scenario versus Alternative Scenario 3 128

Figure 6.10. Heat Map for Base Scenario versus Alternative Scenario 4 130

Figure 6.11. Heat Map for Base Scenario versus Alternative Scenario 5 133

List of Tables

Table 2.1 Indicators used for Pedestrian Level of Service Models 12

Table 2.2. HCM PLOS Threshold for Sidewalk (HCM, 2010) 28

Table 2.3. City of London PLOS Threshold for Sidewalk (City of London, 2010) 29

Table 4.1. Additional Correlation Analysis Between Pedestrian Space and Pedestrian Interaction by PLOS Level and Walking direction 67

List of Acronyms and Abbreviations

CDF	Cumulative Distribution Function
COVID-19	Corona Virus Disease 2019
FHA	Federal Highway Administration
Ft	Feet
GPS	Global Positioning System
HCM	Highway Capacity Manual
IEEE	Institute of Electrical and Electronics Engineer
KDE	Kernel Density Equation
LiDAR	Light Detection And Ranging
M	Metres
MATLAB	MATrix LABoratory
Min	Minute
NACTO	National Association of City Transportation Officials
OTC	Ontario Traffic Council
Ped	Pedestrians
PLOS	Pedestrian Level-of-Service
PPMM	Pedestrian per Metre of Clear Footway Width per Minute
Q	Quartile
S	Second
SFM	Social Force Model
2D	Two Dimensional
3D	Three Dimensional

Chapter 1. Introduction

Chapter 1 introduces the background and motivation for this study. It begins by discussing the importance of pedestrian facilities and Pedestrian Level of Service (PLOS) in evaluating sidewalk performance. The chapter then identifies the limitations of traditional PLOS frameworks, particularly their reliance on pedestrian space as a single indicator and their limited ability to capture pedestrian interactions, such as movement and constraints with respect to others. Based on this gap, the problem and opportunities statement, research objectives, and study scope are presented. Finally, the chapter outlines the organization of the study and explains how each chapter contributes to the development, application, and evaluation of the proposed PLOS framework.

1.1 Study Motivation

1.1.1 Pedestrian Facilities

Pedestrian facilities are infrastructures that provide designated spaces for comfortable walking, ensuring separation from other modes of transportation to minimize conflict. Pedestrian facilities are essential for urban infrastructure, allowing individuals to move safely and comfortably within cities and towns, often alongside vehicles, public transport, and cyclists. Properly designed pedestrian facilities facilitate movement and contribute to the overall walkability and accessibility of urban environments (Ferrer et al., 2015; Sharifi et al., 2020). Pedestrian facilities also play a critical role in promoting active travel, reducing reliance on motorized vehicles, and fostering healthier communities. Ensuring the usability and accessibility of these facilities remains paramount in supporting sustainable urban development (Ribeiro and Hoffimann, 2018; Huang et al., 2019; Fonseca et al., 2022)

Sidewalks are the most widely used pedestrian facility and serve as key connections within many urban environments. They provide dedicated space along high-activity areas such as university campuses and commercial districts that facilitate effective and continuous pedestrian movement. Sidewalk characteristics, such as width, alignment, and adjacent features, directly influence the walking experience of pedestrians. This makes their evaluation particularly important in places that experience consistently high pedestrian demand, including university campuses, which is the focus of the case study for this study (Jaskiewicz, 2000; Ehrenfeucht and Loukaitou-Sideris, 2010; Holmes et al., 2018; Fonseca et al., 2022).

1.1.2 Pedestrian Level-of-Service

Pedestrian Level-of-Service (PLOS) is a commonly used measure for evaluating the design and operational performance of pedestrian facilities (Wang et al., 2015; Gorrini et al., 2023). It serves as a decision-making tool for engineers and planners to assess whether existing or proposed facilities meet acceptable performance standards and to identify necessary improvements. The application of PLOS in sidewalk design has been shown to improve functionality and user experience. For example, poorly designed and deteriorating pedestrian facilities result in a high probability that pedestrians experience a lower PLOS (Zannat et al., 2019; Vallejo-Borda et al., 2020; Rodriguez-Valencia et al., 2022). PLOS helps prioritize improvements by quantifying the impact of design changes on pedestrian conditions. This information is especially valuable for cities with limited financial budgets as it provides them a better understanding of how to optimize their resource allocation. Engineers and planners follow an established PLOS framework that guides their decision-making to effectively implement these improvements (HCM, 2000; Petritsch et al., 2006; HCM, 2016; Nag et al., 2020; Ontario Traffic Council, 2022; TRB, 2020).

This study adapts the conventional PLOS evaluation approach into a systematic four-step framework. Conventional PLOS framework typically evaluate pedestrian facilities using measurable input indicators and predefined thresholds (HCM, 2000; HCM, 2016; TRB, 2020). PLOS frameworks are widely used by transportation engineers and planners to assess the design quality and operational performance of pedestrian environments. Their primary objective is to evaluate how effectively sidewalks can accommodate pedestrian needs (Petritsch et al., 2006; Nag et al., 2020; Rodriguez-Valencia et al., 2022). In the first step (Develop Input Indicators), engineers introduce quantitative input indicators (e.g., pedestrian space, which measures the specific space available to a pedestrian within a defined time frame) to capture pedestrian experiences. In the second step (Design 2D Microsimulation Model and 3D Visualization), they collect pedestrian data (e.g., pedestrian volume) manually or by using an automated monitoring camera system. The collected data is used to calculate the input indicator and create the 2D microsimulation model and 3D visualization. In the third step (Develop PLOS Model), the calculated input indicator is compared with predefined thresholds to create a new PLOS model. In the last step (Apply New PLOS model in a Case Study Area), we identify a Base Scenario and Alternative Scenarios to implement the new PLOS model by evaluating the PLOS of a specific pedestrian facility. Based on the results, if a pedestrian facility has a low PLOS, city planners and engineers address the issue by implementing design improvements, such as increasing sidewalk width, to enhance the facility's effectiveness and improve the experience of pedestrians. This framework provides a foundation for assessing pedestrian facilities, as it often uses basic and simple indicators such as pedestrian space and volume to measure PLOS.

While this framework provides a structured approach, traditional PLOS models rely heavily on measurable single indicators such as pedestrian space, density, volume, and flow rate**.** These

indicators are useful because they describe pedestrian demand and available walking space in a clear and quantitative way (Pushkarev and Zupan, 1975; HCM, 2000; HCM, 2016). Pedestrian space is one of the most commonly used indicators and is the inverse of pedestrian density, expressed in square metres per person (m²/ped) (Pushkarev and Zupan, 1975; HCM, 2000; Petritsch et al., 2006; HCM, 2016; Nag et al., 2020). Although pedestrian space is effective in representing overall crowding conditions, it does not capture the interactions between pedestrians (City of London, 2010; Kim et al., 2014; Nag et al., 2020). In real sidewalk environments, pedestrians may adjust their speed, shift their walking path, or change their trajectory to avoid other pedestrians, obstructions, or constrained areas. These movement adjustments can affect pedestrian comfort and walking conditions, even when the overall pedestrian space appears to be acceptable. Other pedestrian comfort approaches have recognized that restricted movement, including shoulder brushing and collisions, can affect pedestrian walking conditions beyond pedestrian space alone (City of London, 2010; Finch et al., 2010). As a result, important aspects of walking behaviour, such as pedestrian interaction, including shoulder brushing and the need to adjust walking paths to avoid others, are not reflected in conventional PLOS models and assessments of sidewalks (Campisi et al., 2022; Raj and Vedagiri, 2022).

This limitation reduces the ability of traditional PLOS models to fully represent actual pedestrian experience, particularly in high-activity or high-density environments where interactions are more frequent (City of London, 2010; Kim et al., 2014; Nag et al., 2020). In such conditions, pedestrians may experience constrained movement even when sufficient space appears to be available. Therefore, relying solely on pedestrian space may overlook variations in walking conditions that arise from pedestrian interactions. This highlights the need for a new PLOS model that evaluates sidewalk performance using both available pedestrian space and pedestrian interaction. By

combining these two indicators, the proposed model provides a more detailed assessment of sidewalk conditions than a pedestrian-space-only method.

1.1.3 Problem and Opportunities Statement

Building on these limitations, the indicators commonly used in traditional PLOS frameworks fail to capture important qualitative aspects of pedestrian experience, particularly those related to pedestrian interactions (Asadi-Shekari et al., 2013; Kadali and Vedagiri, 2016). While pedestrian space reflects overall crowding conditions, it does not account for how pedestrians adjust their movement in response to others, such as slowing down, changing direction, or avoiding contact or collisions (City of London, 2010; Kim et al., 2014; Campisi et al., 2022; Raj and Vedagiri, 2022). Interactions such as shoulder brushing or bumping into other pedestrians, referred to as restricted movement, have a direct impact on pedestrian comfort and walking experience (City of London, 2010; Finch et al., 2010). In this study, pedestrian interaction builds on the City of London's concept of restricted movement and refers to movement adjustments that pedestrians make in response to nearby pedestrians while walking on a sidewalk, in addition to shoulder brushing and collisions. These adjustments may include slowing down, changing direction, shifting from the intended walking path, as well as avoiding contact, shoulder brushing, or collisions (Moussaid et al., 2010; Kim et al., 2014). Despite their importance, pedestrian interaction remains largely unquantified in existing PLOS models used to assess pedestrian facilities (City of London, 2010; Kim et al., 2014). As a result, current PLOS frameworks may underestimate the level of constraint experienced by pedestrians, especially in high-density environments. There is an opportunity to improve what indicators are used to evaluate the performance of sidewalks and the true walking experience of pedestrians.

Pedestrian interaction can be divided into either a meeting event, where two pedestrians meet each other as they walk in opposite directions, or a passing event, where two pedestrians pass each other as they walk in the same direction (Lam et al., 2003; Lee et al., 2005; Alhajyaseen et al., 2011; Feliciani and Nishinari, 2016).

Figure 1.1. shows the difference between pedestrian space and pedestrian interaction. We assume that each box represents a sidewalk and each circle within the sidewalk represents a pedestrian. The colour coordinated arrow in front of the pedestrian shows their individual walking direction.

Figure 1.1a. shows a uni-directional walking direction (i.e., passing event) with different amounts of pedestrian space over time. Referring to the first row of boxes for example, the following pedestrian (i.e., red dot) behind is walking faster to pass the leading pedestrian (green dot) in the 1st second (t=1) in the yellow box, then the following pedestrian is approaching closer and is almost past the leading pedestrian in the 2nd second (t=2) in the blue box and completely passes in the Nth second (t=N) in the pink box. Studies have shown that decreasing the distance between two pedestrians reduces pedestrian satisfaction and comfort, which further affects the PLOS (Engelniederhammer et al., 2019; El-Didy et al., 2024). Traditional PLOS frameworks only captures the pedestrian space (i.e., vertical changes in **Figure 1.1a.**) and cannot capture the pedestrian interaction between (i.e., horizontal changes in **Figure 1.1a.**) over time.

Figure 1.1b. shows a bi-directional walking direction (i.e., meeting event) where two pedestrians are approaching in 1st second (t=1) in the yellow box, meeting in 2nd second (t=2) in the blue box, and completely meet and are both turned around from each other's back in the Nth second (t=N) in the pink box.

The first row of boxes in **Figure 1.1.** shows the situation when only two pedestrians are present on the sidewalk. As you move downward through the rows, pedestrian space decreases as the number of pedestrians increases because more people are sharing the same sidewalk area. The second row contains more pedestrians than the first, and the third row contains even more pedestrians. By showing the same passing and meeting events at different pedestrian space conditions, the figure highlights how vertical changes represent pedestrian space, while the horizontal changes illustrate pedestrian interaction in passing and meeting events.

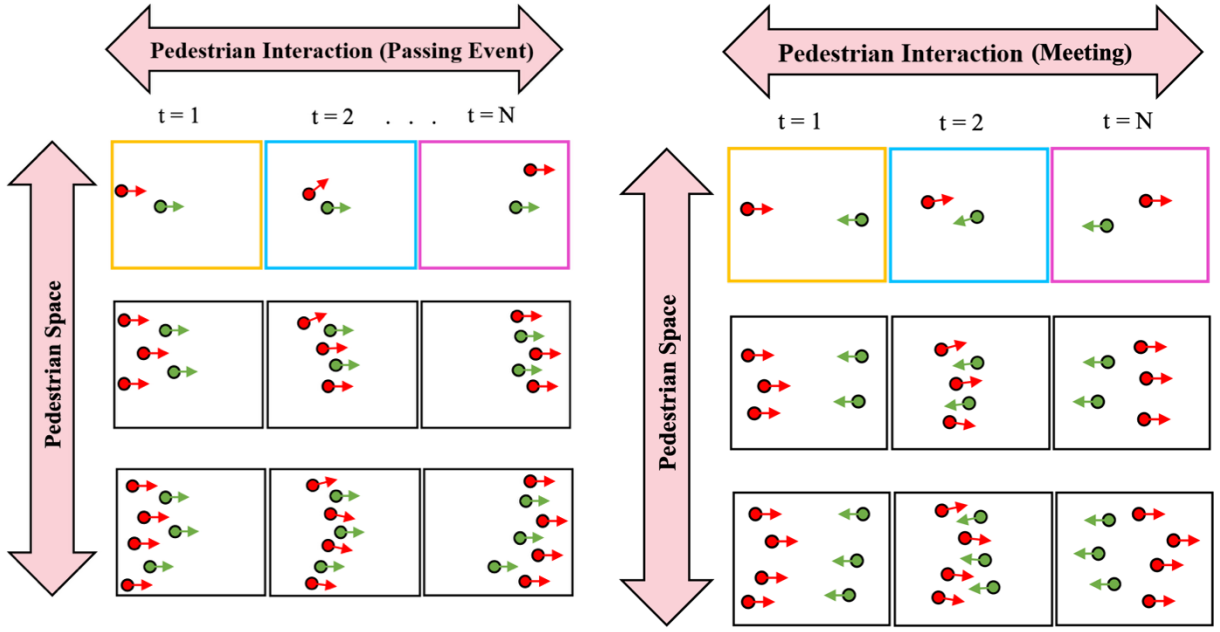

a) Uni-directional walking direction (passing event)

b) Bi-directional walking direction (meeting event)

Figure 1.1. Pedestrian Space versus Pedestrian Interaction

In municipal applications, the City of London uses restricted movement when assessing the PLOS of pedestrian facilities such as sidewalks. However, a key weakness of this approach is the manual

collection of data. An observer is deployed on site to manually counts the number of shoulder brushing, pedestrian bumping or collisions that occur within a given time period (City of London, 2010; Finch et al., 2010).. Furthermore, academic research by Kim et al. (2014) found that pedestrians actively try to maintain a certain amount of personal space while walking, and when forced into close contact with others, their walking behaviour and route choices change to best avoid other pedestrians that they do not know.

To address these gaps, researchers have called for integrating qualitative indicators into PLOS frameworks to better reflect real-world pedestrian experiences (Zannat et al., 2019; Rodriguez-Valencia et al., 2022). By incorporating these indicators, there is an opportunity for future PLOS frameworks to provide a more holistic assessment of pedestrian facilities, enabling planners to design spaces that prioritize both efficiency and user comfort.

1.2 Study Goal and Objectives

This study proposes a new PLOS model that captures pedestrian space and pedestrian interaction using microsimulation outputs. The 3D visualization is used as a supporting tool to interpret and communicate the results from application of the PLOS model through a case study.

There are three objectives to reach our goal:

1) Develop input indicators to capture pedestrian space and pedestrian interaction.
2) Propose a novel PLOS model capturing both pedestrian space and pedestrian interaction to evaluate the performance of sidewalks.
3) Apply the novel PLOS model in a selected study area and use visualization outputs to support the interpretation of the results.

1.3 Study Scope

The key constraints of this study are as follows:

1) The impact of pedestrians intentionally moving together, such as in social groups, is not considered
2) The PLOS framework and approach proposed in this study are limited to pedestrian sidewalks. Other indoor facilities (e.g., commercial malls, airports, hospitals) and outdoor pedestrian facilities (e.g., crosswalks, pedestrian bridges and underpasses, multi-use paths) are not considered.
3) External environmental factors, including weather, lighting, and surface conditions of the sidewalk are not considered in this study.
4) The study focuses on short-term pedestrian interactions within a 15-minute microsimulation period and does not account for long-term variations in pedestrian walking experience over a 15-minute period, or across different days, seasons, or special events..
5) The proposed PLOS framework evaluates pedestrian interactions at a micro-level and does not explicitly consider broader network-level effects or connectivity between multiple pedestrian facilities or facilities that serve other modes of transportation (i.e., cycling, driving, public transit, and micromobility).
6) The proposed PLOS framework is calibrated and demonstrated using one sidewalk case study and does not include site-specific validation or sensitivity testing across other pedestrian facilities.

1.4 Study Structure

We organize the rest of the study in six additional chapters. In **Chapter 2** (Literature Review), we review relevant academic and government studies within the existing PLOS framework. In **Chapter 3** (Methodology), we describe the process of creating a novel PLOS model. In **Chapter 4** (Develop PLOS Model), we present the numerical results obtained from developing the novel PLOS model. In **Chapter 5** (Apply the PLOS Model), we identify the case study area at York University to apply the new PLOS model and evaluate the performance of sidewalks using the new input indicators identified, pedestrian space and pedestrian interaction. In **Chapter 6** (Results of Analysis), we present the results of applying the novel PLOS model that is applied through a case study at York University using the new input indicators identified, specifically pedestrian space and pedestrian interaction. In **Chapter 7** (Conclusion and Recommendations), the key findings of this study are summarized and recommendations for future research and direction for key decision-makers are provided.

Chapter 2. Literature Review

Chapter 2 reviews academic literature and government publications related to PLOS frameworks, including indicator development, data collection, model development, and Base and Alternative Scenario selection (Fonseca et al., 2022). First, this chapter reviews the existing indicators used to measure and evaluate the PLOS of pedestrian facilities, specifically for sidewalks. Next, it explores various data collection methodologies to obtain the necessary input data. Third, we examined existing PLOS models currently implemented in academia and government. Finally, it reviews various scenarios that may affect the PLOS of sidewalks.

2.1 Existing PLOS Indicators

In this section, we examine scientific databases and government sources to review the existing indicators used in PLOS models. Scientific databases include Google Scholar, IEEE Xplore, Scopus, ScienceDirect, while government sources, include Federal Highway Administration, 2004; New York City, 2008; Transport Canada, 2010; Transportation Association of Canada, 2018; City of Brampton, 2022; City of Toronto, 2025, and a British governmental website, City of London, 2010. The search process yielded 200 documents, which were screened and narrowed down to 100 studies and papers. Many indicators have been used in existing PLOS models to evaluate pedestrian facilities (HCM, 2000; Asadi-Shekari et al., 2013; HCM, 2016; Nag et al., 2020; Shu et al., 2021). The input indicators used to evaluate the effectiveness of sidewalks are identified through the literature review . The key findings are summarized in **Table 2.1**.

Table 2.1 summarizes the key indicators identified in this literature review, including traditional PLOS indicators and additional microscopic pedestrian interaction indicators relevant to pedestrian movement and comfort.

Table 2.1 Indicators used for Pedestrian Level of Service Models

ID	Indicator	Independent input	Units	Quantifiable	Target area	Reference	Walking Direction	Definition
1	Pedestrian Space (Inverse of Density)	-	$Meter^2/ped$	Yes	Sidewalk	City of Toronto (2025) City of Brampton (2022) Yang et al. (2022) Mohammadi et al. (2021) Minegishi et al. (2022) Ontario Traffic Council (2022) Lui et al. (2019) Ye et al. (2019) HCM (2016) Kim et al. (2014) Rahayuningsih et al. (2014) New York City (2008) Muraleetharan (2004) Federal Highway Association Administration (2000)	No	Number of pedestrians divided by the area
2	Flow Rate	-	Ped/min/ meter	Yes	Sidewalk	Feliciani and Nishinari (2018) HCM (2016) Rahayuningsih et al. (2014) City of London (2010) Kuang et al. (2008) Lam et al. (2003)	No	Number of pedestrians in a unit distance for a specific time interval
3	Effective Footway Width, Sidewalk Space	-	Meter	Yes	Sidewalk	HCM (2016) Kim et al. (2014), City of London (2010)	No	Total width of sidewalk minus obstacle widths
4	Pedestrian Speed	-	Meter/s	Yes	Sidewalk	HCM (2016) Seer et al. (2014) Shekari et al. (2011)	No	Walking speed of pedestrian
5	Volume/ Capacity Ratio	-	Ratio	Yes	Sidewalk	HCM (2016)	No	Ratio of pedestrian volume to capacity in a sidewalk

ID	Indicator	Independent input	Units	Quantifiable	Target area	Reference	Walking Direction	Definition
6	Radius between Pedestrians, Spacing Distance	-	Meter	Yes	Sidewalk	Minegishi et al. (2022) Song et al. (2018) Kim et al. (2013) Helbing and Molnar (1995) Moussaid et al. (2010)	No	Direct distance/space of pedestrians between each other
7	Pedestrian Volume	-	Ped/min	Yes	Sidewalk	Alhassan and Mashros, (2015) Christopoulou et al. (2012)	No	Number of pedestrians passing a given point on the sidewalk in a certain period of time
8	Pedestrian Density		Ped/meter	Yes	Sidewalk	Feliciani and Nishinari (2018) Rahayuningsih et al. (2014) Zhang et al. (2012) Khuang et al. (2008) Mōri and Tsukaguchi (1987)	No	Number of pedestrians per meter
9	Restricted Movement	-	Percentage	No	Sidewalk	City of London (2010)	No	The number of people who experienced pedestrian interaction was recorded. Pedestrian interaction is when people had to change their speed, route, experienced “shoulder brushing” or bumped into other users
10	Flow Ratio	Volume	Ratio	Yes	Sidewalk	Feliciani et al. (2018) Lam et al. (2003)	Yes	Percentage of one-way pedestrian flow out of the two-way pedestrian flow. (Major and minor flow direction)
		Bearing	Degrees	Yes	Sidewalk	Fu et al. (2022) Akimov et al. (2019) Dabiri and Heaslip, (2018) Chiarandini (2015) Daamen and Hoogendoorn (2003) Greenfeld (2002)		Angle between 2 connecting lines of a point (defined by latitude and longitude) and a reference point (true north).

ID	Indicator	Independent input	Units	Quantifiable	Target area	Reference	Walking Direction	Definition
		Orientation Using Image Processing	Degrees	Yes	Sidewalk	Lallemand et al. (2014) Khan (2013) Zhao et al. (2012) Enzweiler and Gavrila (2010) Gandhi and Trivedi (2008) Anjum and Cavallaro (2008) Shimizu and Poggio (2004) Curio et al. (2000)		Estimate the orientation of pedestrian using computer science techniques (e.g., feature extraction)
		Gazing Direction	Degrees	Yes	Sidewalk	Gallup et al. (2012) Moussaid et al. (2010)		Measuring the angle of pedestrians' head rotation from a specific point of origin
11	Trajectory Clustering	-	Unitless	Yes	Sidewalk	Bian et al. (2019) Bisagno et al. (2018) Sawas et al. (2018) Bensebaa and Lcarabi (2018) Da Silva et al., (2016) Lian et al. (2015) Pelekis et al. (2012)	Yes	Trajectory clustering aims at discovering the similarity in moving object database, grouping similar trajectories into the same cluster, and finding the most common movement behaviors
12	Local density for each pedestrian (Voronoi method)	-	$Meter^2$	Yes	Sidewalk	Cepolina et al., (2018) Xiao et al. (2016) Steffen and Seyfried (2010)	No	Each pedestrian needs a required space to move freely. Violation of this required space by another pedestrian results in decreasing comfort level. This violation can be calculated by direct distance.
13	Local density for each pedestrian (counting method)	-	Number of $ped/meter^2$	Yes	Sidewalk	Jia et al., (2022)	No	Each pedestrian needs a required space to move. Presence of other pedestrians in the required space is considered as violation.
14	Crowd pressure	-	$1/second^2$	Yes	Sidewalk	Feliciani and Nishinari (2018) Ma et al. (2013)	Yes	Estimates if the state of a pedestrian crowd it close to "collapse" or is too crowded. Obtained by multiplying pedestrian density and speed variance.

ID	Indicator	Independent input	Units	Quantifiable	Target area	Reference	Walking Direction	Definition
		Velocity variance	Unitless	Yes	Sidewalk	Feliciani and Nishinari (2018) Kretz (2011) Helbing et al., (2007)		The mean square deviation from the mean velocity of pedestrians. The lower the variance of pedestrian speed, the more comfortable they feel.
15	Congestion Level	-	1/meter	Yes	Sidewalk	Feliciani and Nishinari (2018) Dixon (1996)	No	Measure the smoothness of pedestrian flows within different pedestrian streams and defines thresholds for congestion under safe conditions. Obtained from collected trajectories and velocity.
16	Temporal Changes	-	Seconds	Yes	Sidewalk	Raman et al. (2016)	Yes	Uses vision technology and HMM to determine the walking direction of a person and map 4/8 directions.
		-	Padding	Yes	Sidewalk	Raman et al. (2016)		Is the displacement direction of centroid of the pedestrian which is used to distinguish the direction of movement
17	Self-organization in pedestrian counterflow	-	Unitless	No	Sidewalk	Wang et al. (2012) Ma et al. (2010) Schadschneider et al. (2010) Johansson et al. (2008) Khuang et al. (2008) Hoogendoorn et al. (2005) Tajima et al. (2002) Takimoto et al. (2002)	Yes	Pedestrians display self-organizing features to collective patterns such as lane formation during counterflow. Pedestrians do this self-organize as a form of collision avoidance behaviour especially from people who are moving opposite to their own direction. This influences safety and comfort level of pedestrians.
18	Vanishing Point	-	Degrees	Yes	Sidewalk	Huang et al. (2016) Yu et al. (2009) Lv et al. (2006) Caprile and Torre (1990)	Yes	In the area of computer vision, the head/feet positions on the ground plane is used to determine the vanishing point with respect to the walking direction. This technique is a camera-based calibration method that can be applied using CCTV cameras, videos or still images.

ID	Indicator	Independent input	Units	Quantifiable	Target area	Reference	Walking Direction	Definition
19	Social Force / Interaction Force	Interpersonal distance	m/s² or unitless interaction index	Yes	Sidewalk	Li et al. (2024) Siddharth and Perumal (2024) Hagos and Adnan (2020)	Yes	Estimates pedestrian interaction intensity based on how nearby pedestrians influence one another. This indicator can represent movement constraint and avoidance behaviour.
20	Time-to-Collision	Relative trajectory	Seconds	Yes	Sidewalk / pedestrian facility	Huber et al. (2014) Jafari and Liu (2024) Karamouzas et al. (2014);	Yes	Estimates the time before two pedestrians or sidewalk users may reach a conflict point if they continue along their current movement paths. Lower values indicate greater interaction or conflict potential.
21	Deviation from Walking Path	Pedestrian trajectory	Degrees or metres	Yes	Sidewalk / pedestrian facility	Yang et al. (2019) Lee (2016) Huber et al. (2014)	Yes	Measures how much a pedestrian's actual walking path deviates from the expected walking path. Higher deviation may indicate greater movement constraint or avoidance behaviour.
22	Walking Acceleration / Deceleration	Pedestrian speed	m/s²	Yes	Sidewalk / pedestrian facility	Yang et al. (2019) Lee (2016) Huber et al. (2014)	Yes	Measures changes in pedestrian speed over time. Frequent acceleration or deceleration can indicate unstable walking conditions, slowing, or evasive movement.

The first column, ID, represents the special number we allocated to each indicator that was identified from the review. The ID is unique for each indicator. For example, pedestrian space has an ID of 1, and flow rate has an ID of 2, with a total of 22 IDs to represent 22 input indicators.

The second column, Indicator, is the name for each input indicator.

The third column, Independent Input, indicates whether an indicator depends on other inputs. For instance, the flow ratio (ID: 10) relies on other various indicators, including volume, bearing, orientation, and gazing direction.

The fourth column lists the unit of measurement for each indicator. Some indicators have a unit of measurement, while certain indicators are unitless. For example, pedestrian space (ID: 1) has a measurement of square meters per pedestrian, whereas trajectory clustering (ID: 11) is unitless, as it groups pedestrians together, which has no units.

The fifth column identifies whether the indicator is quantifiable or if it is measurable and typically expressed numerically. Examples of quantifiable indicators include pedestrian space, flow ratio, sidewalk width, and volume (IDs 1, 2, 3, and 4). In contrast, non-quantifiable indicators, such as restricted movement (ID: 9), involve subjective interpretation and are not easily measured. A binary value is used to denote quantifiability: ‘1’ indicates quantifiable, while “0” indicates non-quantifiable.

The sixth column specifies the target area. The target area of this study focuseson sidewalk facilities; therefore, the majority of the literature reviewed focused on sidewalks.

The seventh column lists the references where each indicator was found or observed during the literature review. Certain indicators that are more widely used include multiple references in

academia and federal and municipal sources, such as pedestrian space (ID: 1). Some indicators, for example those that are newly proposed by research and are not used by municipal or federal governments, only include references in academic papers, for example, crowd pressure, congestion level, and vanishing point (ID: 14, 15, and 18 respectively).

The eighth column shows whether an indicator accounts for the walking direction of pedestrians within a sidewalk facility. This is also represented as a binary value, with '1' indicating that walking direction is considered, and "0" indicating that walking direction is not considered. For example, flow ratio (ID: 10) takes walking direction into account while pedestrian space (ID: 1) does not.

Finally, the last column provides a brief description of the concept and application of each indicator.

Many indicators have been used in existing PLOS models to evaluate pedestrian facilities (HCM, 2000; HCM, 2016; Nag et al., 2020; Shu et al., 2021). These indicators include pedestrian space, density, flow rate, speed, sidewalk width, volume, restricted movement, walking direction, and other factors that influence pedestrian walking conditions. Traditional PLOS methods often rely on pedestrian space, density, or flow-based measures, while more recent studies have considered additional qualitative factors relating to pedestrian comfort, perception, and interaction (Asadi-Shekari et al., 2013; Kim et al., 2014; Cepolina et al., 2018; Nag et al., 2020). This shows that PLOS evaluation has gradually expanded beyond a single space-based or quantitative measure.

To better understand which indicators are most useful for sidewalk PLOS evaluation, the indicators in **Table 2.1.** were reviewed based on their purpose, how they are measured, whether they are quantifiable, whether they apply to sidewalks, and whether they consider walking direction (Asadi-

Shekari et al., 2013; Cepolina et al., 2018; Nag et al., 2020; Shu et al., 2021). This comparison shows that some indicators are useful for describing general sidewalk conditions, such as pedestrian space, flow rate, sidewalk width, and volume (HCM, 2000; Landis et al., 2001; Petritsch et al., 2006; HCM, 2016). Other indicators are more useful for describing pedestrian interaction and movement, such as restricted movement, social force, flow ratio, trajectory clustering, crowd pressure, and congestion level (City of London, 2010; Finch et al., 2010; Kim et al., 2014; Feliciani and Nishinari, 2018; Bian et al., 2019). Not all indicators are equally suitable for the proposed model, but reviewing them in this way helps explain the strengths and limitations of each indicator before identifying the most appropriate indicators for the proposed PLOS model in the following chapter.

The expanded indicators in **Table 2.1.** further show that PLOS evaluation can include measures related to available walking area, pedestrian movement, interaction, and comfort. This supports the need to consider more than one aspect of pedestrian walking conditions when developing a PLOS model. However, not all indicators are equally suitable for direct use in a proposed model because some require additional data, calibration, or are more appropriate as supporting measures. Overall, the literature review shows that pedestrian space is widely used to represent available walking area, while restricted movement, social force, and walking direction are relevant for describing pedestrian interaction and movement constraint. These indicators provide the basis for identifying and developing the input indicators used in the proposed PLOS model in **Section 4.3**. Based on our literature review, pedestrian space is the most widely used indicator in both academic and municipal contexts.

Pedestrian space refers to the amount of available walking area per pedestrian, usually expressed in square meters per person (m^2/ped). It reflects the amount of available space per pedestrian at

any given time. For example, in North America, New York City, the City of Brampton, and the City of Toronto use this indicator to evaluate sidewalks (New York City, 2008; City of Brampton, 2022; City of Toronto, 2025). The FHWA in the US and the OTC in Canada are transportation agencies that also use or recommend using pedestrian space as an indicator to measure the effectiveness of sidewalk facilities (FHWA, 2004; OTC, 2022). In academia, Kim et al. (2014) used pedestrian space as an indicator to measure the PLOS and evaluate the effectiveness of sidewalks. Rahayuningsih et al. (2014) also used pedestrian space along with other indicators in their model to assess the performance of sidewalks and highlight areas of improvement to enhance PLOS.

Restricted movement refers to the limitations that pedestrians face when freely navigating a space due to physical obstacles, crowding or behavioural constraints caused by other pedestrians or general environmental conditions (City of London, 2010; Finch et al., 2010; Kim et al., 2014). Unlike indicators such as pedestrian space, which can be objectively measured or quantified (Zhang et al., 2012; Seer et al., 2014), restricted movement often depends on subjective observation, making it a non-quantifiable indicator as identified in **Table 2.1.** This indicator captures instances where pedestrians must frequently alter their path to avoid other pedestrians (City of London, 2010; Kim et al., 2014; Huber et al., 2014). Due to its subjective nature, restricted movement is difficult to quantify. For example, the City of London (2010) has integrated restricted movement into their PLOS frameworks. Their model measures PLOS by manually observing and counting instances of shoulder brushing and minor collisions during designated observation periods (City of London, 2010). In high-density urban areas, the pedestrian interaction can significantly impact the pedestrian experience by forcing individuals to deviate from their preferred walking paths and speeds to avoid colliding with other pedestrians (Kim et al., 2014;

Mohammadi et al., 2021; Yang et al., 2022). These limitations can reduce both the perceived walking experience and actual PLOS and are therefore critical to understanding the overall effectiveness of pedestrian facilities, specifically within sidewalks.

Social-force-based approaches were also reviewed as part of the PLOS indicator identification process. Social force models are commonly used to represent pedestrian interaction effects, including how pedestrians respond to nearby pedestrians and movement constraints (Helbing and Molnar, 1995; Johansson et al., 2007; Kretz et al., 2018). Some formulations use simplified interaction terms, while extended models can represent pedestrian movement direction as a vector (Helbing and Molnar, 1995; Johansson et al., 2007; Karamouzas et al., 2014). Vector-based formulations can capture both the direction and magnitude of pedestrian movement in greater detail. However, for the purpose of developing a practical PLOS model, this study uses social force with a simplified walking direction term to quantify pedestrian interaction consistently across the proposed PLOS categories.

Walking direction plays an important role in shaping the PLOS of sidewalks. When people walk in opposite directions on the same sidewalk, they are more likely to face interruptions such as sudden stops, path adjustments, or evasive movements to avoid collisions with other pedestrians (Lee et al., 2005; Feliciani et al., 2018). These changes in movement can influence pedestrian interaction by increasing the likelihood of shoulder brushing. Studies have shown that bi-directional walking conditions tend to result in lower PLOS in comparison to uni-directional walking conditions (Yang et al., 2022). This is largely because people have less freedom to move smoothly in a consistent walking path (Alhajyaseen et al., 2011; Corbetta et al., 2016). By considering walking direction when measuring PLOS on sidewalks, the model can better identify how pedestrians navigate their environment and where discomfort or conflicts may occur.

2.2 Pedestrian Data Collection and Simulation Approaches

In this section, we review two common approaches for collecting pedestrian-related data, including real-world field data collection and simulation tools.

2.2.1 Real-World Data Collection

Real-world data collection for PLOS assessments involves gathering information from pedestrian facilities. This includes direct observation (e.g., manual pedestrian counts), questionnaire surveys, and sensor-based techniques. The direct observation (e.g., manual pedestrian counts) and questionnaire survey methods allow researchers to assess pedestrian volume, walking speeds, and pedestrians' interactions with other pedestrians, vehicular traffic or other features within a sidewalk. This method is often convenient as it does not require additional tools or software. (Asadi-Shekari et al., 2015). However, sensor-based techniques have enabled the use of automated tools such as LiDAR, GPS tracking, and computer vision-based pedestrian detection systems to enhance accuracy and reduce observer bias (Rahman et al., 2021). These methods provide valuable insights into pedestrian behaviours, infrastructure utilization, and environmental factors affecting pedestrian flow that direct observation and questionnaire surveys are unable to. (Jiang et al., 2017).

The real-world data collection method plays an important role in calibrating detection systems for pedestrians by helping PLOS models reflect actual and more accurate pedestrian experiences when walking on sidewalks. Real-world data provides insight into pedestrian volumes and speeds but is often limited by subjectivity and scale (Kim et al., 2018). Sensor-based methods offer more detailed and consistent data, making them suitable for crowded or complex pedestrian facilities (Jiang et al., 2017). However, they can be costly and require technical setup that can become

complicated. In smart cities, real-time monitoring allows for more responsive planning and management (Shamsuddin et al., 2019).

A key drawback of the real-world data collection method is that it can be time-consuming and expensive since it requires an individual to be physically on the observation site. It also only captures what is happening in one location at a given time, which makes it harder to implement alternative scenarios that consider different design layouts, such as adding benches or setting up a construction zone, that might affect pedestrian movement and PLOS. Additionally, repeated observations may be needed to account for variability caused by time of day, weather, or special events. As a result, real-world data collection does not always provide sufficient or consistent information to evaluate different design options or anticipate how conditions might change under alternative layouts. This limitation makes it difficult to test potential changes to design layout that may affect the walking experience of pedestrians before implementation, which is why researchers often supplement real-world data collection with simulation tools that allow controlled experimentation across multiple alternative scenarios.

2.2.2 Simulation Tools

This section discusses two widely used simulation tools applied in this study: 1) PTV Viswalk, used for pedestrian behaviour modelling and data collection, and 2) Unity, used for enhanced visualization and interactive analysis.

1) PTV Viswalk

Micro-simulation is a computational technique that enables the modelling of pedestrian movement and interactions within a virtual environment that can simulate real-world existing conditions (Papadimitriou et al., 2018). It allows researchers to explore various pedestrian scenarios with

varying volume, flow, and walking direction, which allows us to assess the effects of alternative urban design scenarios on PLOS. Compared to real-world data collection, microsimulation offers several advantages, including the ability to conduct multiple iterations, test hypothetical or future scenarios, and analyze complex interactions that would be difficult to manually observe in real-world settings (Papadimitriou et al., 2018). PTV Viswalk is a reliable tool for simulating pedestrian facilities and environments, as well as collecting pedestrian data for future scenarios that the real-world data collection methods cannot capture. This tool is beneficial for comparing existing conditions and proposed changes or improvements to design layouts to assess how alternative scenarios may potentially affect sidewalk operations.

PTV Viswalk is one of the most widely used simulation software programs for pedestrian dynamics. It is based on the Social Force Model (SFM), which represents pedestrians as agents influenced by forces that dictate their movement and behaviour (Helbing and Molnar, 1995; Kretz, 2018). The microsimulation software can model how pedestrians move in different environments and can provide second-by-second data, making it useful for evaluating PLOS in sidewalks. Researchers have used PTV Viswalk to study pedestrian behaviour under various conditions, including uni- and bi-directional walking direction, crowding, and social distancing during COVID-19 (Mohammadi et al., 2021; Adwitiya and Sumabrata, 2022; Rodriguez-Valencia, 2022). One of the main advantages of using PTV Viswalk for simulation is that it allows researchers to test "what-if" scenarios, such as widening sidewalks and changing crosswalk layouts without the need for costly real-world changes (Papadimitriou et al., 2018).

Many researchers have used PTV Viswalk for various applications to model pedestrian behaviour and movement, particularly in studies examining the impact of social distancing and behavioural changes in response to crowding conditions. Mohammadi et al. (2021) introduced a new PLOS

model called Level of Pedestrian Physical Distancing by simulating North American sidewalks during the COVID-19 pandemic and incorporating distancing requirements into the model. PTV Viswalk was used to simulate the virtual sidewalk environment of the study area in Toronto, Canada, and demonstrate the application of the proposed model. Espitia et al. (2022) used PTV Viswalk to explore how social distancing affected pedestrian route choices in large-scale spaces in Venice, Italy. Social distancing conditions were simulated in the software, which helped the development of predictive crowd management strategies.

In contrast, other studies have applied PTV Viswalk to evaluate pedestrian interactions and infrastructure performance under varying design and operational conditions. Rodriguez (2022) tested whether PTV Viswalk can model the interactions of pedestrians and cyclists in shared multi-use paths for different scenarios, including conditions with and without obstacles. The simulations were run ten times, with a warm-up period of 15 minutes and a running period of 1 hour. For each scenario tested, data were collected and averaged for walking speed, riding speed, and the density of both pedestrians and cyclists. The study confirmed that the software can be used as a conceptual design tool, even for complex scenarios, as long as it is properly calibrated. Adwitiya and Sumabrata (2022) conducted a microscopic simulation of a transit-oriented area in Jakarta, Indonesia. PTV Viswalk was used to evaluate the PLOS of a multi-purpose crossing bridge for two scenarios based on the pedestrian flow ratio. Based on the outcomes from PTV Viswalk, improvements, including changing the entrance and exit locations of the bridge and converting the elevator to a staircase, were proposed to improve the PLOS of the existing conditions.

Figure 2.1a. illustrates a real-world data collection approach, where field staff observe and record pedestrian activity (City of London, 2010). In contrast, **Figure 2.1b.** displays a simulation-based

approach using PTV Viswalk, which generates pedestrian flow data virtually through a calibrated model (Adwitiya & Sumabrata, 2022).



a) Real-World Data Collection (City of London, 2010)

b) Data Collection using Simulation Tools (Viswalk) (Adwitiya and Sumabrata, 2022)

Figure 2.1. Data Collection Approaches

2) Unity Game Engine

Unity is a software game engine released in June 2005 (Haas, 2014). It is a widely used tool for simulation and visualization. Researchers have used Unity to enhance the visualization from other pedestrian simulation software, such as PTV Viswalk, and to analyze pedestrian behaviour using virtual reality.

For example, Lv and Hu (2020) used Unity's scene implementation features to simulate different scenarios of pedestrian evacuation in an indoor commercial facility. The simulations included multiple camera angles for existing conditions and scenarios, including indoor multi-exit locations and different obstacles. Researchers are also using Unity to develop different pedestrian crowd simulations and the results from Unity are used to predict and prevent crowd-rush accidents. Abu Alatta and Moman (2021) utilized Unity to enhance the visualization of pedestrian facilities. The study area in an urban neighbourhood in Amman, Jordan, was visualized by different study

participants using various formats, including physical models, animated walkthrough videos, and an interactive, real-time demo from Unity. The use of the game engine also led to a better understanding of the design layout and details in comparison to the other methods. It also provided an enhanced simulation of pedestrian movement and understanding of how sidewalk design layouts can affect the PLOS. Choi et al. (2025) used Unity to create a pedestrian crowd simulation of a high-density sidewalk in Seoul, Korea. Pedestrians were tracked in real time, and areas of high interactions and conflicts were identified. Visual heat maps and graphs of pedestrian density and congestion were modelled. Multiple scenarios were tested, including cultural events and emergencies for past incidents. The effectiveness of creating alternative scenarios, such as modified venue layouts, additional exit routes, were also evaluated in Unity before implementing it into the real world, to ensure the success of the changes (Lv and Hu, 2020; Abu Alatta and Momani, 2021; Choi et al., 2025).

Unity provides an opportunity to improve the visualization of microsimulations presented by other microsimulation softwares (Lv and Hu, 2020; Abu Alatta and Momani, 2021; Choi et al., 2025). With its built-in programming capabilities, it also enables advanced pedestrian analysis that cannot be achieved with microsimulation software alone. This is an advantage because it can help explore pedestrian behaviour and interactions, compare various design scenarios in greater depth, and develop new PLOS frameworks.

2.3 Existing PLOS Models

Here, we reviewed the two most common PLOS models that consider pedestrian space and restricted movement, including: 1. HCM PLOS and 2. City of London PLOS.

2.3.1 HCM PLOS

The HCM (2000) introduced a PLOS model originating from the research of Fruin in 1971. The PLOS model emphasizes that the performance of sidewalks and crossings that is based on a single indicator; for example, pedestrian space (Fruin, 1971; Pushkarev and Zupan, 1975). It compares the indicator with different thresholds to achieve different categories that form the PLOS table, as shown in **Table 2.2**. The first column represents six levels varying from the best walking conditions (A) to the worst conditions (F). The second column shows the pedestrian space for each PLOS level. This indicates the different thresholds for the average area that is available to each pedestrian within a sidewalk and is measured in square meters per pedestrian (m^2/ped). For example, if the average pedestrian space over a 15-minute observation period is 5.7 m^2/ped, the sidewalk would be classified as PLOS A; if the average pedestrian space is 1.8 m^2/ped, then it would be classified as PLOS D, and if the average pedestrian space is 0.74 m^2/ped, then it would be classified as PLOS F.

Table 2.2. HCM PLOS Threshold for Sidewalk (HCM, 2010)

Pedestrian Level-of-Service (PLOS)	Pedestrian Space (m^2/ped)
A	> 5.6
B	$3.7 - 5.6$
C	$2.2 - 3.7$
D	$1.4 - 2.2$
E	$0.75 - 1.4$
F	< 0.75

2.3.2 City of London PLOS

The City of London developed a PLOS model that considers two indicators: pedestrian crowding and restricted movement (City of London, 2010; Finch et al., 2010). Pedestrian crowding is

measured in pedestrians per metre of clear footway width (ppmm), while restricted movement quantifies the percentage of pedestrians who need to adjust their walking path or speed to avoid shoulder brushing or bumping with other pedestrians, measured manually through visual observation. The higher the percentage, the higher the indication of uncomfortable walking conditions for pedestrians. The first column model represents five main levels ranging from A (very comfortable) to E (very uncomfortable). The second, third, and fourth column, shows how the main level is subdivided into 3 categories (+ / 0 / -) giving a total of 15 levels as shown in **Table 2.3** (City of London, 2010). Therefore, the three-level "+ / 0 / -" classification structure used to describe varying walking conditions within a main comfort level is attributed to the City of London PLOS model.

Table 2.3. City of London PLOS Threshold for Sidewalk (City of London, 2010)

Pedestrian Comfort Level	Restricted Movement (+)	Restricted Movement (0)	Restricted Movement (-)
A	A+ (3ppmm) < 3% Restricted Movement	A0 (3 to 5 ppmm) 13% Restricted Movement	A- (6 to 8 ppmm) 22% Restricted Movement
B	B+ (9 to 11 ppmm) 31% Restricted Movement	B0 (12 to 14 ppmm) 41% Restricted Movement	B- (15 to 17 ppmm) 50% Restricted Movement
C	C+ (18 to 20 ppmm) 59% Restricted Movement	C0 (21to 23 ppmm) 69% Restricted Movement	C- (24 to 26 ppmm) 78% Restricted Movement
D	D (27 to 35 ppmm) 100% Restricted Movement		
E	E (>35 ppmm) 100% Restricted Movement		

The restricted movement concept used in this study is related to the City of London approach because both focus on how movement constraints affect pedestrian walking comfort and movement. However, the City of London method is based on manually observed events, such as shoulder brushing, bumping, and collisions (City of London, 2010; Finch et al., 2010). In comparison, this study uses a simulation-based calculation to represent movement constraints using pedestrian proximity, social force, and walking direction, rather than relying only on manually counted contact events (Helbing and Molnar, 1995; Moussaid et al., 2010; Kim et al., 2014).

2.3.3 Limitations of Existing PLOS Models

Although existing PLOS methods provide a useful foundation for evaluating pedestrian facilities, many of these methods rely on indicators that primarily describe quantitative aspects, such available pedestrian space, density or volume. These indicators are important for assessing capacity and general operating conditions, but they do not fully capture interaction-related walking behaviours. For example, sidewalks with similar pedestrian space values may still provide different walking experiences if pedestrians experience different levels of speed adjustment, path deviation, avoidance movement, or shoulder brushing and collisions. This limitation shows that pedestrian space alone may not be sufficient to evaluate sidewalk performance. Therefore, a second indicator is incorporated into the PLOS model in this study to better represent pedestrian interactions and provide a more detailed assessment of walking conditions that is more accurate and reflective of real world conditions.

2.4 Scenario-Based Application of PLOS Models

The application of PLOS models commonly involves the use of Base and Alternative Scenarios to evaluate how changes to the design of pedestrian facilities influence walking conditions (Asadi-Shekari et al., 2014; Papadimitriou et al., 2018). In the literature, a Base Scenario typically represents existing conditions, while Alternative Scenarios introduce modifications to the physical environment to assess their impact on established pedestrian indicators, such as pedestrian space (Asadi-Shekari et al., 2014). This scenario-based approach allows researchers to examine how changes to the design layout affect these indicators and identify potential improvements to sidewalk performance that enhance the pedestrian walking experience. However, these applications are primarily limited to traditional PLOS indicators and do not account for pedestrian interactions that influence direct movement behaviour (City of London, 2010; Finch et al., 2010; Kim et al., 2014; Mohammadi et al., 2021; Yang et al., 2022).

Design layout modifications are the most common changes that are typically considered and implemented along sidewalks by municipalities (Loukaitou-Sideris et al., 2007; Oliver-Solà et al., 2009). Design layout modifications are changes to the design of the physical environment and typically influence how pedestrians navigate and experience sidewalks. These physical changes are especially important in crowded areas, such as university campuses. Common physical changes include widening of available walking area, reallocation of sidewalk furniture, and minimizing physical obstructions (Ehrenfeucht and Loukaitou-Sideris, 2010; Saltarin-Molino et al., 2023; Ulhaq et al., 2024). These physical changes help improve the indicators used for evaluating PLOS on sidewalks, such as pedestrian space and pedestrian interaction.

Sidewalk widening is one of the most common changes in the design layout, especially within crowded pedestrian areas where pedestrian movement may become constrained. By increasing the available pedestrian space during peak pedestrian periods, such as campus events or class transitions, a larger walking area increases space and may potentially reduce pedestrian interaction. Research shows that a greater walking space improves PLOS (Loukaitou-Sideris et al., 2007; Asadi-Shekari et al., 2015). A study by Holmes et al. (2018) also illustrated that wider sidewalks in crowded areas, such as university campuses, reported better movement for bi-directional walking direction and fewer shoulder brushing and conflicts between pedestrians.

Sidewalk furniture, such as benches and trash bins, can obstruct sidewalks when poorly placed. When these are clustered near entrances or exits, or placed too close to the pedestrian walking area, they reduce the usable sidewalk width and interrupt walking paths. This may potentially lead to frequent changes in walking directions and patterns, increased shoulder brushing or pedestrian interaction, and ultimately, a lower PLOS. Pedestrians are also more likely to have unpredictable movement patterns due to the need to avoid fixed infrastructure that acts as obstacles along the sidewalk (Jaskiewicz, 2000; Nikiforiadis & Basbas, 2019). The Urban Design Guide by the National Association of City Transportation Officials (NACTO) emphasizes maintaining clear walking areas for sidewalks (NACTO, 2013).

Advertisements and promotional posters are often installed along walking paths or hung from walls. Too many advertisements placed along sidewalks are a common issue on crowded sidewalks. According to studies, pedestrians often pause for an average of 5 to 12 seconds to view advertisements and posters, also known as dwell time, especially when they are visually appealing or informative (Kong et al., 2019; Konovalova and Petrova, 2023; Mishra and Chowdhury, 2023). These pauses can reduce the available walking area and prompt other pedestrians to change their

walking direction unexpectedly, which can increase pedestrian interactions and worsen the PLOS (Alhajyaseen et al., 2011; Corbetta et al., 2016).

Construction and maintenance activities can also disrupt the effectiveness of a sidewalk. Equipment and barriers restrict the available walking area and disrupt walking patterns. This can require pedestrians to modify their walking direction or navigate through cramped sections of the sidewalk to avoid obstacles, narrow paths, or unsafe walking conditions. Research shows that poorly managed construction and maintenance areas within a sidewalk have been linked to an increase in pedestrian interaction experienced and can lead to a lower PLOS (Fitzpatrick et al., 2001; Yoon et al., 2025).

2.5 Chapter Summary

Chapter 2 reviewed existing PLOS indicators used in academic literature and government publications to evaluate sidewalk performance. The review showed that pedestrian space is the most commonly used indicator because it provides a quantifiable measure of available space per pedestrian. However, relying on pedestrian space alone does not fully capture pedestrian interactions such as shoulder brushing, collision avoidance, or changes in walking direction. Restricted movement was also reviewed as an important indicator for representing pedestrian interactions, although existing approaches often rely on manual observation, which can be subjective and difficult to apply consistently.

The chapter also examined pedestrian data collection and simulation approaches used in PLOS studies. Real-world data collection methods, including direct observation, surveys, and sensor-based techniques, provide useful information but can be costly, time-consuming, and limited when testing alternative design conditions. Simulation tools such as PTV Viswalk and Unity were

reviewed as useful approaches for modelling pedestrian movement, generating trajectory data, testing "what-if" scenarios, and improving visualization of pedestrian interactions.

The chapter also reviewed existing PLOS models, with a focus on the HCM PLOS framework and the City of London PLOS framework. The HCM PLOS model uses pedestrian space as its main indicator, making it simple and widely applicable but limited in its ability to represent interaction-based walking experiences. In contrast, the City of London model incorporates two indicators, pedestrian crowding and restricted movement. However, a key drawback was the manual observation of visible shoulder brushing, bumping and collision events to evaluate the PLOS of sidewalks.

Finally, the chapter reviewed scenario-based applications of PLOS models. Previous studies commonly use Base and Alternative Scenarios to evaluate how sidewalk design changes affect pedestrian conditions. These scenarios often include modifications to design layouts such as sidewalk widening, changes to sidewalk furniture, advertisements, and construction-related obstructions. However, most scenario-based applications focus on traditional indicators and do not explicitly quantify how pedestrian interactions change under different design conditions.

Overall, **Chapter 2** established the research gap addressed in this study. Existing PLOS indicators and models provide useful methods for evaluating sidewalk performance, but they either rely heavily on pedestrian space or require subjective observation of pedestrian interaction. To address these limitations, this study develops a PLOS framework that uses two indicators, pedestrian space and a measurable form of pedestrian interaction. The literature reviewed in this chapter also supports the use of PTV Viswalk, Unity, and scenario-based analysis to evaluate how design layout modifications influence pedestrian walking conditions.

Chapter 3. Methodology

Chapter 3 outlines the methodology for achieving the research objectives presented in this study. This study follows a structured framework to improve how we analyze PLOS in pedestrian facilities, specifically in sidewalks (See **Figure 3.1.**) Firstly, we begin by identifying the key input indicators that capture PLOS and the true pedestrian walking experience. Secondly, we create 2D microsimulation models to extract relevant pedestrian input data that we need to develop a novel PLOS model and 3D visualizations to support the calculation of the indicators and enhance the presentation of the sidewalk environment and results from the PLOS analysis. Thirdly, we use the pedestrian input data obtained from the 2D microsimulation model and 3D visualization to develop a novel PLOS model for the chosen study area. This incorporates the input indicators pedestrian space and pedestrian interaction. Finally, we apply the new PLOS model by testing it on the study area's Base Scenario and Alternative Scenarios to evaluate how these affect pedestrian conditions along a sidewalk.

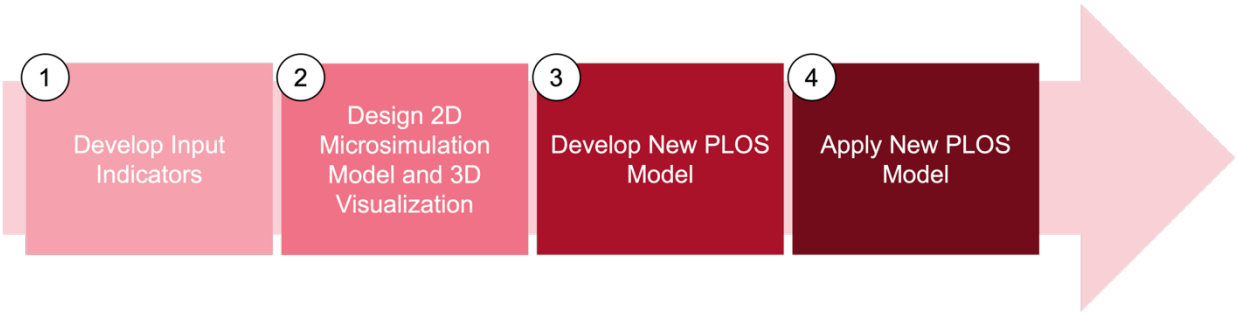

Figure 3.1. Study Methodology

3.1 Process to Develop Input Indicator

This section describes the process of identifying and developing the chosen input indicators, pedestrian space and pedestrian interaction, which form the foundation of the novel PLOS model.

3.1.1 Develop and Identify Input Indicators

Pedestrian space is the first input indicator we used for the PLOS model (Pushkarev and Zupan, 1975; HCM, 2000; HCM, 2016; TRB, 2020). As discussed in **Chapter 2**, it is a traditional indicator used in existing PLOS models that academic literature and government publications commonly use to evaluate PLOS in sidewalks. **Equation 3.1.** shows the formula for pedestrian space:

$$PS = \frac{S_P}{V_P} \qquad \textbf{Equation 3.1.}$$

Where

PS represents pedestrian space (m²/ped),

S_P represents pedestrian speed (m/min), and

V_P represents pedestrian flow per unit width (ped/min/m)

The second input indicator we use for the model is pedestrian interaction because it represents movement constraints caused by pedestrian interactions due to proximity effects, evasive changes to pedestrian movement such as speed and walking path, differences in walking direction, as well as shoulder brushing and collisions, as outlined in **Chapter 2** (City of London, 2010; Finch et al., 2010; Kim et al., 2014). We develop a mathematical equation for pedestrian interaction derived from two sub-indicators: social force and walking direction (Helbing and Molnar, 1995; Moussaid

et al., 2010). These two sub-indicators quantify how pedestrians adjust their movement in response to others, such as slowing down, maneuvering, or deviating from their intended original walking path to avoid colliding or shoulder brushing with other pedestrians (Kim et al., 2014; Lee et al., 2005; Feliciani and Nishinari, 2018).

In this study, the pedestrian interaction indicator is proposed as a simulation-based indicator that represents and extends the restricted movement concept identified in existing PLOS literature. In the City of London approach, restricted movement is measured through manual observation of visible events such as shoulder brushing, bumping, and collisions. However, because this approach is based on manual observation, it does not directly quantify second-by-second changes in pedestrian speed, trajectory, proximity, or walking direction. The pedestrian interaction indicator we develop in this study extends the restricted movement concept by calculating constraints or changes in movement from pedestrian trajectory outputs, proximity between pedestrian pairs, social force, and walking direction. Therefore, the proposed indicator captures both visible restricted movement events and earlier movement adjustment effects, such as slowing down, changing path, or adjusting trajectory that pedestrians make before shoulder brushing or collision occurs (City of London, 2010; Finch et al., 2010; Moussaid et al., 2010; Kim et al., 2014; Lee et al., 2005; Feliciani and Nishinari, 2018).

3.1.2 Combine Pedestrian Interaction Sub-Indicators

Social force represents the influence pedestrians have on one another based on their proximity while walking (Helbing and Molnar, 1995; Helbing et al., 2000; Lakoba et al., 2005; Kretz, 2018). For a pedestrian pair i and j on a sidewalk, we calculate the social force by using the required personal space of each pedestrian and the actual distance separating them at a given time. As the

distance between two pedestrians decreases, the social force increases, as shown in **Equation 3.2.** (Helbing and Molnar, 1995; Helbing et al., 2000; Lakoba et al., 2005). In practical terms, this means that when pedestrians walk very close to one another, they become more aware of each other and are more likely to adjust their speed, direction, or path to avoid contact. When pedestrians are farther apart, these interactions are minimal and have little influence on their intended original movement. As a result, higher social force values indicate situations where pedestrians experience stronger interactions and greater constraints on their movement (Helbing and Molnar, 1995; Helbing et al., 2000; Moussaid et al., 2010; Kim et al., 2014).

Within this study, social force serves as a key sub-indicator of pedestrian interaction (Helbing and Molnar, 1995; Kretz, 2018; Li et al., 2024; Siddharth and Perumal, 2024). Higher social force corresponds to higher levels of pedestrian interaction because pedestrians must make more noticeable adjustments to their walking paths to maintain their preferred personal space and avoid shoulder brushing or collisions. In contrast, lower social force reflects more comfortable walking conditions where pedestrians don't experience as frequent interruptions due to other pedestrians.

Equation 3.2. shows the formula for social force.

$$SF_{ij} = Ae^{\frac{(RS_i - d_{ij})}{B}} \qquad \textbf{Equation 3.2.}$$

where

SF_{ij} represents the social force of pedestrian i to j (m/s²),

RS_i represents the required personal space required by pedestrian i (m), and

d_{ij} represents the actual distance of pedestrian i to j (m)

A and B are constants of 11 m/s² and 0.77 m, respectively (Helbing and Molnar, 1995; Kretz, 2018)

The A and B values are applied only in the post-processing calculation of the pedestrian interaction indicator. They are not used to modify pedestrian behaviour within PTV Viswalk. PTV Viswalk first generates the pedestrian trajectories, and the separate social force-based calculation is then applied to the exported pedestrian positions and distances to quantify interaction intensity. This post-processing calculation follows a simpler social force formulation based on Helbing and Molnar (1995) and is not intended to reproduce PTV Viswalk's internal Social Force Model. In this study, PTV Viswalk is used as to simulate pedestrian behaviour, while the post-processing social force calculation is used as a comparative interaction indicator applied to the exported pedestrian trajectories. This separation between simulation-generated trajectories and externally calculated PLOS input indicators is common in transportation simulation. For example, previous studies have used VISSIM-generated trajectories and then calculated externally defined surrogate-safety indicators, such as time-to-collision and post-encroachment time, for scenario comparison (Gettman et al., 2008; Fan et al., 2013). Similarly, this study uses PTV Viswalk to generate trajectories and then applies a separate pedestrian interaction calculation to the intensity of interactions and changes to movements across different scenarios.

Walking direction captures the type of interaction that occurs between pedestrians based on their relative movement and direction of travel (Lam et al., 2003; Lee et al., 2005; Alhajyaseen et al., 2011; Feliciani and Nishinari, 2016). In some social force models, pedestrian direction is represented as a vector to capture both movement direction and magnitude (Helbing and Molnar, 1995; Johansson et al., 2007; Karamouzas et al., 2014). In this study, walking direction is used as a sub-indicator for pedestrian interaction and represents a scalar simplification to distinguish

between same-direction and opposite-direction pedestrian walking movements. These interactions include passing events and meeting events. Passing events can occur during uni-directional walking direction, specifically when a faster pedestrian overtakes a slower pedestrian. Meeting events occur during bi-directional walking direction, specifically as two pedestrians approach each other and meet. These two types of interactions influence pedestrian behaviour and walking experience differently (Lam et al., 2003; Lee et al., 2005; Corbetta et al., 2016). Meeting event encounters typically require greater path adjustment and awareness than passing events. By distinguishing between same-direction and opposite-direction walking movements, this sub-indicator helps represent how interaction intensity varies depending on movement direction. We used **Equation 3.3.** to quantify walking direction into binary values for same-direction and opposite-direction walking movements for each pedestrian pair, for example, pedestrian i and j (Lam et al., 2003; Alhajyaseen et al., 2011; Feliciani and Nishinari, 2016).

Equation 3.3. shows the formula for walking direction.

$$WD_{ij} = Maximum(\frac{PSD}{TP}, \frac{POD}{TP}) \quad \textbf{Equation 3.3.}$$

where

WD_{ij} represents the quantified walking direction of pedestrian i to j (i.e., uni-directional or bi-directional)

PSD represents the number of pedestrians walking in the same direction

POD represents the number of pedestrians walking in the opposite direction

TP represents the total number of pedestrians, in our case, this is 2

Walking direction is included because pedestrian interactions differ between same-direction and opposite-direction movement, and previous studies have shown that bi-directional walking movement can significantly influence walking behaviour, capacity, and movement efficiency (Lam et al., 2003; Lee et al., 2005; Alhajyaseen et al., 2011; Feliciani and Nishinari, 2016). Using **Equation 3.3.**, when a pedestrian pair is walking in the same direction, the end value is 1. Similarly, when a pedestrian pair is walking in the opposite direction, the end value is 0.5. Ultimately, we obtain the binary values 1 and 0.5 for same-direction and opposite-direction walking movements, respectively.

In this study, opposite-direction movement represents counterflow movement at the pedestrian-pair level. Therefore, the walking direction formula captures whether two pedestrians are moving in the same direction or toward one another, but it does not evaluate broader counterflow characteristics such as directional split percentages, lane formation, or capacity changes in sidewalks. Based on **Equation 3.3,** the walking direction term also acts as a scaling factor in the pedestrian interaction calculation. For uni-directional pedestrian interactions, both pedestrians are walking in the same direction. Therefore, $WD_{ij} = \frac{2}{2} = 1$, and the direction scaling factor is $\frac{1}{WD_{ij}} = 1$. For bi-directional pedestrian interactions, both pedestrians are walking in the opposite direction. Therefore, $WD_{ij} = \frac{1}{2}$, and the direction scaling factor is $\frac{1}{WD_{ij}} = 2$. The bi-directional scaling factor is therefore defined as $T_B = 2$. This gives a higher weight to bi-directional walking movement interactions because pedestrians walking toward one another generally require more movement adjustment than pedestrians walking in the same direction. Previous studies have also shown that bi-directional walking movements can significantly influence pedestrians' walking behaviour,

capacity, and movement efficiency (Lam et al., 2003; Lee et al., 2005; Alhajyaseen et al., 2011; Feliciani and Nishinari, 2016).

We combine the two sub-indicators, social force and walking direction, using multiplication, which is a commonly adopted aggregation method in composite indicator development (OECD, 2008). We combine the sub-indicators, social force and walking direction to get the pedestrian interaction for each pedestrian pair (i.e., pedestrian i and j) for a specific duration using **Equation 3.4**. This scalar formulation was created to keep the pedestrian interaction calculation practical and consistent with the proposed PLOS model classification structure. However, it does not capture the full direction and magnitude of pedestrian movement in the same way as vector-based social force models (Helbing and Molnar, 1995; Johansson et al., 2007; Karamouzas et al., 2014).

Equation 3.4. shows the formula for pedestrian interaction.

$$RM_{ij} = SF_{ij} \times \frac{1}{WD_{ij}} \qquad \textbf{Equation 3.4.}$$

where

RM_{ij} represents the pedestrian interaction of pedestrian i to j (m/s²),

SF_{ij} represents the social force of pedestrian i to j (m/s²),

WD_{ij} represents the quantified walking direction of pedestrian i to j (uni-directional or bi-directional)

Figure 3.2. summarizes the concept through a time-based representation of pedestrian interaction for passing (i.e., uni-directional walking direction) and meeting (i.e., bi-directional walking direction) events. The two circles represent the pedestrian pair i and j, and the colours represent whether a pedestrian is experiencing a social force and pedestrian interaction. A green circle

indicates that the pedestrian is experiencing a social force and pedestrian interaction, and a red circle indicates that they are not. In a passing event during a uni-directional walking direction (see **Figure 3.2a.** and **Figure 3.2b.)**, both pedestrians i and j walk in the same direction. The passing event commonly occurs when one pedestrian walks faster than another on a sidewalk.

Figure 3.2a. shows that since pedestrian i is behind pedestrian j, pedestrian i is experiencing a social force greater than 0, which we indicated by the colour green, since it is aware of pedestrian j and has a view of them in front and needs to be mindful of their movements. This means that pedestrian i may need to alter their walking direction, adjust their speed or maneuver around to avoid colliding with pedestrian j, the slower walking pedestrian, before successfully passing them. In contrast, pedestrian j is experiencing no social force, which we indicate by the colour red, since pedestrian i is behind them, meaning that they do not need to adjust their walking direction or speed to avoid pedestrian i because they are unaware of the events that are occurring behind their back.

Figure 3.2b. shows the following time-stamp where pedestrian i is now ahead of pedestrian j, highlighting that pedestrian i has a faster walking speed than pedestrian j. Once overtaking is complete in the passing event, the faster pedestrian, pedestrian i, no longer experiences any social force or pedestrian interaction, which we indicate by the colour red. However, the slower pedestrian, pedestrian j, behind now does, which we indicated by the colour green, because their view is now occupied by the faster pedestrian walking ahead. This means that pedestrian j needs to be more mindful of the movement of pedestrian i.

In a meeting event during a bi-directional walking direction (see **Figure 3.2c.** and **Figure 3.2d.)**, meeting events happen when two pedestrians are walking toward each other and they must adjust

their paths to avoid shoulder brushing or colliding with each other. **Figure 3.2c.** shows that pedestrians i and j are walking towards each other and are approaching closer to meet. Pedestrians i and j are both facing each other, and both experience a social force and pedestrian interaction greater than 0, which we indicate by the colour green, since they both may need to adjust their walking direction or speed to avoid colliding with each other. **Figure 3.2d.** shows that both pedestrians have met and are no longer facing each other. This means that neither pedestrian experiences any social force or pedestrian interaction, which we indicate by the colour red, since they no longer need to adjust their paths to avoid each other and are no longer aware of the other person and their movements.

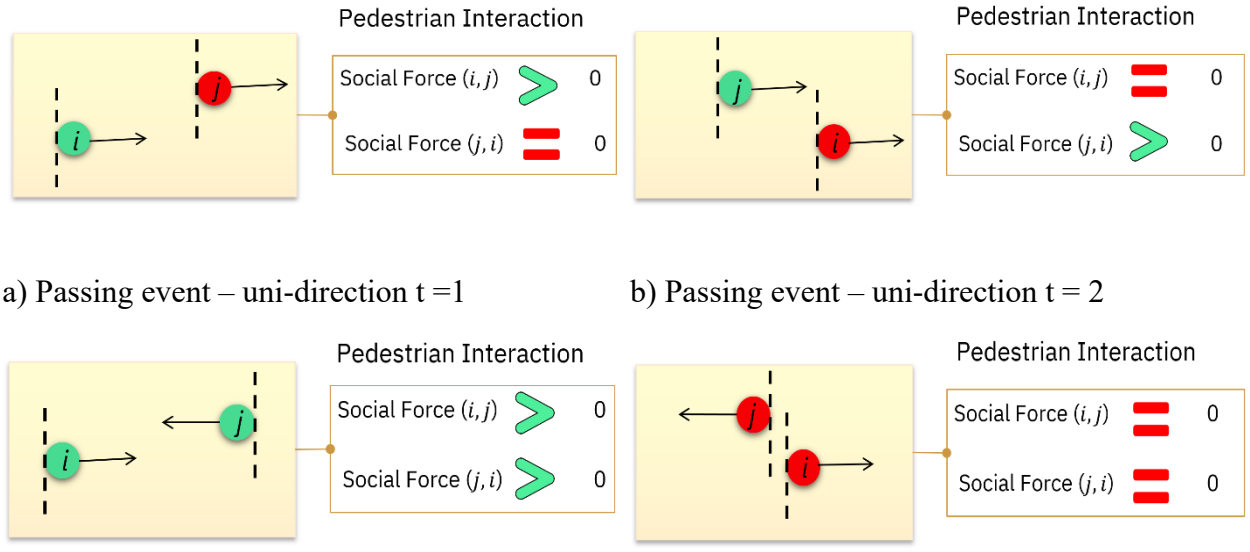

a) Passing event – uni-direction t =1 b) Passing event – uni-direction t = 2

c) Meeting event – bi-direction t = 1 d) Meeting event – bi-direction t = 2

Figure 3.2. Passing versus Meeting Event for Pedestrian Interaction

3.1.3 Calculate Aggregated Pedestrian Interaction

When more than two pedestrians are present on a sidewalk, each pedestrian has an interaction with every other pedestrian on the sidewalk (Moussaid et al., 2010; Kim et al., 2014; Feliciani and Nishinari, 2018). This results in several pedestrian pairs, each experiencing its own pedestrian interaction value at a given time. These pedestrian pair interactions occur simultaneously at any given time and also vary over time. Accounting for all pedestrian pair interactions is an important step to determine the aggregated pedestrian interaction experienced by each pedestrian at every second and over the full 15-minute simulation period that we account for and evaluate in this study.

Aggregated pedestrian interaction represents the cumulative effect of multiple pedestrian pair interactions experienced by a single pedestrian at a given time. Since a pedestrian may experience multiple pedestrian interactions due to several pedestrian pair interactions at a given time, a single aggregated pedestrian interaction value is required to represent their overall walking constraint of the sidewalk. Rather than averaging individual pedestrian interaction values, we use the aggregated pedestrian interaction value to better reflect the true restriction and conditions experienced by the pedestrian. This approach ensures that all meaningful interactions influencing walking behaviour are captured, including those that can be underestimated or lost if the average pedestrian interaction value is used.

Aggregated pedestrian interaction is a key input to our proposed PLOS model. Higher aggregated pedestrian interaction values correspond to lower PLOS levels, as pedestrians experience greater constraints on their movement. Lower PLOS levels reflect more difficult and less comfortable walking conditions. On the other hand, lower aggregated pedestrian interaction values are more commonly associated with higher PLOS levels and more comfortable pedestrian movement in

sidewalks. By incorporating aggregated pedestrian interaction, the PLOS model accounts for the cumulative impact of pedestrian pair interactions, rather than evaluating isolated interactions only.

Figure 3.3 summarizes the concept described above by illustrating each stage where there are more than two pedestrians on a sidewalk. In this example, there are four pedestrians on a sidewalk at a given time. Stage 1 shows all the pedestrian pair interactions that each pedestrian is experiencing. Stage 2 highlights the pedestrian pair interaction that pedestrian 1 is experiencing with pedestrians 2, 3, and 4 simultaneously at a given time. This creates three different pedestrian pairs, specifically with pedestrian 1-2, pedestrian 1-3, and pedestrian 1-4. Lastly, Stage 3 visualizes the aggregated pedestrian interaction for pedestrian 1 as a red bar at a given time. We use **Equation 3.4.** to calculate the pedestrian interaction for pedestrian 1, and similarly, we also calculated the pedestrian interaction for pedestrians 2, 3, and 4. Finally, we calculated the aggregated pedestrian interaction value by summing all of the pedestrian interaction for pedestrians 1, 2, 3, and 4. The aggregated pedestrian interaction accounts for every pedestrian pair interaction for all the pedestrians present on the sidewalk at a given time.

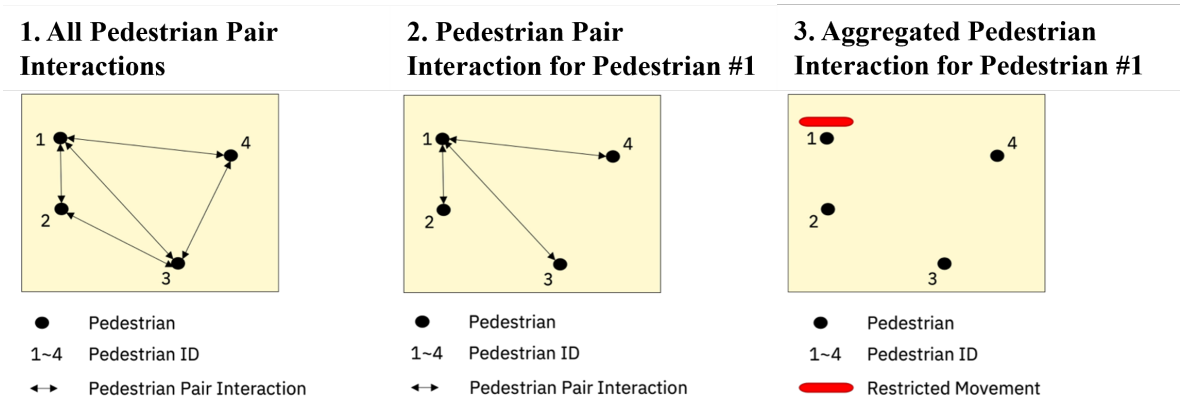

Figure 3.3. Identifying Aggregated Pedestrian Interaction

3.1.4 Develop Heat Map

Heat maps are a type of visualization that uses colour to show how values change across an area (Lv and Hu, 2020; Choi et al., 2025). In this study, we create heat maps to show how aggregated pedestrian interaction varies across space and time within the study area. By presenting these variations visually, heat maps help identify locations where pedestrians experience higher or lower levels of pedestrian interaction and PLOS along the sidewalk.

We create the heat maps for this study using a four-step approach. First, we calculate the pedestrian interaction value for each pedestrian pair for every second of the microsimulation period, using the pedestrian position (x,y,z) extracted from the 2D microsimulation model. To plot the heat map, we only keep pedestrian pair interactions where pedestrians are in close proximity to each other (i.e., within the distance threshold used in the model of 0.68) and the pedestrian interaction value is greater than zero. The distance threshold of 0.68 m used for heat map generation is based on pedestrian personal space findings reported in the Pedestrian Level of Service Study, Phase 1 (New York, 2008), which identifies minimum desirable occupancies of approximately 0.5–1 m² per pedestrian. The midpoint value of this range is used to represent close-proximity pedestrian pair interactions where pedestrians are likely to experience pedestrian interaction. The recorded (x,y,z) position corresponds to the pedestrian who is experiencing pedestrian interaction at that specific time (i.e., the pedestrian assigned a non-zero pedestrian interaction value). Second, we treat the aggregated pedestrian interaction values as weights, and we attach them to their recorded positions (x,y,z). Third, this process is repeated for every second over the full 15-minute microsimulation duration, which produces a collection of weighted points that represent where the pedestrian interaction occurs over time. Lastly, because pedestrian positions are continuous, the weighted points used to create the heat map do not need to have exactly identical (x,y,z) coordinates. Nearby

positions are grouped, and we combine and scale the pedestrian interaction values relative to the highest value we observe. This allows the heat map to show colours that effectively illustrate areas with lower and higher levels of pedestrian interaction and PLOS along the sidewalk.

This process produces a visual heat map that highlights areas with higher and lower levels of pedestrian interaction and PLOS. Higher values indicate locations where pedestrian pair interactions occur more frequently or where pedestrians need to adjust their paths more noticeably. Overall, the heat maps make it easier to observe where pedestrian interaction tends to concentrate and where pedestrians have more available space, providing a clearer picture of how pedestrian movement patterns emerge and evolve along the sidewalk when different alternative scenarios come into play.

3.2 Process to Design 2D Microsimulation Model and 3D Visualization

This section describes the study area, the development of the 2D microsimulation model using PTV Viswalk, and the development of the 3D visualization using Unity.

3.2.1 Case Study Area

The study area is a sidewalk at York University in Toronto, Ontario, Canada, commonly referred to as York Lanes. The sidewalk dimensions are approximately 72 m in length and 3 m in width. Adjustments are made to account for physical features such as seating and stairs along the sidewalk to determine the effective walking width available to pedestrians. York Lanes serves as a key pedestrian connection between the university's central shopping area, which includes a bookstore, drugstore, medical offices, and several fast-food restaurants, and the main academic buildings on

campus. The sidewalk is used throughout the day by students, faculty, and staff, with pedestrian activity increasing during peak periods such as class changes and meal times. These conditions create frequent pedestrian pair interactions and variations in movement patterns, making the study area well-suited for evaluating pedestrian space, pedestrian interaction, and the novel PLOS model.

Figure 3.4. illustrates the study area used in this study. **Figure 3.4a.** shows the study area through the camera monitoring system and represents real-world conditions. **Figure 3.4b.** shows the 2D microsimulation model for the study area using PTV Viswalk. **Figure 3.4c.** shows the 3D visualization using Unity.

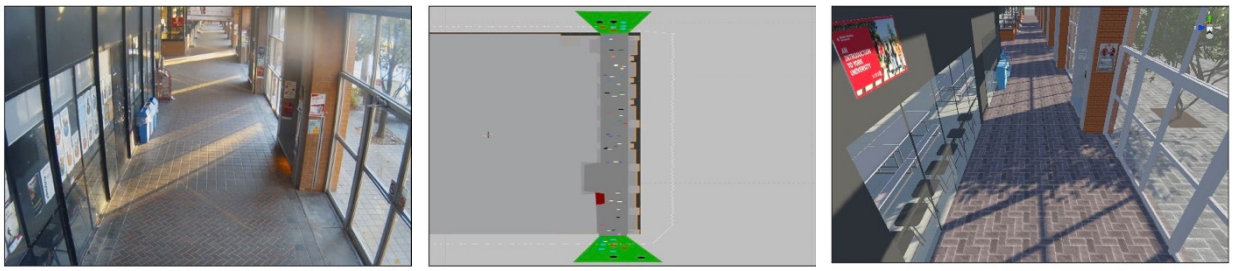

a) Camera Monitoring System | b) Development of 2D Microsimulation | c) Development of 3D Visualization

Figure 3.4. Study Area

3.2.2 Develop a 2D Microsimulation Model and 3D Visualization

We use PTV Viswalk to create 2D microsimulation models of the study area. The simulation includes a 15-minute warm-up period to allow pedestrian flows to stabilize, followed by a 15-minute data collection period, which we use for the analysis of pedestrian space, pedestrian interaction, and PLOS. The 2D microsimulation model provides us with important pedestrian data, including pedestrian trajectory data, walking speeds, and pedestrian volumes (Hoogendoorn et al.,

2003; Boltes et al., 2010). These outputs serve as the primary input data for calculating pedestrian space and pedestrian interaction, and they form the basis for subsequent visualization and analysis in the 3D visualization using Unity. Therefore, the 2D microsimulation outputs form the basis of the proposed PLOS calculation, while the 3D visualization supports the interpretation and communication of the results.

PTV Viswalk uses a social-force based walking behaviour model to generate pedestrian movement and trajectory outputs. The model includes interaction components that have been discussed and calibrated in previous Social Force Model studies, including circular or isotropic interaction components and velocity-dependent interaction components (Johansson et al., 2007; Kretz et al., 2008; Kretz et al., 2018). In this study, the internal walking-behaviour parameters in PTV Viswalk were not modified between scenarios. The same unmodified PTV Viswalk settings were applied to all microsimulation models for all scenarios because site-specific pedestrian trajectory data for the study area were not available to support separate model calibration. Changing these parameters without empirical calibration data could introduce additional assumptions and uncertainty into the simulation (Johansson et al., 2007; Kretz et al., 2008; Kretz et al., 2018).

We use Unity to develop a 3D visualization that replicates the real-world surveillance perspective of the study area. The 3D environment completely aligns with the same sidewalk geometry, dimensions and design layout used for the study area in the 2D microsimulation in PTV Viswalk. This allows pedestrian movements and interactions to be viewed from a camera-based monitoring perspective and as an accurate representation for comparison. In addition to 3D visualization, Unity enables the tracking and calculation of pedestrian space and pedestrian interaction on a second-by-second basis that is not feasible through the 2D microsimulation from PTV Viswalk. It also supports the computation of aggregated pedestrian interaction for all pedestrian pairs during

the 15-minute simulation period. Unity also supports the calculation and visualization of pedestrian space, pedestrian interaction, and heat map outputs (Lv and Hu, 2020; Abu Alatta and Momani, 2021; Choi et al., 2025). The 3D visualization adds value by helping interpret pedestrian interaction patterns and areas where pedestrian interaction is concentrated when evaluating the PLOS of sidewalks. It also helps present the results in a way that connects the numerical PLOS outputs with observable pedestrian movement behaviour that are easily interpretable (Abu Alatta and Momani, 2021).

3.3 Process to Develop PLOS Model

This section outlines the methodology used to develop the novel PLOS model, which integrates pedestrian space and pedestrian interaction as input indicators to evaluate sidewalks. The PLOS model builds on the traditional framework by introducing a second indicator and refining each PLOS level into subcategories. The development process consists of defining PLOS categories, generating microsimulation model scenarios, quantifying pedestrian interaction, analyzing statistical distributions, and establishing threshold boundaries for PLOS classification. Each step is designed to ensure that the PLOS model captures both the availability of walking space and the intensity of pedestrian interactions consistently and accurately.

3.3.1 Develop Three Categories for Each PLOS

The development of the PLOS model begins by adopting pedestrian space thresholds from the Highway Capacity Manual, as presented in **Table 2.2.**to define six PLOS levels, ranging from A to F (HCM, 2010). Each level is further divided into three subcategories, denoted as “-”, “0”, and “+”, to represent varying walking conditions within the same PLOS level. The “-” category represents more constrained conditions, the “0” category represents average conditions, and the

"+" category reflects more comfortable conditions. Representative pedestrian space values are then randomly selected within each PLOS category and used as inputs for the 2D microsimulation models. This structured classification allows the PLOS model to maintain consistency with established standards while incorporating additional detail through a second input indicator.

Creating separate 2D microsimulation models for uni-directional and bi-directional walking directions accounts in PTV Viswalk allows the PLOS model to account for differences in pedestrian interaction types for both walking directions. For each randomly selected pedestrian space value, corresponding microsimulation models are created for both walking directions across all PLOS categories. The microsimulation parameters include an average desired walking speed of 1.3 m/s, while individual pedestrian speeds are allowed to vary within a defined range to reflect realistic behaviour (TRB, 2020). The microsimulation models generate detailed trajectory data, including (x,y,z) coordinates for each pedestrian at each time step. These trajectory data provide the foundation for calculating pedestrian interaction and enable a detailed assessment of pedestrian interactions under different walking conditions.

Pedestrian interaction is calculated for each pedestrian pair based on their proximity and walking direction and then aggregated to represent the overall level of interaction within the sidewalk at each second of the 15-minute data collection period. The pedestrian interaction values for all pedestrian pairs present are added at a given time. Data collection begins after a 900-second warm-up period to ensure stable pedestrian conditions, with analysis conducted over the subsequent simulation period from 901 to 1800 seconds. Through this, we can calculate the aggregated pedestrian interaction for each pedestrian for each second that we start collecting data. The use of second-by-second aggregated pedestrian interaction for each pedestrian allows for a detailed

representation of pedestrian interactions and ensures that short-term changes are preserved in the dataset.

The next step is to conduct a correlation test to examine the relationship between pedestrian space and pedestrian interaction to support the PLOS model development. This step is important when introducing a second indicator to ensure that it provides additional information rather than duplicating the first indicator. In this study, the first input indicator, pedestrian space, is calculated over the 15-minute data collection period using an area-based method where the (i.e., the total area is divided by the pedestrian volume in each second). The second input indicator, pedestrian interaction, is calculated every second using **Equation 3.4.** As a result, the two indicators capture distinct aspects of pedestrian behaviour, and the correlation test is used as an initial check to examine whether pedestrian interaction provides complementary information for the PLOS model. This correlation analysis is not used as the only justification for the second indicator; rather, it supports the broader model development process along with the within-level variation in pedestrian interaction values.

The distribution of aggregated pedestrian interaction values is then analyzed using statistical methods, including histograms and probability density functions for uni-directional and bi-directional walking movements. Histograms are generated to visualize how pedestrian interaction values are distributed over time for each microsimulation scenario. To improve clarity and enable comparison across all microsimulation scenarios, probability density functions are developed using the Kernel Density Estimation (Chen, 2017; Węglarczyk, 2018). This approach produces smooth curves that represent the distribution of pedestrian interaction values and allows multiple scenarios to be compared without the limitations of overlapping histograms. MATLAB is used to generate both the histograms and the probability density functions for all microsimulation outputs.

3.3.2 Identify PLOS Model Thresholds and Boundary Values

The next step is to develop box plots to further identify the thresholds and boundaries of the PLOS model by summarizing the distribution of pedestrian interaction values, including the minimum, first quartile, median, third quartile, and maximum. These plots provide insight into the variability of the dataset and help identify the range of values associated with different PLOS conditions. In addition, cumulative distribution functions are used to determine percentile-based thresholds. Specifically, the 33rd and 67th percentiles are identified as cutoff points to divide each PLOS level into the three subcategories. These percentile thresholds provide a consistent and data-driven method for defining the boundaries between "-", "0", and "+" classifications within each PLOS level of the novel model.

3.3.3 New PLOS Model

Finally, the proposed PLOS model is developed by integrating pedestrian space and pedestrian interaction into a unified PLOS framework. Pedestrian space defines the first input indicator of the PLOS model based on established thresholds from the HCM for each PLOS level (TRB, 2020). Pedestrian interaction defines the second input indicator that divides each PLOS level into the three subcategories (-/0/+). The combination of these two indicators allows the PLOS model to capture variations in pedestrian interactions that are not reflected by pedestrian space alone. This results in a more detailed and practical classification system that can represent differences in walking conditions within the same PLOS level while maintaining consistency with established standards.

3.4 Process to Apply New PLOS Model

This section describes the general process used to apply the novel PLOS model to the selected study area. After developing the input indicators and establishing the PLOS model thresholds, the next step is to test the model using a Base Scenario and a set of Alternative Scenarios. The Base Scenario represents the existing sidewalk conditions of the case study area, while the Alternative Scenarios represent changes to the design layout or surface elements of the same sidewalk. This approach allows the proposed model to evaluate how different sidewalk modifications affect pedestrian space, pedestrian interaction, and the resulting PLOS.

Before applying the PLOS model, consistent input parameters are defined for all scenarios. These include the target pedestrian space, corresponding pedestrian volume, and average desired walking speed. Keeping these parameters consistent ensures that any changes in the resulting pedestrian space, pedestrian interaction and PLOS analysis are mainly caused by the design modifications introduced in each scenario, rather than differences in pedestrian demand or walking speed assumptions. The same simulation duration is also applied to all scenarios so that the results can be compared on a minute-by-minute basis and over the full 15-minute microsimulation period.

For each scenario, a 2D microsimulation model is developed in PTV Viswalk to generate pedestrian trajectory data, including pedestrian coordinates and walking speeds. These outputs are then transferred into Unity to support 3D visualization and to calculate pedestrian space and pedestrian interaction throughout the simulation period. The proposed PLOS model is applied by first identifying the PLOS level based on the first input indicator, pedestrian space and then refining the classification using the second input indicator, pedestrian interaction. This produces

both minute-by-minute PLOS classifications and an overall PLOS for the Base Scenario and Alternative Scenario for evaluation and comparison.

The results from each Alternative Scenario are then compared with the Base Scenario to determine how the design modification affects sidewalk performance. Alternative Scenarios that reduce pedestrian interaction indicate improved PLOS and walking conditions, while scenarios that increase pedestrian interaction indicate more constrained PLOS and pedestrian movement. Heat maps are also generated to support the interpretation of the numerical results by showing where pedestrian interaction is concentrated across the sidewalk. This process allows the novel PLOS model to be applied as a practical evaluation tool for comparing existing and modified sidewalk conditions.

3.5 Chapter Summary

Chapter 3 presented the methodology used to develop the proposed PLOS model. The chapter first introduced the overall research framework, which includes developing input indicators, creating 2D and 3D microsimulation models, developing the proposed PLOS model, and applying the model to base and alternative scenarios. This framework was designed to evaluate sidewalk performance using both available walking space and pedestrian interactions.

The chapter then described the development of the two main input indicators: pedestrian space and pedestrian interaction. Pedestrian space was used as the first input indicator. At the same time, pedestrian interaction was developed to capture pedestrian interactions that occur when individuals adjust their paths, speeds, or directions in response to others. Pedestrian interaction was calculated using social force and walking direction, then aggregated to account for multiple pedestrian pair interactions occurring at the same time.

This chapter also introduced the study area, simulation environment, and methodology to develop the new PLOS model and heat map. The York Lanes sidewalk at York University was selected as the case study area, and PTV Viswalk was used to generate pedestrian trajectory data, walking speeds, and pedestrian volumes. Unity was used to support 3D visualization and calculate pedestrian interaction outputs. It outlines how pedestrian space thresholds, pedestrian interaction distributions, and percentile-based boundaries were used to develop the proposed PLOS model.

Finally, **Chapter 3** described the general process for applying the proposed PLOS model. The model is applied by first defining a Base Scenario that represents existing conditions and then comparing it with Alternative Scenarios that modify the sidewalk design layout or surface elements. Consistent input parameters, including pedestrian space, pedestrian volume, and walking speed, are used across all scenarios so that differences in PLOS can be attributed to the design changes being tested.

Overall, **Chapter 3** provides the methodology framework for the study by connecting input indicator development, 2D microsimulation and 3D visualization, PLOS model development and application into a structured framework. These methodological steps allow the novel PLOS model to be tested in later chapters and help determine whether it can capture walking conditions that traditional PLOS approaches may overlook.

Chapter 4. Develop PLOS Model

Chapter 4 presents the quantitative results that we obtained to develop the new PLOS model based on the methodology outlined in **Chapter 3**. While **Section 3.3** describes the procedures for calculating input indicators pedestrian space and pedestrian interaction and generating data from microsimulation models to create the new PLOS model and apply it to the case study area, this chapter focuses on the numerical outcomes of that process. The analysis examines how pedestrian interaction varies across PLOS levels, walking directions, and subcategories, and identifies the threshold values used to define the proposed PLOS framework.

4.1 Develop Three Categories for Each PLOS

We develop a PLOS model with six levels, ranging from LOS A to LOS F (HCM, 2000; HCM, 2016; TRB, 2020). We use the HCM PLOS thresholds for LOS A to F based on pedestrian space, as outlined in HCM's PLOS Threshold for Sidewalks in **Table 2.2** (HCM, 2000; HCM, 2016; TRB, 2020). Each PLOS level is further divided into three categories, specifically (-/0/+) (City of London, 2010; Finch et al., 2010). We evenly divide each PLOS level into the three categories to find the thresholds for pedestrian interaction. The first PLOS category "-" is meant to represent the worst walking condition in the same PLOS level, followed by the second category "0", and the third category "+" which represents the better walking condition. Then, we randomly select a pedestrian space value in each category. We use these pedestrian space values as the inputs to create the 2D microsimulation models using PTV Viswalk, for both uni-directional and bi-directional walking directions.

Figure 4.1. illustrates the process used to define the categories for PLOS A to E for the study area. In **Figure 4.1a.**, PLOS A is defined by pedestrian space being greater than 5.6 m^2/ped based

on **Table 2.2**. To establish representative subcategories within PLOS A, an upper limit of 108 m^2/ped was calculated to represent the lowest pedestrian space conditions within the microsimulation environment by selecting 2 pedestrians in the study area. With the study area having a length of 72 m and a width of 3 m, this provides a total area of 216 m^2, and a maximum pedestrian space of 108 m^2 for 2 pedestrians. In **Figure 4.1b.**, The range between 5.6 m^2/ped and 108 m^2/ped was then divided into three equal intervals of 34.1 m^2/ped to define the three PLOS A subcategories (-/0/+). As a result, the first category ranges from 5.6 m^2/ped to 39.5 m^2/ped, the second category ranges from 39.5 m^2/ped to 73.4 m^2/ped, and the third category ranges from 73.4 m^2/ped to 108 m^2/ped for PLOS A. In **Figure 4.1c.**, representative pedestrian space values were then randomly generated within each interval using the "Random" function in Microsoft Excel and used as inputs for the 2D microsimulation models. The randomly generated pedestrian space values for the first PLOS A category "-" is 9.7 m^2/ped, the second PLOS A category "0" is 41.4 m^2/ped, and the third category "+" is 83.5 m^2/ped. The same procedure was repeated for all PLOS levels from B to E to generate pedestrian space values and corresponding microsimulation models. PLOS F was excluded from the calibration process because it represents breakdown conditions associated with extremely limited pedestrian movement and pedestrian space values below 1.80 m^2/ped. Since the proposed PLOS framework focuses on typical pedestrian operating conditions rather than over capacity walking situations, PLOS F was not included in the model development process. Each randomly generated pedestrian space value produces 1,800 rows of datasets.

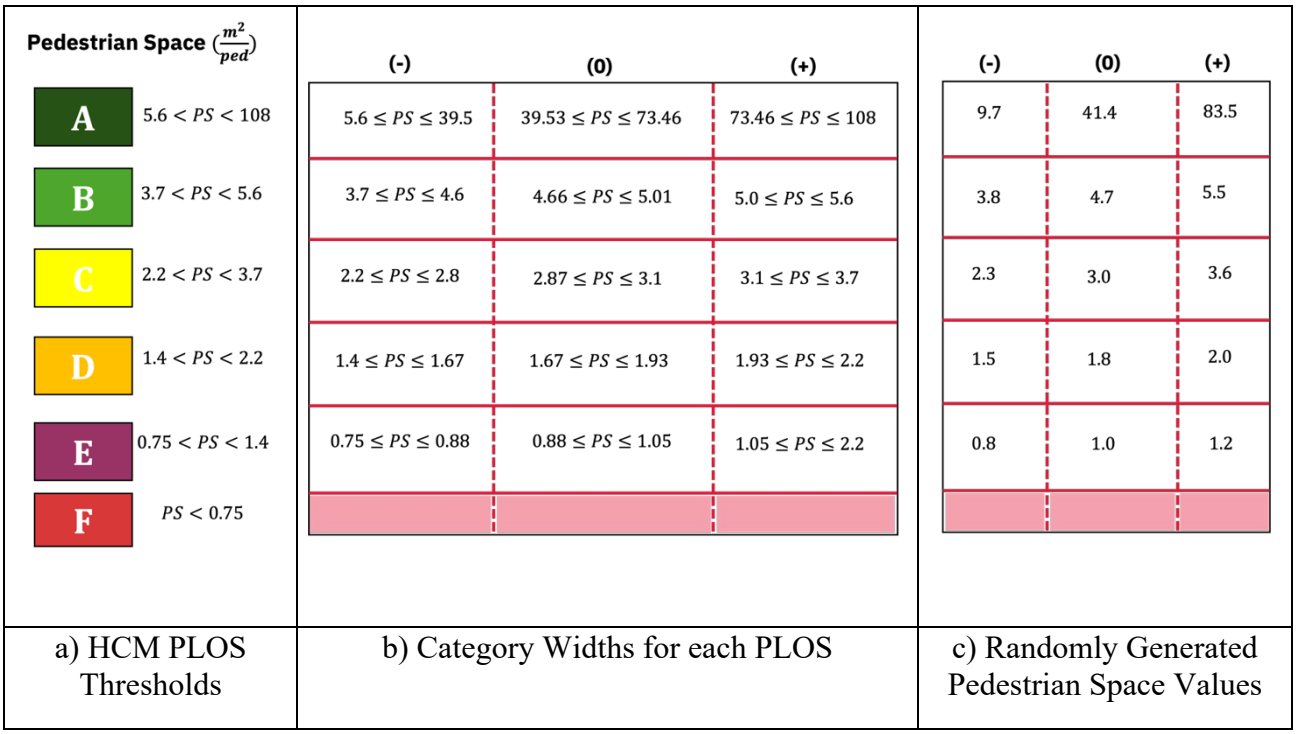

a) HCM PLOS Thresholds

b) Category Widths for each PLOS

c) Randomly Generated Pedestrian Space Values

Figure 4.1. Data Sampling Process for Model Calibration

We use the randomly generated pedestrian space in each category to develop uni-directional and bi-directional walking direction pedestrian 2D microsimulation models in PTV Viswalk. Each microsimulation model was generated using the selected pedestrian space. We also inversely calculated the pedestrian volume per hour for each of the 2D microsimulation models. Therefore, we create uni-directional and bi-directional walking direction models for each randomly selected pedestrian space value for each of PLOS A+, A0, A-, B+, B0, B-, C+, C0, C-. D+, D0, D-, E+, E0, E-. This yields 30 micro-simulation models, with a 15-minute warm-up period and a 15-minute running period.

The parameters of the 2D microsimulation model in PTV Viswalk include an average desired walking speed of 1.3 m/s, although the model was set so that individual pedestrian walking speeds can vary within a defined range, for example, 0.8 to 1.8 m/s (TRB, 2020) as discussed in **Section**

3.3. This creates more realistic movements by preventing all pedestrians from walking at the same walking speed while keeping the overall speeds centred around the average value. In the analysis, we extracted the trajectory data (i.e., x-y-z coordinates) for each pedestrian's second-by-second movement along the simulated sidewalk. The microsimulation models produce 27,000 raw data sets in total (i.e., 15-min × 60-sec x 30 simulations). This equates to 5,400 rows of datasets per PLOS level.

The next step is to evaluate the difference in the pedestrian interaction that pedestrians experience for uni-directional and bi-directional walking direction within the different categories (-/0/+) in the same PLOS level and within different PLOS levels (i.e., A-E). To do this, we need to find the aggregated pedestrian interaction per second by adding the pedestrian interaction for each pedestrian pair within the sidewalk at a given time. The aggregated pedestrian interaction is important because it is a key value when developing the new PLOS model. We collect the pedestrian interaction data for each pedestrian pair starting from 901 seconds, because this is when the 900-second running period begins, following the 900-second warm-up period.

Figure 4.2. below shows a sample of the partial raw dataset from the microsimulation of a bi-directional walking direction for PLOS C. This uses the randomly generated pedestrian space value of 2.3 as shown in **Figure 4.1c**. We conduct a similar process for other PLOS levels B-E. This shows the aggregated pedestrian interaction for the initial pedestrian pairs for pedestrian number 925 for the first second after the 900s warm-up period. The first column shows the time in seconds that we collect the data. For this example, it only captures the raw dataset at 901 seconds. The second column shows the aggregated pedestrian interaction that we calculate for each second. For this example, the aggregated pedestrian interaction for all the pedestrian pairs for pedestrian number 925 in the sidewalk at 901 seconds is 446.09, and we calculate this by aggregating the

pedestrian interaction value for every pedestrian pair interaction for number 925 in the sidewalk at the time of 901 second of the microsimulation period. The third column shows the ID of the respective pedestrian pair that was present in the sidewalk during that second. The fourth and fifth column shows the (x,y,z) coordinates for each pedestrian pair. The sixth column shows the distance between the pedestrian pair. The seventh column shows the social force calculated using **Equation 3.2.** for each pedestrian pair. The eighth column is a binary value of either 0.5 or 1, representing whether the pedestrian pair's walking direction is either bi-directional or uni-directional, respectively. Lastly, the ninth column shows the second indicator, pedestrian interaction for each pedestrian pair by combining the sub-indicators, social force and walking direction, from the seventh and eighth columns, respectively.

Time (Seconds)	Aggregated Pedestrian Interaction	Pedestrian Pair	Ped A Position	Ped B Position	Distance	Social Force	Walking Direction	Restricted Movement
901	446.09	925-927	(1.9, 0.0, 0.8)	(9.2, 0.0, 0.4)	7.31	1.71E-04	1	1.71E-04
901		925-930	(1.9, 0.0, 0.8)	(15.5, 0.0, 0.8)	13.61	1.21E-08	1	1.21E-08
901		925-937	(1.9, 0.0, 0.8)	(70.0, 0.0, 0.2)	68.19	1.49E-44	0.5	2.98E-44
901		925-938	(1.9, 0.0, 0.8)	(14.2, 0.0, 0.4)	12.36	8.05E-08	1	8.05E-08
901		925-942	(1.9, 0.0, 0.8)	(17.2, 0.0, 0.9)	15.36	8.57E-10	1	8.57E-10
901		925-944	(1.9, 0.0, 0.8)	(66.8, 0.0, 0.7)	64.95	2.02E-42	0.5	4.05E-42
901		925-947	(1.9, 0.0, 0.8)	(65.5, 0.0, 0.8)	63.6	1.55E-41	0.1	3.11E-41
901		925-948	(1.9, 0.0, 0.8)	(14.8, 0.0, 2.6)	13.02	2.99E-08	1	2.99E-08
901		925-949	(1.9, 0.0, 0.8)	(9.6, 0.0, 2.6)	7.89	7.04E-05	1	7.04E-05
901		925-950	(1.9, 0.0, 0.8)	(27.5, 0.0, 0.5)	25.65	1.46E-16	1	1.46E-16
901		925-953	(1.9, 0.0, 0.8)	(37.2, 0.0, 0.3)	35.31	6.44E-23	1	6.44E-23
901		925-954	(1.9, 0.0, 0.8)	(18.8, 0.0, 1.1)	16.92	8.04E-11	1	8.04E-11
901		925-957	(1.9, 0.0, 0.8)	(4.2, 0.0, 2.5)	2.86	1.45E-01	1	1.45E-01
901		925-958	(1.9, 0.0, 0.8)	(69.9, 0.0, 1.0)	68.08	1.76E-44	0.5	3.53E-44
901		925-959	(1.9, 0.0, 0.8)	(62.6, 0.0, 0.7)	60.76	1.15E-39	0.5	2.30E-39
901		925-962	(1.9, 0.0, 0.8)	(72.8, 0.0, 0.6)	70.97	2.18E-46	0.5	4.37E-46
901		925-963	(1.9, 0.0, 0.8)	(19.5, 0.0, 1.2)	17.63	2.77E-11	1	2.77E-11
901		925-964	(1.9, 0.0, 0.8)	(7.5, 0.0, 2.6)	5.88	1.49E-03	1	1.49E-03
901		925-966	(1.9, 0.0, 0.8)	(10.1, 0.0, 0.4)	8.28	3.91E-05	1	3.91E-05
901		925-967	(1.9, 0.0, 0.8)	(26.6, 0.0, 1.3)	24.75	5.73E-16	1	5.73E-16
901		925-968	(1.9, 0.0, 0.8)	(31.1, 0.0, 1.7)	29.21	6.61E-19	1	6.61E-19
901		925-969	(1.9, 0.0, 0.8)	(16.3, 0.0, 2.2)	14.49	3.19E-09	1	3.19E-09
901		925-970	(1.9, 0.0, 0.8)	(61.7, 0.0, 0.6)	59.82	4.79E-39	0.5	9.58E-39
901		925-971	(1.9, 0.0, 0.8)	(40.8, 0.0, 2.2)	39	2.39E-25	0.5	4.78E-25
901		925-972	(1.9, 0.0, 0.8)	(17.1, 0.0, 2.1)	15.32	9.07E-10	1	9.07E-10
901		925-973	(1.9, 0.0, 0.8)	(52.4, 0.0, 1.3)	50.59	5.66E-33	0.5	1.13E-32

Figure 4.2. Raw Dataset Calibration Results for the 1st Second (901 seconds) for PLOS C

Figure 4.3 presents the aggregated pedestrian interaction values from 901 to 925 seconds for all pedestrians under both uni-directional and bi-directional walking directions for PLOS C**.** The values shown are based on three randomly generated pedestrian space values within PLOS C, 2.3,

3.0, and 3.6 m²/ped as shown in **Figure 4.1c**,**.** These values represent the three subcategories within PLOS C, where lower pedestrian space corresponds to more constrained conditions and higher pedestrian space corresponds to less constrained walking conditions. For both walking directions, the aggregated pedestrian interaction decreases as pedestrian space increases. For example, at 901 seconds, the uni-directional pedestrian interaction decreases from 310.36 at 2.3 m²/ped, to 281.40 at 3.0 m²/ped, and to 218.28 at 3.6 m²/ped.

A similar pattern is observed for the bi-directional walking direction, where pedestrian interaction decreases from 446.09, to 394.35, and to 310.80 for the same pedestrian space values. This indicates that greater pedestrian space generally reduces the level of pedestrian interaction experienced by pedestrians. This confirms how pedestrian interaction varies across pedestrian space values and walking directions within the same PLOS level. The results support the need to subdivide each PLOS level into "-", "0", and "+" categories, since pedestrian conditions can differ even when they remain within the same overall PLOS range.

	Uni-directional				Bi-directional		
Time (s)	2.3	3.0	3.6		2.3	3.0	3.6
901	310.36	281.40	218.28		446.09	394.35	310.80
902	301.36	280.63	213.99		423.08	375.96	296.60
903	297.35	278.23	213.55		422.73	371.27	270.03
904	290.74	272.07	205.88		421.07	364.72	262.68
905	287.60	270.51	205.54		419.64	363.00	259.92
906	285.51	268.90	203.67		415.99	361.92	256.11
907	284.96	264.91	202.91		409.94	353.33	255.57
908	281.61	264.79	202.44		403.90	352.57	254.78
909	280.08	264.49	201.25		403.12	347.58	253.17
910	280.04	263.58	200.64		397.12	346.56	252.57
911	278.69	263.44	199.61		393.60	342.17	252.51
912	274.25	260.21	199.51		392.41	340.10	251.93
913	270.80	259.52	198.91		390.62	337.23	251.88
914	269.16	258.54	198.68		379.27	335.79	250.25
915	268.36	257.44	197.65		376.46	335.19	248.58
916	267.48	254.41	196.17		376.18	335.07	248.39
917	267.10	253.60	196.06		373.65	333.68	246.51
918	266.88	249.77	195.81		372.61	333.52	245.53
919	266.59	248.23	195.62		370.78	332.45	244.11
920	265.63	248.01	194.61		370.62	328.90	243.18
921	265.53	247.72	194.56		368.85	326.68	241.26
922	264.16	247.68	194.08		365.96	326.14	234.86
923	264.07	247.05	193.29		364.77	325.86	231.61
924	262.69	246.82	192.96		362.75	325.75	227.75
925	260.61	246.42	192.58		356.32	325.57	227.35

Figure 4.3. Model Development Calibration Results for 901-925 seconds for LOS C

A correlation test is usually performed when introducing a second indicator (i.e., pedestrian interaction) to verify that the second indicator is not redundant to the first indicator (i.e., pedestrian space) (OECD, 2008; Saisana et al., 2005; Greco et al., 2019). In our study, the correlation test was conducted to confirm whether pedestrian space and pedestrian interaction capture similar or different aspects of pedestrian walking conditions. For this analysis, the first input indicator, pedestrian space, is calculated for each second of the 15 minute analysis period, while the second input indicator, pedestrian interaction, is calculated every second. However, we calculated

pedestrian space in each second using a different formula than the formula proposed by HCM, which is called an area-based method (i.e., the total area is divided by the pedestrian volume in each second) (HCM, 2000; HCM, 2016). This provides a distinct value for both indicators in each second. The pooled result from calculating the correlation between the two indicators is -0.28. This weak negative correlation indicates that pedestrian interaction is not strongly related to pedestrian space across the pooled dataset and is therefore not fully redundant to the first indicator. It also shows that there is a negative correlation between the two indicators, meaning that they have an inverse relationship. This provides an initial descriptive check supporting the use of pedestrian interaction as a second indicator because it captures effects of movement adjustments and constraints that are not fully represented by available walking space alone. However, the pooled correlation value is not used as the only justification for the second indicator because it combines all PLOS levels and walking-direction conditions.

An additional level-specific correlation analysis was conducted. The results show that the relationship between pedestrian space and pedestrian interaction is not uniform across PLOS levels, as shown in **Table 4.1**. All correlation coefficients are negative, indicating that pedestrian interaction generally increases as pedestrian space decreases. However, the strength of this relationship differs substantially between PLOS levels and does not increase consistently with the degree of constraint. For PLOS A, B, and C, the correlations are weak to moderate and show no consistent ordering, ranging from -0.510 to -0.010 for uni-directional movement and from -0.539 to -0.348 for bi-directional movement. Each coefficient is calculated from second-by-second observations obtained from three pedestrian space values per PLOS level, so small differences between these levels may reflect sampling variability rather than a whole systematic effect. The near-zero value for PLOS B under uni-directional movement is interpreted in this context and is

not treated as evidence of a distinct behavioural pattern. For PLOS D and E, the correlations are consistently strong, ranging from -0.835 to -0.961, indicating that pedestrian interaction becomes largely determined by available pedestrian space once spacing between pedestrians is severely constrained. Therefore, the level-specific correlation results are interpreted together with the fixed-pedestrian-space analysis to show whether pedestrian interaction varies enough within the same pedestrian space range to support the - / 0 / + subcategories.

These differences are relevant to how the proposed PLOS model would be applied in practice. Sidewalk design guidance commonly identifies PLOS C as the minimum acceptable operating condition for pedestrian facilities, specifically in sidewalks (New York City, 2006; City of London, 2010; TRB, 2020; City of Brampton, 2022; Hong Kong Transportation Department, 2023). Within this design-relevant range of PLOS A to C, pedestrian space and pedestrian interaction are only weakly to moderately correlated, which indicates that pedestrian interaction captures movements and effects that pedestrian space does not represent. Two sidewalk configurations with comparable pedestrian space may therefore produce different walking conditions, and the proposed model is able to distinguish between them. At PLOS D and E, pedestrian interaction is closely related to pedestrian space and provides limited additional information. This has minimal practical consequence, because sidewalks operating at these levels already fall below common design targets and would be identified as requiring intervention on the basis of pedestrian space alone. Pedestrian interaction is therefore most informative in the range where sidewalk design and operational decisions are actually made, which supports its inclusion as a second input indicator in the proposed PLOS model.

Table 4.1. Additional Correlation Analysis Between Pedestrian Space and Pedestrian Interaction by PLOS Level and Walking direction

PLOS Level	Uni-directional Walking Movement (100-0)	Bi-directional Walking Movement (50-50)
A	-0.510	-0.539
B	-0.010	-0.348
C	-0.410	-0.437
D	-0.835	-0.914
E	-0.961	-0.944

We then process the raw datasets per microsimulation to calculate the aggregated pedestrian interaction for every pedestrian pair interaction per second for every 15-minute running period. We use the aggregated pedestrian interaction for each second to create the histogram and probability density function (smoothed version of the histogram). We do this for each of the uni-directional walking direction and bi-directional walking direction microsimulation models for each pedestrian space value from each category within a PLOS level. This is important because it allows us to compare the maximum and minimum aggregated pedestrian interaction values between the categories (-/0/+) for each PLOS level. This is useful when identifying how pedestrian interaction differs for uni-directional walking direction and bi-directional walking direction in different categories (i.e., (-/0/+)) in the same PLOS level (i.e., A-E) and how pedestrian interaction differs for uni-directional and bi-directional walking direction for each PLOS level. **Figure 4.4. to Figure 4.8.** shows histograms and a smoothed version of the histogram (i.e., probability density function) for 30 microsimulation models (from A+ to E- in both uni and bi-directional walking direction). The probability density function allows an easy comparison by overlaying multiple shapes, while overlapping histograms can be messy and not easily understandable. We used the most common of producing probability density functions, which is the KDE (Chen, 2017; Węglarczyk, 2018).

We use the MATLAB software to create the histograms and probability density function (Higham and Higham, 2016). The outputs show how aggregated pedestrian interaction values are spread out across time for uni-directional and bi-directional walking directions (Chen, 2017; Węglarczyk, 2018). In **Figure 4.4. to Figure 4.8.,** the horizontal axis shows the bins for pedestrian interaction and the vertical axis shows the probability density function.

Figure 4.4. shows the histograms and probability density function of pedestrian interaction for uni-directional and bi- directional walking direction for each PLOS A categories "-", "0", and "+".

In the uni-directional case (**Figure 4.4a.)**, the category "+" group is tightly concentrated near zero with a steep left-skewed peak, indicating minimal restriction for most observations. The category "0" group shifts right and broadens, showing moderately higher restriction. The category "-" group exhibits the largest rightward shift and a long right tail, reflecting both higher central tendency and greater variability in pedestrian interaction. Overall, increasing pedestrian presence is associated with larger and more variable restricted-movement values. In the bi-directional case (**Figure 4.4b.**), the category "+" and category "0" groups cluster near zero, indicating mostly minor restriction with short right tails. The category "-" group shows a substantial rightward shift and a heavy, extended tail (visible well beyond 30 units), evidencing both higher central tendency and much greater variability in pedestrian interaction when counterflows are dense. Comparing uni- and bi-directional walking directions, both show the same monotonic pattern: increasing presence moves the probability density function to the right and widens it. However, for bi-directional, the category "-" exhibits a longer and heavier tail than the uni-directional walking direction for the category "-", implying more frequent severe restriction events under different walking directions.

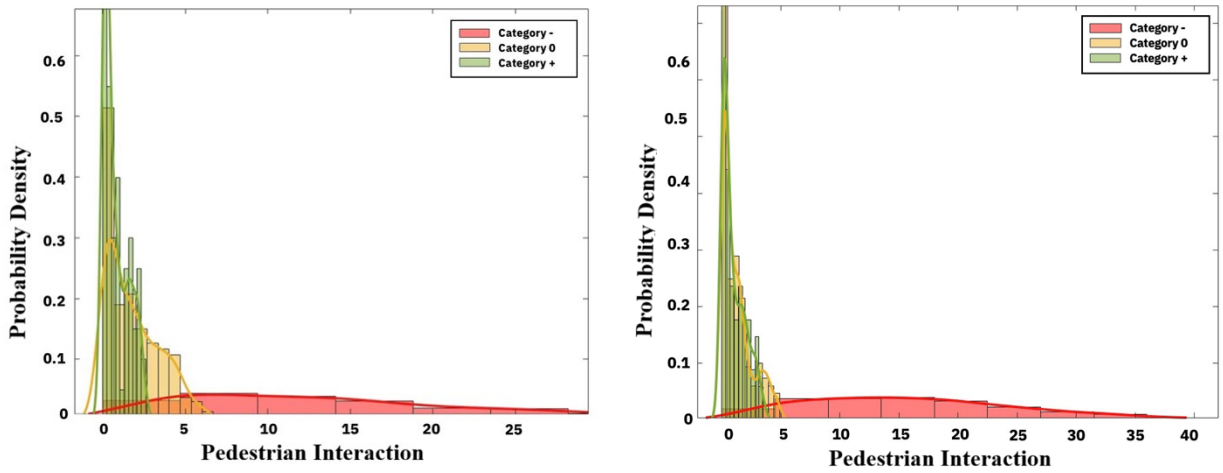

a) PLOS A – Uni-directional b) PLOS A – Bi-directional

Figure 4.4. Normalized histograms with smoothed probability density functions of Pedestrian Interaction for PLOS A under (a) uni-directional and (b) bi-directional walking

Figure 4.5. show the histograms and probability density function of pedestrian interaction for uni-directional and bi- directional walking direction for each PLOS B categories "-", "0", and "+".

In the uni-directional walking direction (**Figure 4.5a.**), the "+" category is compact with peaks at low pedestrian interaction; "0" shifts right and widens; "-" moves further right and exhibits a long right tail (extending beyond approximately 200), reflecting higher typical pedestrian interaction and more frequent higher pedestrian interaction events in uni-directional walking direction as the number of pedestrians increases.

In the bi-directional walking direction (**Figure 4.5b.**), a similar monotonic pattern appears, but the "-" category shows an even heavier tail (stretching toward approximately 300) and greater

spread, consistent with stronger interaction effects under counterflow. The "+" and "0" categories remain concentrated between roughly 40–80, with moderate overlap with one another.

Both cases display a rightward shift and increasing dispersion from "+" to "0" to "-". Compared with uni-directional, the bi-directional walking direction, the "-" category exhibits a broader probability density function and longer right tail, indicating more frequent severe restriction when opposing streams interact, while differences between "+" and "0" are modest in both cases.

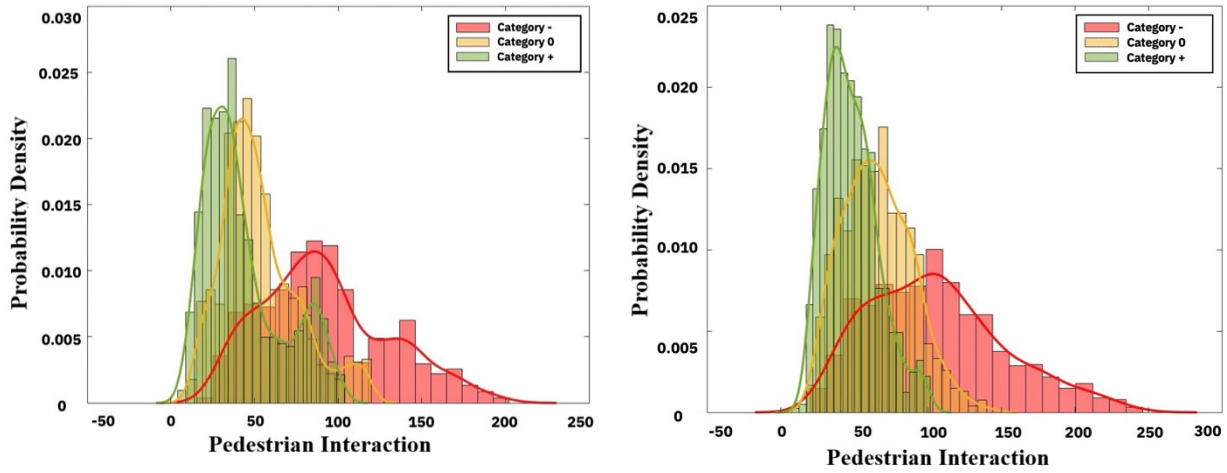

a) PLOS B – Uni-directional b) PLOS B – Bi-directional

Figure 4.5. Normalized histograms with smoothed probability density functions of Pedestrian Interaction for PLOS B under (a) uni-directional and (b) bi-directional walking

Comparing PLOS A and PLOS B shows that all three categories in PLOS B are displaced farther to the right than in PLOS A. For the same category ("+", "0", "-"), Pedestrian interaction is larger in PLOS B. The probability density function for PLOS B is broader with heavier right tails, especially for the "-"category. PLOS A shows short tails for "+" and "0" and a moderate tail for "-". PLOS B shows pronounced long tails (up to approximately 200-300) for "-" category.

In PLOS A, “+” and “0” categories are tightly near zero and overlap substantially; “-” is shifted right but still overlaps the mid-range. In PLOS B, category separation is clearer. “+” category peaks around lower values, “0” sits mid-range, and “-” is distinctly higher, with less overlap.

PLOS A has taller peaks (e.g., up to approximately 0.6-0.7) because its data are tightly concentrated near zero (the y-axis is probability density). In PLOS B, it is spread over larger values, so the peaks are lower (approximately 0.02-0.03).

Figure 4.6. show the histograms and probability density function of pedestrian interaction for uni-directional and bi- directional walking direction for each PLOS C categories “-”, “0”, and “+”.

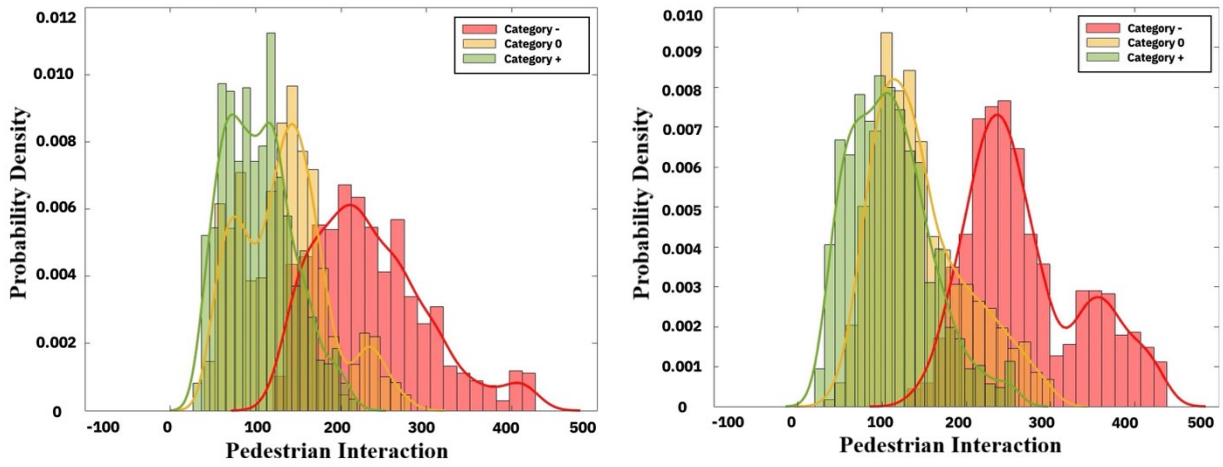

a) PLOS C – Uni-directional b) PLOS C – Bi-directional

Figure 4.6. Normalized histograms with smoothed probability density functions of Pedestrian Interaction for PLOS C under (a) uni-directional and (b) bi-directional walking

Both uni-directional and bi-directional walking direction display a rightward shift and increased spread from “+” to “0” to “-”. The bi-directional case shows more extreme and varied values,

especially in the "-"category, which has a longer tail and two peaks. Relative to PLOS A and B, PLOS C exhibits substantially higher pedestrian interaction values and a broader probability density function, especially under bi-directional walking direction.

Figure 4.7. show the histograms and probability density function of pedestrian interaction for uni-directional and bi- directional walking direction for each PLOS D categories "-", "0", and "+".

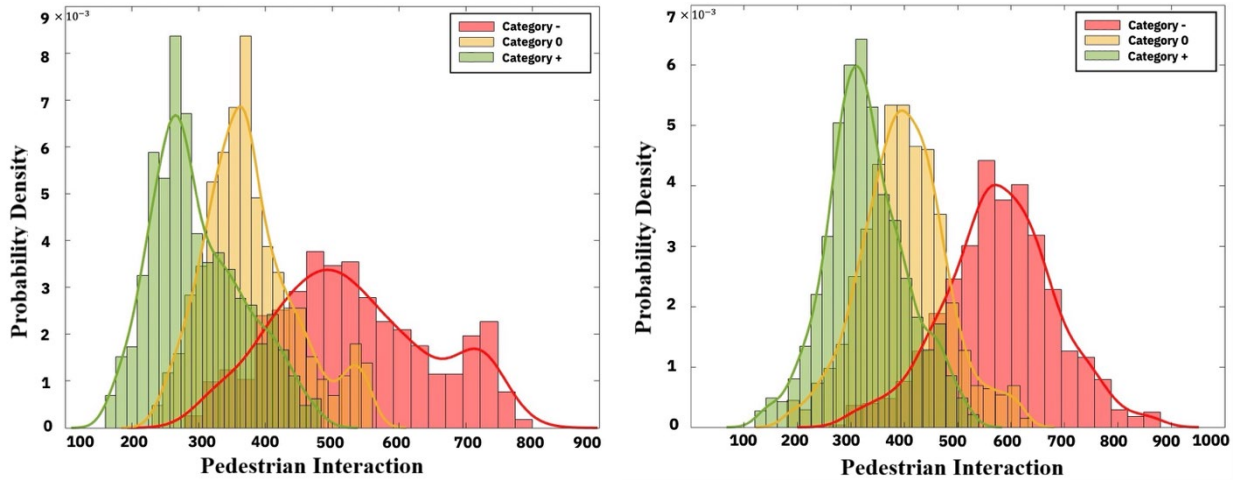

a) PLOS D – Uni-directional b) PLOS D – Bi-directional

Figure 4.7. Normalized histograms with smoothed probability density functions of Pedestrian Interaction for PLOS D under (a) uni-directional and (b) bi-directional walking

Figure 4.8. show the histograms and probability density function of pedestrian interaction for uni-directional and bi-directional walking direction for each PLOS E categories "-", "0", and "+".

Both PLOS D directional cases show the same monotonic pattern: as the category moves from "+" to "0" and then to "-", the probability density function shifts to the right and becomes wider. The bi-directional case, particularly in "-", shows the highest levels and greatest spread. With the bi-directional "-" case most elevated and most dispersed, carrying the longest right tail. Relative

to PLOS C, PLOS D is shifted substantially further right across all categories (higher typical pedestrian interaction), and the category separation is clearer, especially for "-". Whereas PLOS C's "-" group shows two clear peaks and a long tail of very large values, PLOS D presents higher centers but slightly more compact shapes.

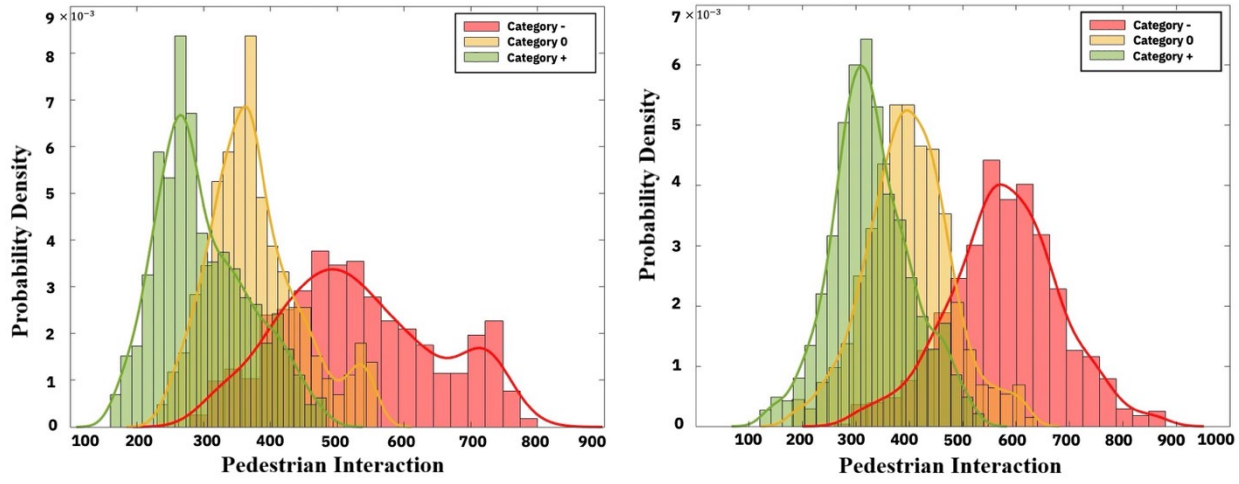

a) PLOS D – Uni-directional b) PLOS D – Bi-directional

Figure 4.8. Normalized histograms with smoothed probability density functions of Pedestrian Interaction for PLOS E under (a) uni-directional and (b) bi-directional walking

The normalized histograms with smoothed probability density functions of the pedestrian interaction for PLOS D and E show that moving from "+" to "0" to "-"increases typical pedestrian interaction and variability. Compared with uni-directional, the bi-directional "-" condition is higher and wider, with the longest right tail, indicating more frequent severe restriction when opposing streams interact.

The results show that bi-directional walking direction consistently produced higher pedestrian interaction compared to uni-directional walking direction at the same PLOS level. This difference

is clear in each PLOS level. The reason for this is that in bi-directional walking direction, pedestrians encounter more frequent meeting events, which require them to adjust their paths, slow down, or change direction to avoid shoulder brushing or colliding with others. In contrast, uni-directional walking direction is generally smoother, as pedestrians move in the same direction with fewer conflicts with each other. These findings highlight how walking direction plays an important role in shaping PLOS, especially under crowded conditions with limited pedestrian space.

4.2 Identify PLOS Model Thresholds and Boundary Values

We first draw box plots for the pedestrian interaction dataset to determine the threshold and boundary values for the PLOS model. The box plot shows the distribution of the data by summarizing five key values: the minimum, the first quartile (Q1), the second quartile (Q2), the third quartile (Q3), and the maximum pedestrian interaction values (Saisana et al., 2005; OECD, 2008). The minimum and maximum represent the lowest and highest observed pedestrian interaction values in the dataset, respectively. Q1 corresponds to the 25th percentile, indicating the pedestrian interaction value below which 25% of the data falls. Q2, also known as the median, represents the 50th percentile and divides the dataset into two sections. Q3 corresponds to the 75th percentile, marking the pedestrian interaction value below which 75% of the data falls. In addition to visualizing the spread of the pedestrian interaction dataset, the box plot also helps to identify outliers (i.e., marked as red crosses in **Figure 4.9a. to Figure 4.13a.**), which are values that lie much lower or higher than the rest of the data.

Next, we develop cumulative distribution functions for the same dataset (Saisana et al., 2005; OECD, 2008). These functions allow us to identify the 33rd and 67th percentiles, which serve as threshold points for the subcategories for each PLOS level. By using these two thresholds, each

PLOS level can be identically divided into three subcategories: “-”, “0”, and “+”. This step provides a clearer way to capture the variations of pedestrian interaction within each PLOS level.

Figure 4.9a. shows two box plots for PLOS A for uni-direction and bi-direction walking direction. For uni-directional walking, the minimum is 0, Q1 is 0, Q2 is 0.97, Q3 is 9.1, and the maximum is 22.8. For bi-directional walking, the minimum is 0, Q1 is 0, Q2 is 0.4, Q3 is 11.5, and the maximum is 28.6. Comparing the two, the values of Q2 are higher in the uni-direction case, but both Q3 and the maximum are higher in the bi-direction walking direction. This indicates that although the middle of the distribution is slightly higher for uni-directional walking direction, bi-directional generally produces larger values of pedestrian interaction at the upper end of the dataset. This occurs because in uni-direction, pedestrians are moving in the same direction and generally experience fewer conflicts, so even when pedestrian interaction occurs, it tends to stay moderate. In contrast, bi-direction introduces opposing movement, which creates more encounters where pedestrians must adjust paths or share limited space. While at lower levels these interactions may not stand out, they accumulate at the higher end, leading to much greater pedestrian interaction in the upper quartiles and maximum values.

Figure 4.9b. shows the CDF using the pedestrian interaction data sets for uni-direction walking direction and bi-direction walking direction for PLOS A after removing outliers. The CDF shows that the 33rd percentile corresponds to a pedestrian interaction value of 0.004, while the 67th percentile corresponds to 5.64. Values below the 33rd percentile represent the “+” category in PLOS A, values between the 33rd and 67th percentiles represent the “0” category in PLOS A, and values above the 67th percentile represent the “-” category in PLOS A. This subdivision gives a clearer picture of conditions within PLOS A and helps show small differences in pedestrian interaction between uni-directional and bi-directional walking.

We repeat the same process for PLOS B-E as shown in **Figure 4.10. to Figure 4.13.** below

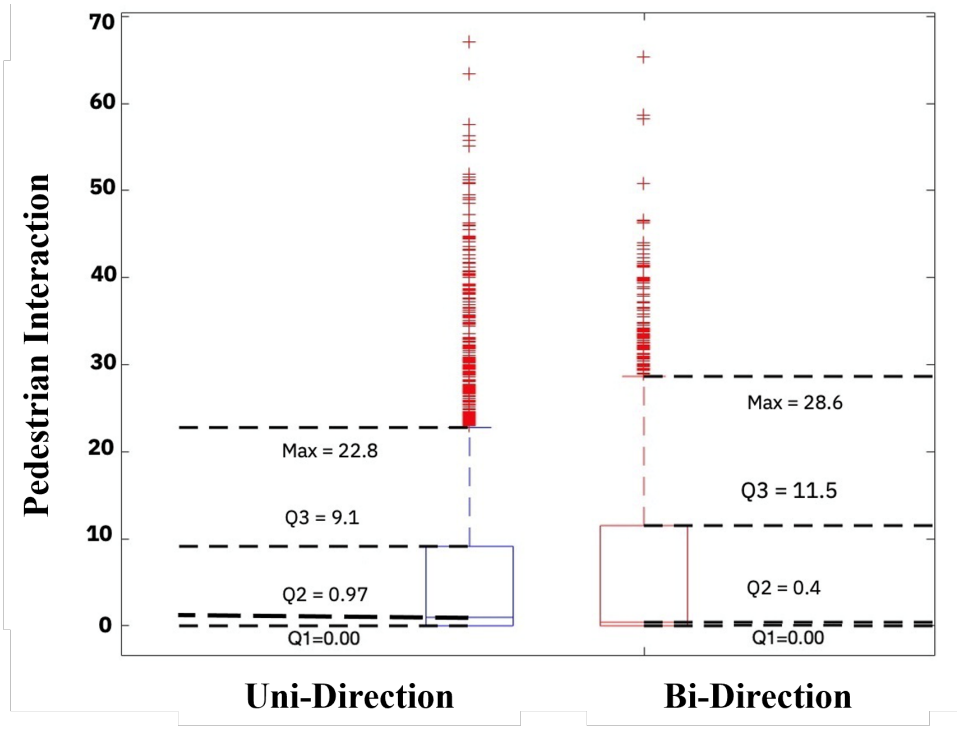

a) Box Plots for Uni-directional and Bi-directional PLOS A

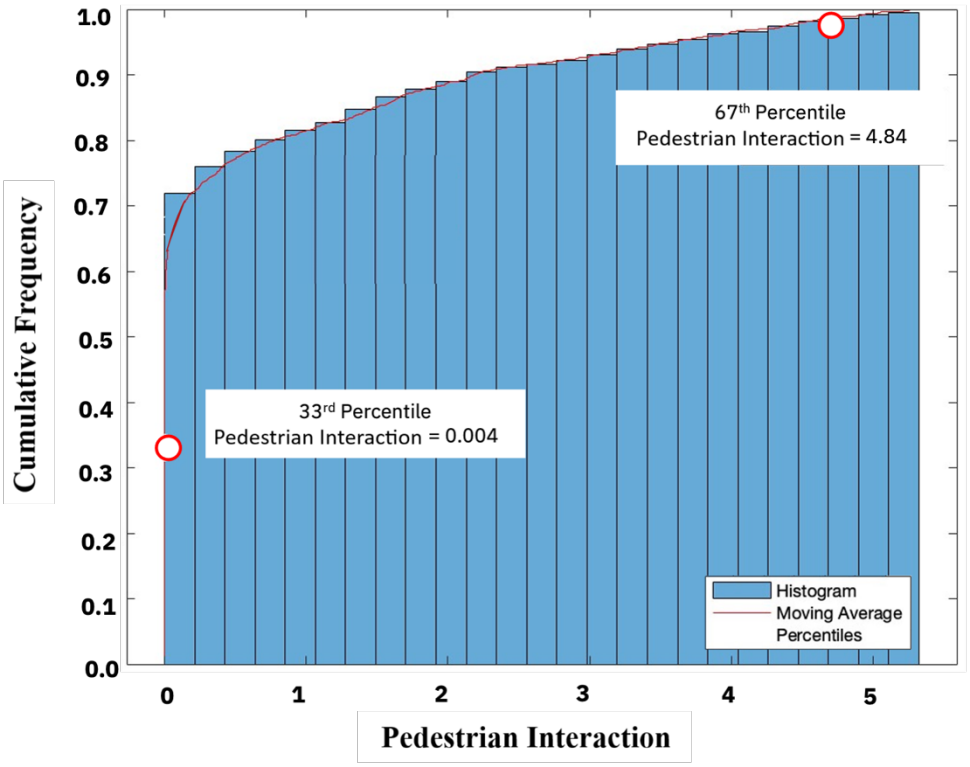

b) Cumulative Distribution Function for Uni-directional and Bi-directional PLOS A

Figure 4.9. Identification of PLOS Model Thresholds and Boundary Values for PLOS A

Figure 4.10a. shows two box plots for PLOS B for uni-direction and bi-direction walking direction. For uni-directional walking, the minimum is 9.88, Q1 is 37.03, Q2 is 54.12, Q3 is 89.77, and the maximum is 168.80. For bi-directional, the minimum is 10.84, Q1 is 44.70, Q2 is 63.91, Q3 is 93.85, and the maximum is 167.30.

Figure 4.10b. shows the cumulative distribution function using the pedestrian interaction data sets for uni-direction and bi-direction walking movement for PLOS B after removing outliers. The cumulative distribution function shows that the 33rd percentile corresponds to a pedestrian interaction value of 45.43, while the 67th percentile corresponds to 78.54. Values below the 33rd

percentile represent the "+" category in PLOS B, values between the 33rd and 67th percentiles represent the "0" category, values above the 67th percentile represent the "-" category in PLOS B.

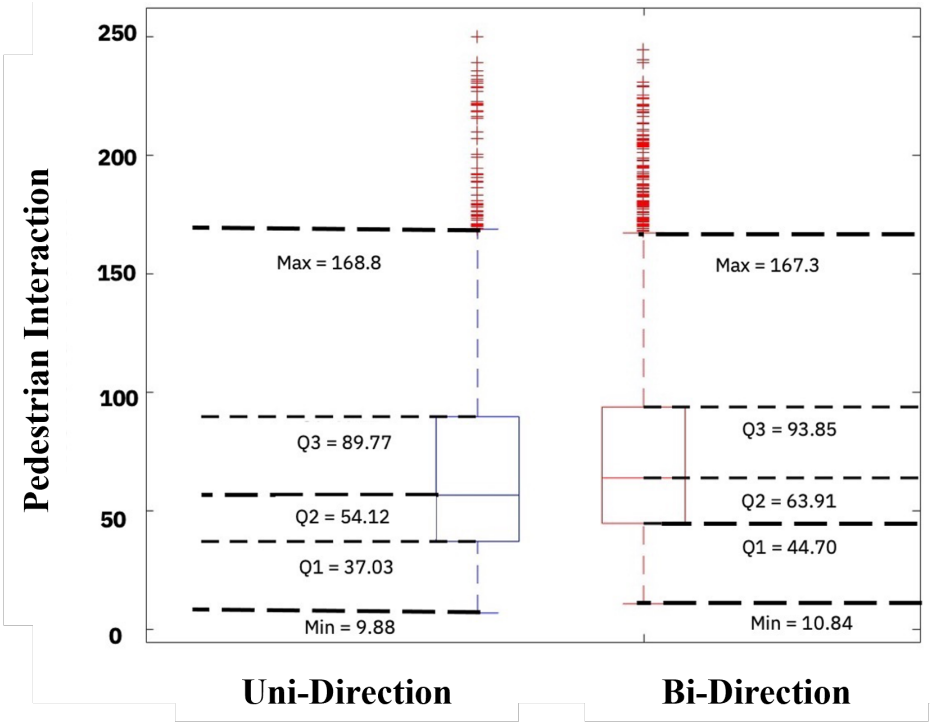

a) Box Plots for Uni-directional and Bi-directional PLOS B

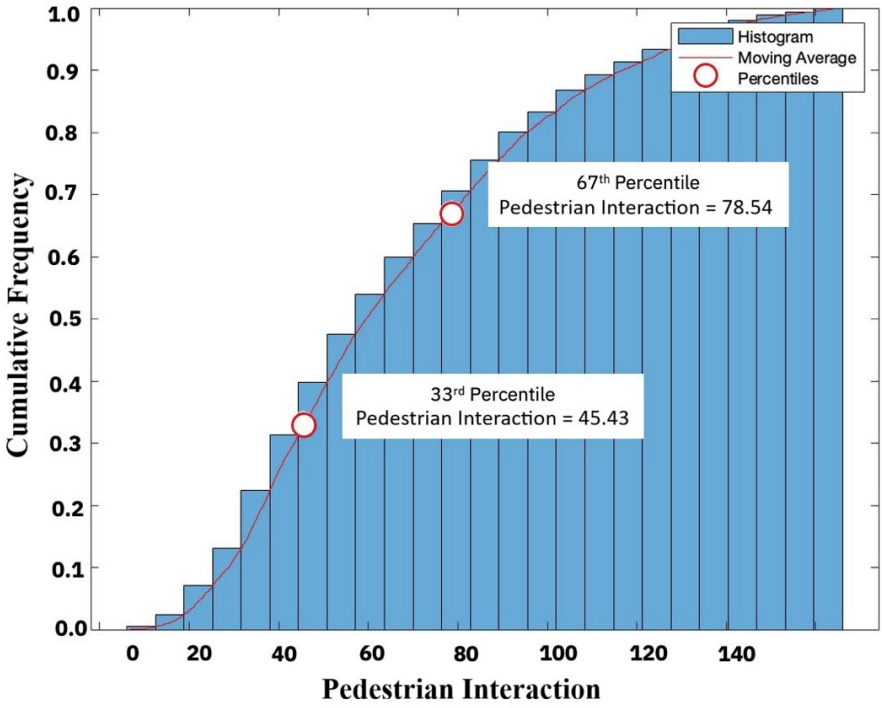

b) Cumulative Distribution Function for Uni-directional and Bi-directional PLOS B

Figure 4.10. Identification of PLOS Model Thresholds and Boundary Values for PLOS B

Figure 4.11a. shows two box plots for PLOS C for uni-direction and bi-direction walking direction. For uni-directional walking direction, the minimum is 34.28, Q1 is 95.86, Q2 is 149.12, Q3 is 203.86, and the maximum is 365.60. For bi-directional, the minimum is 26.16, Q1 is 104.81, Q2 is 159.31, Q3 is 240.85, and the maximum is 444.90. Comparing the two, the minimum pedestrian interaction value is higher in the uni-direction walking direction, but the Q1, Q2, Q3 and the maximum pedestrian interaction values are higher in the bi-directional walking direction.

Figure 4.11b. shows the cumulative distribution function using the pedestrian interaction data sets for uni-direction and bi-direction walking direction for PLOS C after removing outliers. The cumulative distribution function shows that the 33rd percentile corresponds to a pedestrian interaction value of 117.20, while the 67th percentile corresponds to 194.09. Values below the

33rd percentile represent the "+" category in PLOS C, values between the 33rd and 67th percentiles represent the "0" category in PLOS C, and values above the 67th percentile represent the "-" category in PLOS C.

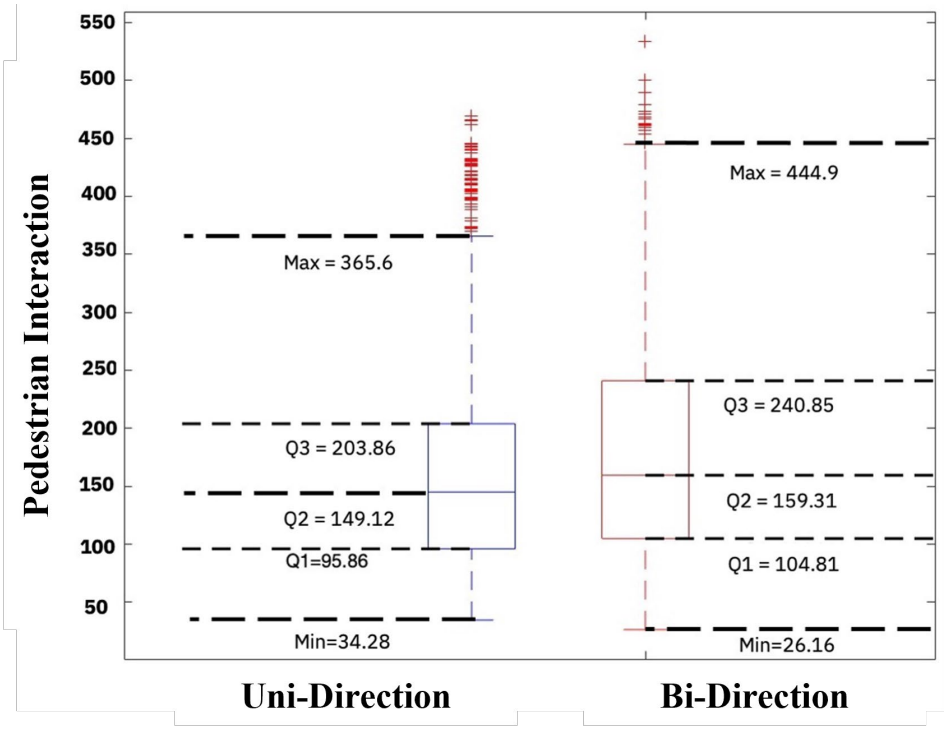

a) Box Plots for Uni-directional and Bi-directional PLOS C

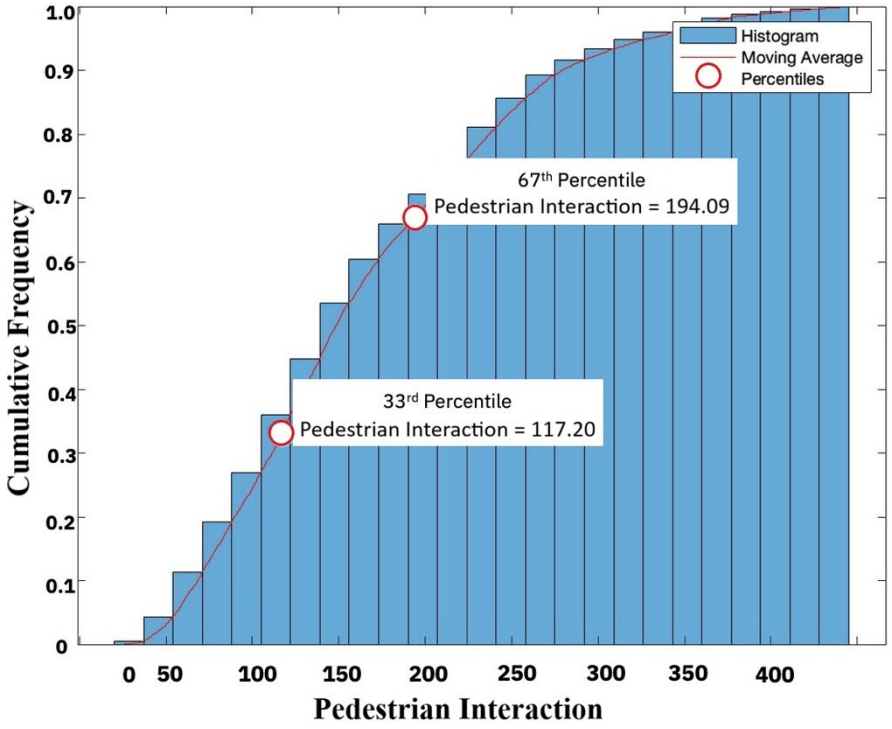

b) Cumulative Distribution Function for Uni-directional and Bi-directional PLOS C

Figure 4.11. Identification of PLOS Model Thresholds and Boundary Values for PLOS C

Figure 4.12a. shows two box plots for PLOS D for uni-direction and bi-direction. For uni-directional walking direction, the minimum is 163.60, Q1 is 307.50, Q2 is 378.20, Q3 is 482.40, and the maximum is 744.20. For bi-directional walking direction, the minimum is 109.20, Q1 is 330.60, Q2 is 414.00, Q3 is 535.10, and the maximum is 838.50. Comparing the two, the minimum pedestrian interaction value is higher in the uni-direction walking direction, but the Q1, Q2, Q3 and the maximum values are higher in the bi-directional walking direction.

Figure 4.12b. shows the cumulative distribution function using the pedestrian interaction data sets for uni-direction and bi-direction walking direction for PLOS D after removing outliers. The cumulative distribution function shows that the 33rd percentile corresponds to a pedestrian interaction value of 342.60, while the 67th percentile corresponds to 462.10. Values below the

33rd percentile represent the "+" category in PLOS D, values between the 33rd and 67th percentiles represent the "0" category in PLOS D, and values above the 67th percentile represent the "-" category in PLOS D.

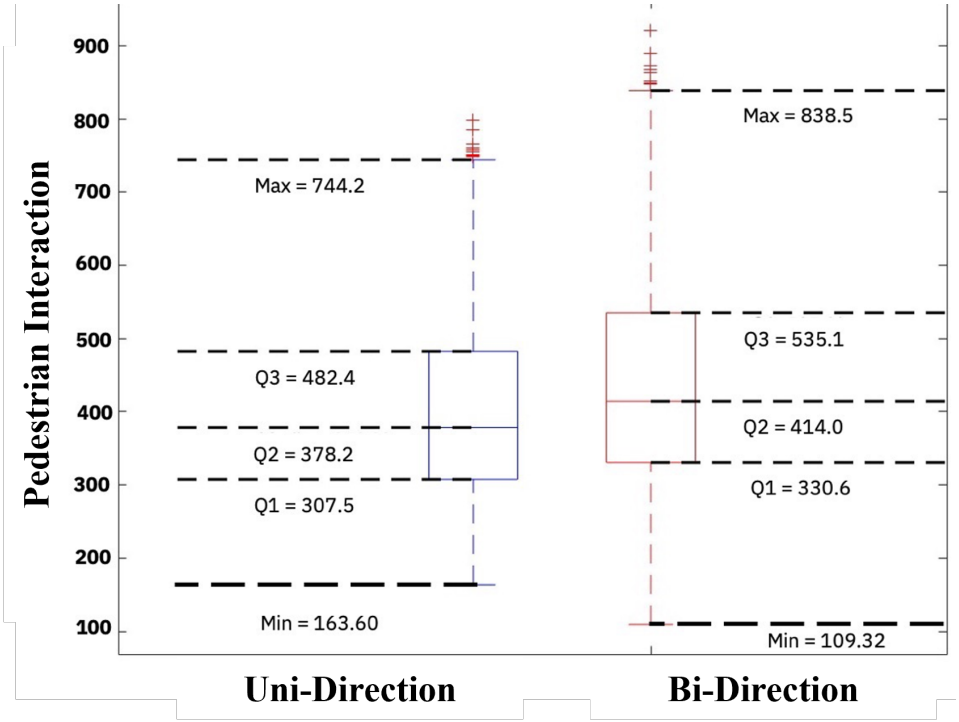

a) Box Plots for Uni-directional and Bi-directional LOS D

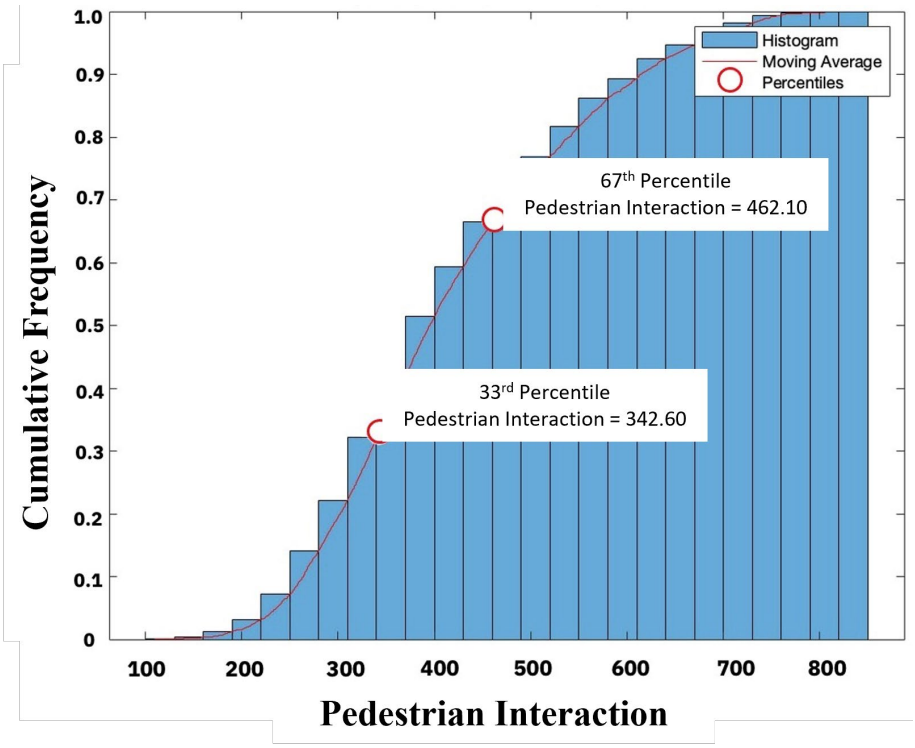

b) Cumulative Distribution Function for Uni-directional and Bi-directional LOS D

Figure 4.12. Identification of PLOS Model Thresholds and Boundary Values for LOS D

Figure 4.13a. shows two box plots for PLOS E for uni-direction and bi-direction walking direction. For uni-directional walking direction, the minimum is 539.05, Q1 is 928.20, Q2 is 1206.50, Q3 is 1475.90, and the maximum is 2038.10. For bi-directional, the minimum is 565.32, Q1 is 1032.70, Q2 is 1344.20, Q3 is 1679.30, and the maximum is 2592.90. Comparing the two, all the pedestrian interaction values are higher in the bi-directional walking direction. Comparing the two, all the pedestrian interaction values are higher in the bi-directional walking direction.

Figure 4.13b. shows the cumulative distribution function using the pedestrian interaction data sets for uni-directional and bi-directional walking direction for PLOS E after removing outliers. The cumulative distribution function shows that the 33rd percentile corresponds to a pedestrian

interaction value of 1082.30, while the 67th percentile corresponds to 1472.70. Values below the 33rd percentile represent the "+" category in LOS E, values between the 33rd and 67th percentiles represent the "0" category in LOS E, and values above the 67th percentile represent the "-" category in LOS E.

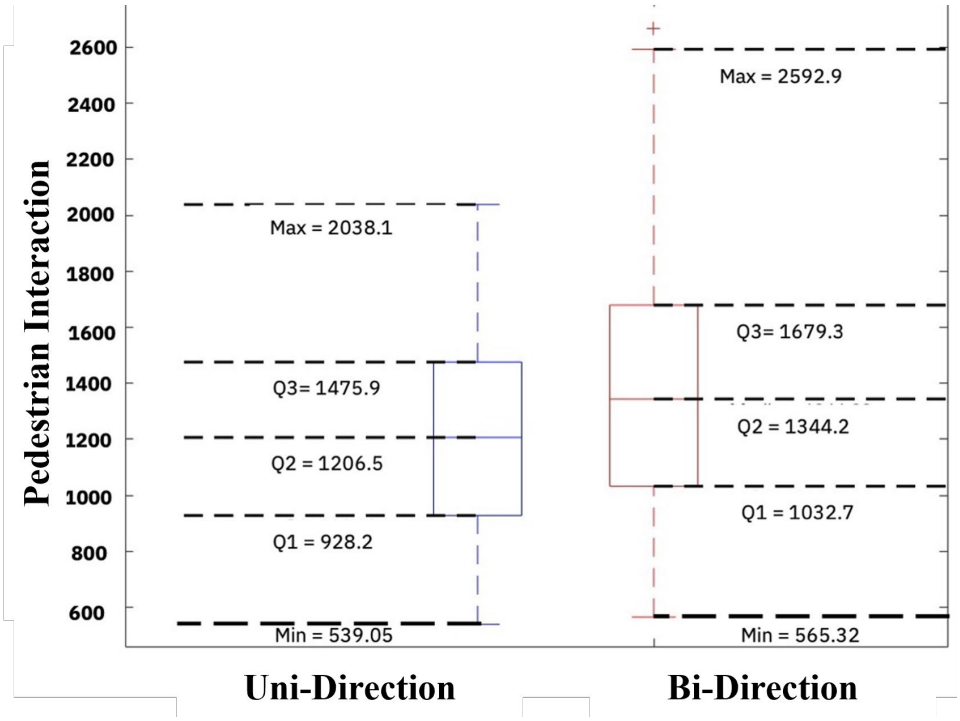

a) Box Plots for Uni-directional and Bi-directional LOS E

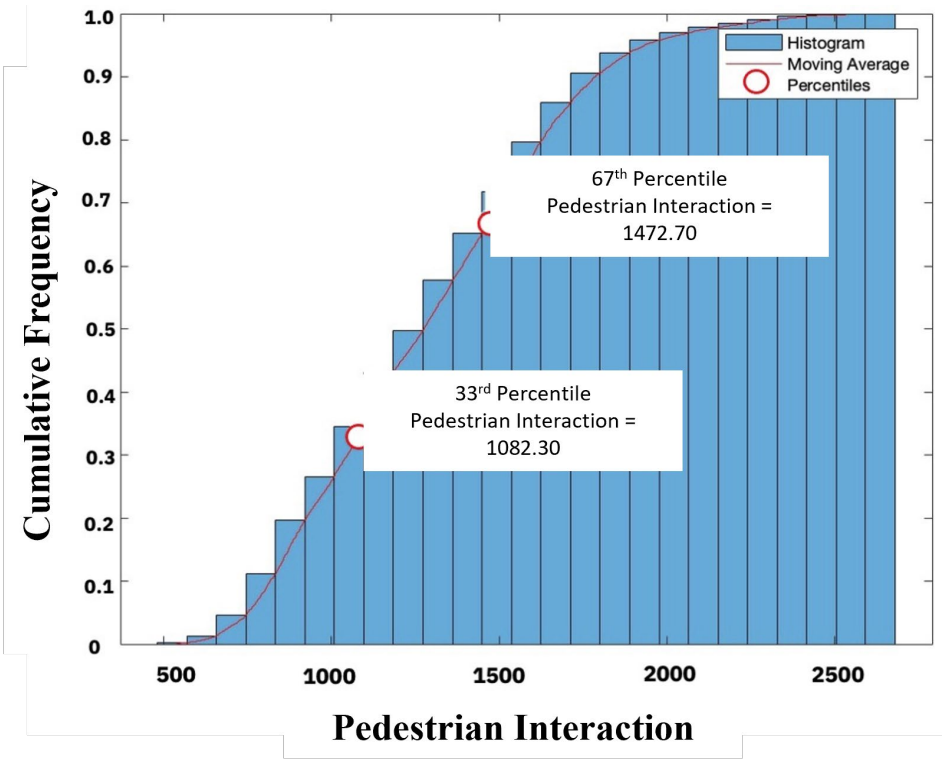

b) Cumulative Distribution Function for Uni-directional and Bi-directional LOS E

Figure 4.13. Identification of PLOS Model Thresholds and Boundary Values for LOS E

4.3 New PLOS Model

We use the minimum and maximum pedestrian interaction threshold values for each PLOS level and the 33rd and 67th percentiles calculated in the previous section, to develop the novel PLOS model. **Figure 4.14.** shows the PLOS model created by combining the threshold and boundary values taken from the box plots and the cumulative distribution functions for uni-directional and bi-directional walking direction for each PLOS level. We note that the novel PLOS model also uses pedestrian space as the first input indicator, with the range for each PLOS level taken directly from the HCM, as mentioned in **Table 2.2** (HCM, 2010).

The "- / 0 / +" classification structure is adapted from the City of London PLOS model, which also uses subcategories to describe different levels of pedestrian comfort (City of London, 2010; Finch et al., 2010). Therefore, the contribution of this study is not the classification structure itself. What is adopted from the City of London model is the three-level form used to describe variation within the first indicator, and not the measurement scale, the units, or the threshold values. City of London's restricted movement is expressed as the percentage of pedestrians observed to adjust their path or speed, and is therefore bounded between 0 and 100 percent (City of London, 2010). Pedestrian interaction in this study is an aggregated interaction quantity expressed in m/s^2, derived from social force and walking direction. Because the two measures are defined on different scales, the City of London threshold values cannot be transferred to the proposed PLOS model, and the subcategory boundaries for pedestrian interaction used in this study are instead derived empirically from the pedestrian interaction distribution obtained for each PLOS level. The contribution is therefore the simulation-based method used to calculate pedestrian interaction, the derivation of the corresponding threshold values, and the application of both within a PLOS model. In this study, pedestrian interaction is calculated using pedestrian trajectory outputs, pedestrian distance, social force, and walking direction, rather than through manual observation of shoulder brushing or collision events (City of London, 2010; Finch et al., 2010).

By integrating both input indicators, each PLOS level is subdivided into three categories ("-", "0", and "+"). This makes it possible to capture smaller variations in pedestrian interaction within the fixed pedestrian space ranges that are typically not accounted for in traditional PLOS models that are currently being used. This gives the novel PLOS model a more detailed and practical description of pedestrian conditions and walking experiences, showing when walking conditions are more restricted, typical, or more comfortable.

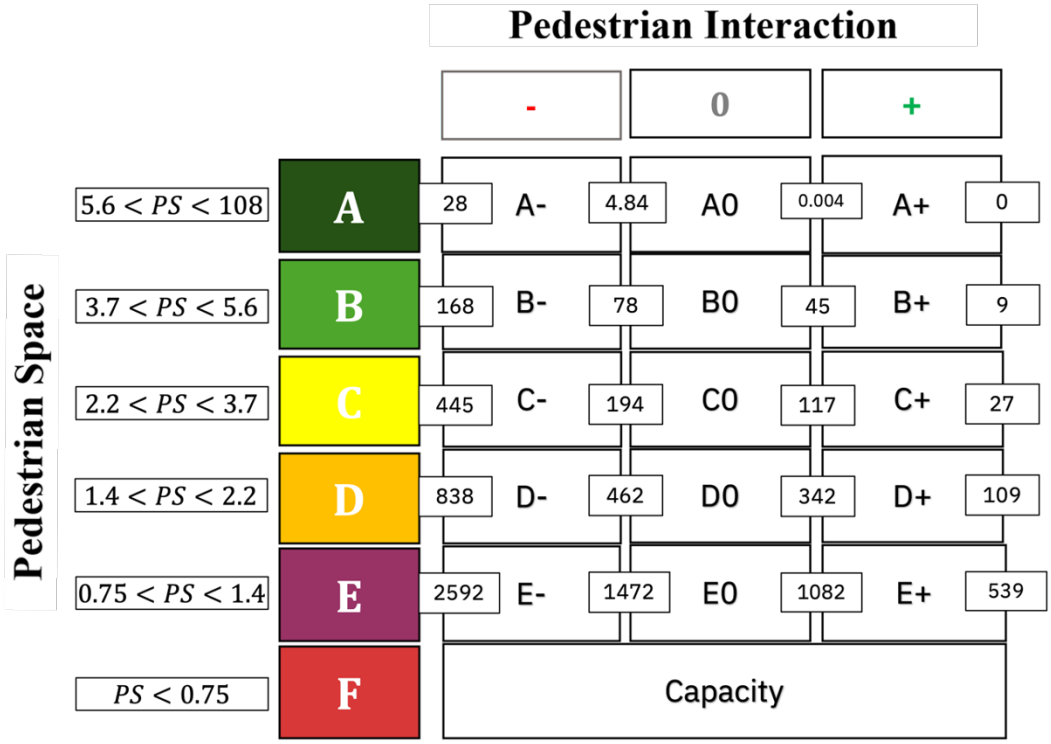

Figure 4.14. New PLOS Model

4.4 Chapter Summary

Chapter 4 presented the quantitative results used to develop the novel PLOS model. Building on the methodology described in **Section 3.3**, this chapter focused on the numerical outcomes from the 2D microsimulation models and 3D visualization in Unity. The analysis examined how pedestrian interaction varied across PLOS levels, walking directions, and subcategories. These results were used to define the threshold values required for the proposed PLOS framework.

The chapter first showed how each PLOS level was divided into "-", "0", and "+" subcategories using pedestrian space values and microsimulation outputs. Both uni-directional and bi-directional walking conditions were modelled in PTV Viswalk, producing trajectory datasets used to calculate

aggregated pedestrian interaction. The results showed that pedestrian interaction generally decreased as pedestrian space increased, while bi-directional walking conditions produced higher pedestrian interaction than uni-directional walking conditions.

This chapter also presented the statistical analysis used to identify PLOS model thresholds and boundary values. Histograms and probability density functions were used to examine the distribution of pedestrian interaction, while box plots and cumulative distribution functions were used to identify the 33rd and 67th percentile thresholds. These thresholds were used to divide each PLOS level into three subcategories. The final PLOS model integrates pedestrian space as the first input indicator and pedestrian interaction as the second input indicator.

Overall, **Chapter 4** establishes the numerical foundation of the proposed PLOS model. The results demonstrate why walking direction and pedestrian interactions should be considered when evaluating sidewalk performance. By combining pedestrian space with pedestrian interaction, the final model can capture variations in walking conditions that are not reflected by pedestrian space alone. The resulting PLOS framework is applied in the following chapters to evaluate how modifications to a sidewalk's design layout affect pedestrian walking conditions.

Chapter 5. Apply the PLOS Model Through Case Studies

Chapter 5 presents the Base and Alternative Scenarios developed to apply the PLOS model through case studies. As discussed in **Chapter 3** and **Chapter 4**, the new PLOS model relies on two input indicators, pedestrian space and pedestrian interaction. To use our PLOS model, we first need a Base Scenario that reflects realistic conditions in the study area. We then compare this Base Scenario with several Alternative Scenarios to see how different modifications affect pedestrian movement and overall PLOS. Before implementing the PLOS model, the pedestrian space, pedestrian volume, and walking speed must be defined so that all scenarios are evaluated consistently. The chapter also shows the heat map results, which help visualize how pedestrian interaction changes when different design layouts or surface elements are added or removed.

5.1 Select Base and Alternative Scenarios

The purpose of creating one Base Scenario and several Alternative Scenarios is to apply the new PLOS model and evaluate how it responds to modifications in design layouts for a sidewalk (Asadi-Shekari et al., 2014; Papadimitriou et al., 2018). Since the PLOS model captures the two input indicators, pedestrian space and pedestrian interaction, it is important to test it under a range of realistic changes that commonly occur in sidewalks. By comparing the Base Scenario to multiple modified Alternative Scenarios of the same environment, we can see how specific design layouts and elements, such as seating, stairs, advertisements, construction zones, or temporary barriers, affect pedestrian space, pedestrian interaction, and the overall PLOS of a sidewalk.

The Base and Alternative Scenarios also allow the PLOS model to be applied in a practical, decision-making context. Cities frequently adjust sidewalks through small-scale modifications rather than completing full redesigns (Ehrenfeucht and Loukaitou-Sideris, 2010; NACTO, 2013;

Saltarin-Molino et al., 2023). Understanding how each modification to the design layout can influence PLOS helps determine its level of impact on pedestrian experience and overall PLOS before committing to any permanent changes. We simulate a total of six scenarios, consisting of one Base scenario and five Alternative Scenarios to apply and implement the novel PLOS model. The Base Scenario represents the existing conditions of the study area, while the Alternative Scenarios introduce different modifications to the original design layout of the sidewalk. These scenarios help identify design layouts and features that may enhance the overall PLOS in a sidewalk.

The six scenarios that were modelled and evaluated include:

1) Base Scenario
2) Alternative Scenario 1: Addition of Advertisements
3) Alternative Scenario 2: Removal of Seats
4) Alternative Scenario 3: Removal of Stairs
5) Alternative Scenario 4: Addition of Construction Zone
6) Alternative Scenario 5: Addition of Hazard Tape

5.1.1 Base Scenario

Figure 5.1. shows a snapshot of the Base Scenario in 2D microsimulation in PTV Viswalk and 3D visualization in Unity. The Base Scenario is the "do nothing" conditions and reflects the current state of the study area without any change. The Base Scenario is the study area described in **Section 3.2.1**, with the sidewalk having 2 entrances and dimensions that are 72 meters in length and 3 meters in width. **Figure 5.1a.** shows a snapshot of the existing pedestrian environment in the Base Scenario in the 2D microsimulation model. In the figure, the sidewalk is the colour gray, the seats

available in the sidewalk are outlined in yellow boxes, and the stairs are outlined in blue and static objects (i.e., a garbage bin) are outlined in red. Additionally, the two entrances at each end of the sidewalk where pedestrians enter the sidewalk are outlined in green boxes, and the yellow arrows represent the walking direction that pedestrians can move towards. **Figure 5.1b.** shows a snapshot of the Base Scenario in a 3D visualization in Unity.

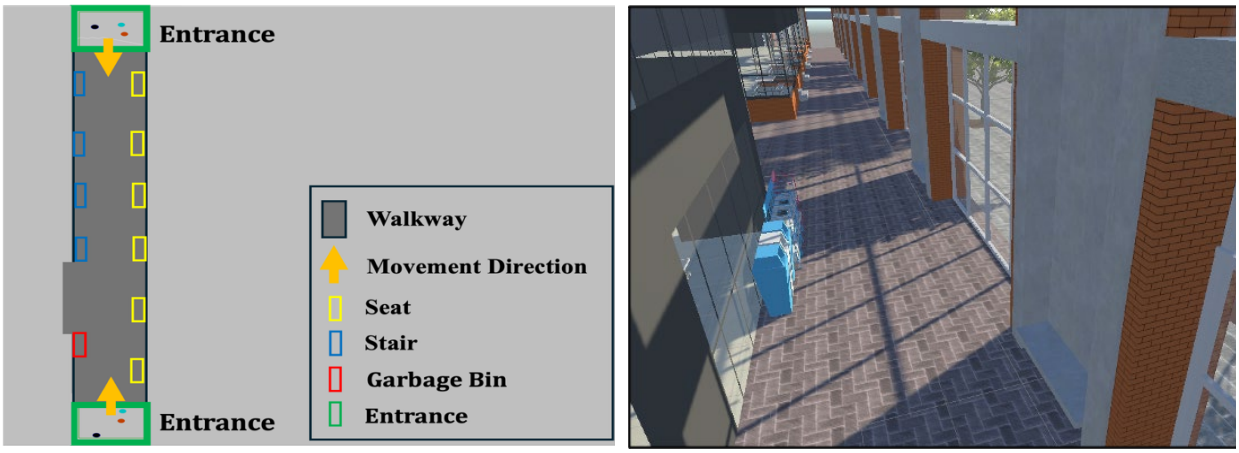

a) Base Scenario in 2D Microsimulation b) Base Scenario in 3D visualization

Figure 5.1. Base Scenario in 2D Microsimulation Model versus 3D Visualization

5.1.2 Alternative Scenario 1: Addition of Advertisements

Figure 5.2. shows a snapshot of the addition of advertisements scenario in 2D microsimulation model and 3D visualization. In Alternative Scenario 1 (addition of advertisements), several advertisements, specifically posters on the wall, are added to the study area. These can serve a functional or commercial purpose but may also reduce available walking space or distract pedestrians, which can potentially affect their movement patterns (Kong et al., 2019; Konovalova and Petrova, 2023; Mishra and Chowdhury, 2023). The analysis evaluates whether the added visual and physical elements impact PLOS and walking conditions.

Figure 5.2a. shows Alternative Scenario 1 in a 2D microsimulation model in PTV Viswalk and shows where the advertisements in the sidewalk are located. The advertisement posters are located in the same location as the seats on the sidewalk, outlined in yellow boxes. In the figure, the gray boxes in front of the seats represent the waiting areas where pedestrians can stand and review the content of the advertisement. **Figure 5.2b.** show Alternative Scenario 1 in 3D visualization using Unity, where the advertisements are specifically added on the walls on top of the seating areas. For that, we design waiting areas for pedestrians in front of each wall and add advertisement posters. In PTV Viswalk, we set the time that pedestrians will wait and assess the advertisement posters within a defined range of 5-15 seconds (Kong et al., 2019; Konovalova and Petrova, 2023; Mishra and Chowdhury, 2023).

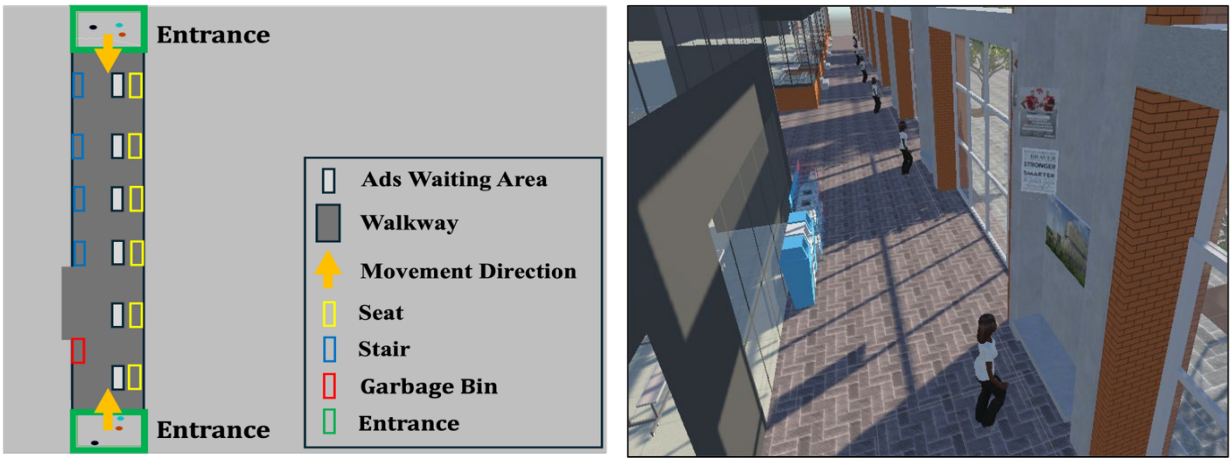

a) Addition of advertisement in 2D Microsimulation

b) Addition of advertisement in 3D Visualization

Figure 5.2. Addition of Advertisement Scenario 2D Microsimulation Model versus 3D Visualization

5.1.3 Alternative Scenario 2: Removal of Seats

Figure 5.3. shows a snapshot of the removal of seats scenario in 2D microsimulation model and in 3D visualization. In Alternative Scenario 2 (removal of seats), the existing stairs are removed from the area. This aims to free up additional pedestrian space, which could improve movement efficiency, especially during peak hours when there are the most students, faculty, and workers walking along the sidewalk (Jaskiewicz, 2000; NACTO, 2013; Holmes et al., 2018). **Figure 5.3a.** shows Alternative Scenario 2 in a 2D microsimulation in PTV Viswalk. In the figure, the yellow boxes representing the seats are taken out to visualize the removal of multiple seats that are positioned throughout the sidewalk. There is a great increase in the gray areas that represent the available space in the sidewalk where pedestrians can walk. **Figure 5.3b.** shows Alternative Scenario 2 in 3D visualization in Unity and visualizes the larger available walking space after the seats are removed.



a) Removal of seats in 2D Microsimulation b) Removal of seats in 3D Visualization

Figure 5.3. Removal of Seats Scenario in 2D Microsimulation Model versus 3D Visualization

5.1.4 Alternative Scenario 3: Removal of stairs

Figure 5.4. shows a snapshot of the removal of stairs scenario in 2D microsimulation model and 3D visualization. In Alternative Scenario 3 (removal of stairs), there is a small section of the existing stairs that protrude along the sidewalk that we will remove. This modification is also meant to provide additional walking space for pedestrians by increasing the effective walking width of the sidewalk (Jaskiewicz, 2000; NACTO, 2013; Holmes et al., 2018). **Figure 5.4a.** shows Alternative Scenario 3 in a 2D microsimulation in PTV Viswalk. In the figure, the blue boxes representing the stairs are taken out to visualize the removal of multiple stairs that are positioned throughout the sidewalk. **Figure 5.4b.** shows Alternative Scenario 3 in a 3D visualization in Unity and shows how more walking space is provided for the pedestrians in the sidewalk when the stairs were removed, especially because the stairs were slightly encroaching certain areas of the sidewalk that could have been used as a walking space.

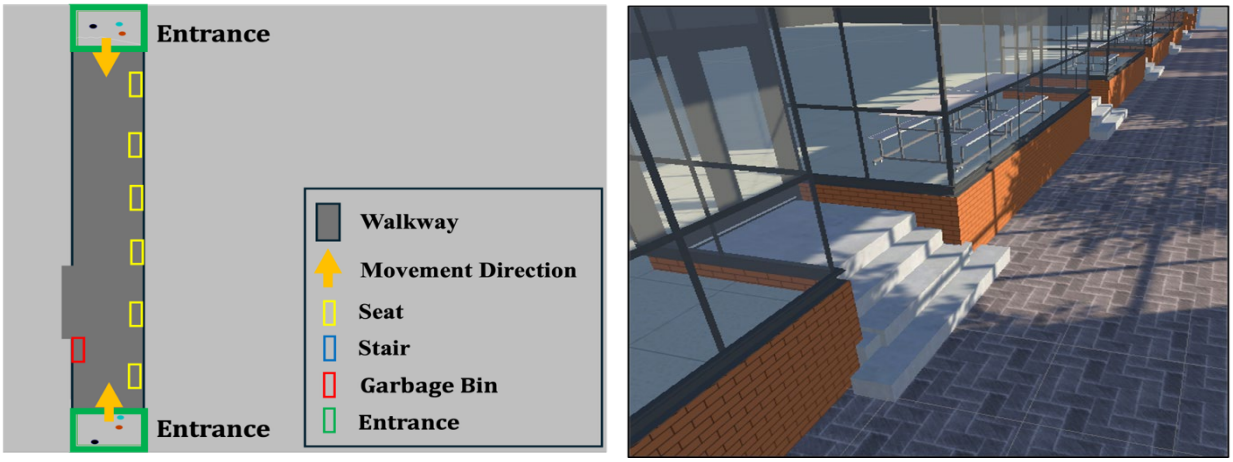

a) Removal of stairs in 2D Microsimulation b) Removal of stairs in 3D Visualization

Figure 5.4. Removal of Stairs Scenario in 2D Microsimulation Model versus 3D Visualization

5.1.5 Alternative Scenario 4: Addition of Construction Zone

Figure 5.5. shows a snapshot of the addition of a construction zone scenario in 2D microsimulation model and 3D visualization. In Alternative Scenario 4 (addition of a construction zone), we add a construction zone in the middle of the sidewalk to represent the common temporary disruption during construction. **Figure 5.5a.** shows Alternative Scenario 4 in a 2D microsimulation model in PTV Viswalk. In the figure, the exact location where the construction zone is added is shown as a purple box, on the southern end of the sidewalk. **Figure 5.5b.** shows Alternative Scenario 4 in 3D visualization in Unity. The construction zone acts as a barrier, and a restricted area is introduced to simulate the reduced pedestrian walking space and the altered routes pedestrians must take to navigate around the restricted area (NACTO, 2013; Yoon et al., 2025).

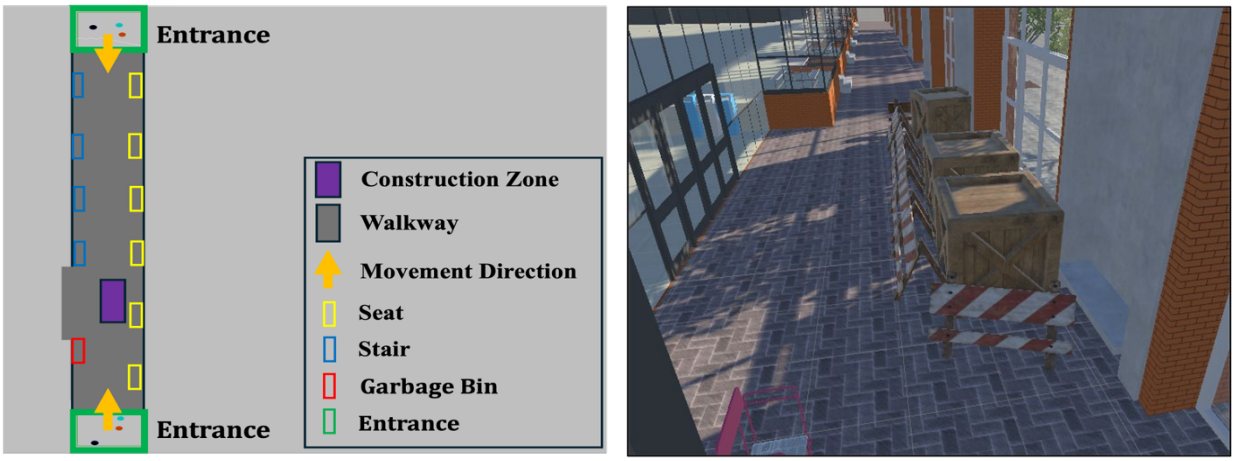

a) Addition of a construction zone in 2D Microsimulation

b) Addition of a construction zone in 3D Visualization

Figure 5.5. Addition of A Construction Zone Scenario 2D Microsimulation Model versus 3D Visualization

5.1.6 Alternative Scenario 5: Addition of Hazard Tape

Figure 5.6. shows a snapshot of the addition of a hazard tape scenario in 2D microsimulation model and 3D visualization. In Alternative Scenario 5 (addition of hazard tape), we add a hazard tape along a designated section of the sidewalk that fully spans its length. This creates a complete barrier to pedestrian movement within that section, forcing pedestrians to divert around the restricted area (NACTO, 2013; Yoon et al., 2025). **Figure 5.6a.** shows Alternative Scenario 5 in a 2D microsimulation in PTV Viswalk. In the figure, the restrictions from the added hazard tape spanning the sidewalk length is outlined as hatched markings in orange. **Figure 5.6b.** shows Alternative Scenario 5 in 3D visualization in Unity. Since the taped-off section covers a section of the full sidewalk length of the sidewalk, the resulting unwalkable area is greater than that in the construction area scenario, where the obstructions are only confined to a specific area.

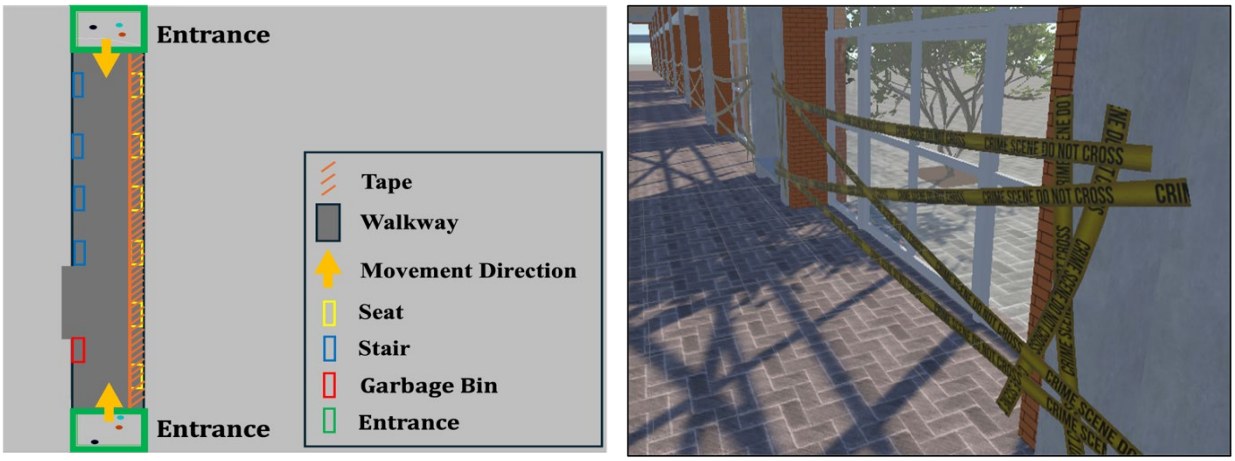

a) Addition of hazard tape in 2D Microsimulation

b) Addition of hazard tape in 3D Visualization

Figure 5.6. Addition of Hazard Tape Scenario in 2D Microsimulation versus 3D Visualization

5.2 Determine the Required Parameters for Scenarios

5.2.1 Selecting PLOS C

Many municipalities in North America and around the world widely adopt PLOS C as the planning benchmark or target for sidewalks to ensure reasonable pedestrian space while maintaining cost-effective design layout and operational standards (New York City, 2006; City of London, 2010; TRB, 2020; City of Brampton, 2022; Hong Kong Transportation Department, 2023). It represents a balance between pedestrian comfort and infrastructure efficiency since conditions are neither too congested to be unsafe or uncomfortable (Pushkarev and Zupan, 1975; HCM, 2010; TRB, 2020).

Our study area at York University is a busy sidewalk that accommodates high volumes of pedestrians, especially during peak periods during class and meal times. York Lanes is the main shopping centre with a bookstore, drugstore, medical services and several fast-food joints, that connects to the rest of the academic buildings at York University's Keele campus. It is reasonable to assume that the sidewalk was designed to operate around PLOS C during peak period conditions or worst-case scenario. Modelling the Base Scenario under PLOS C conditions reflects realistic municipal planning practice and provides a meaningful reference point for evaluating how the novel PLOS model performs under typical design assumptions for sidewalks.

5.2.2 Pedestrian Volume and Speed as Input Parameters

The Base and Alternative Scenarios require a pedestrian volume and walking speed to build the 2D microsimulation models in PTV Viswalk. To determine these inputs, we randomly select a pedestrian space value within the PLOS C level. We select 2.7 m² per pedestrian as the random pedestrian space value using Microsoft Excel. We then convert this into a corresponding pedestrian volume for all the microsimulation model runs in PTV Viswalk.

For walking speed, we use an average desired speed of 1.3 m/s based on recommendations from the HCM (TRB, 2020). Using the same pedestrian space and walking speed for all the Base and Alternative Scenarios ensures that any changes in PLOS result from the modifications to the design layout in comparison to the Base Scenario and not from differences in basic pedestrian movement or behaviour assumptions.

5.2.3 Collecting the outputs from PTV Viswalk to input into Unity

Once the 2D microsimulation model was generated for the Base and Alternative Scenarios, we collect the required outputs to calculate the second indicator, pedestrian interaction. The outputs we obtain include the (x,y,z) coordinates and walking speed for each pedestrian who is on the sidewalk for every second of the 15-minute simulation period. We then use Unity to generate the 3D visualization and calculate the pedestrian space and pedestrian interaction values using the input parameters from PTV Viswalk.

5.3 Chapter Summary

Chapter 5 presented the application setup for the novel PLOS model using the York Lanes sidewalk as the case study. One Base Scenario and five Alternative Scenarios were developed to evaluate how different design layout modifications affect pedestrian space, pedestrian interaction, and overall PLOS. The Base Scenario represented existing conditions, while the Alternative Scenarios included the addition of advertisements, removal of seats, removal of stairs, addition of a construction zone, and addition of hazard tape.

The chapter also defined the required input parameters for the Base and Alternative Scenarios. PLOS C was selected as the target operating condition because it is commonly used as a planning benchmark and reflects a balance between pedestrian comfort and infrastructure efficiency. A

pedestrian space value of 2.7 m² per person was selected within the PLOS C range and applied consistently across all scenarios. The average desired walking speed was set at 1.3 m/s based on HCM recommendations. Outputs from PTV Viswalk, including pedestrian coordinates and walking speed, were then transferred into Unity to calculate pedestrian space and pedestrian interaction.

Overall, **Chapter 5** establishes the case study conditions needed to apply the PLOS model. By keeping pedestrian space and walking speed assumptions consistent across all scenarios, the analysis can focus on how each design modification affects pedestrian interaction and pedestrian walking conditions. These scenario definitions and input parameters provide the basis for the numerical and heat map results presented in **Chapter 6**.

Chapter 6. Results of PLOS Analysis

Chapter 6 presents the numerical results for pedestrian space, pedestrian interaction, and the resulting PLOS for the evaluation of the Base Scenario and the five Alternative Scenarios for the case study area discussed in **Chapter 5**. We also discuss the heat maps that we develop to support and interpret the quantitative results we observe.

6.1 Results of PLOS Analysis for Case Studies

These values are calculated from five microsimulation model runs for each scenario to ensure consistency and reliability in the results. For every scenario, we evaluate the pedestrian space and pedestrian interaction for each minute of the 15-minute microsimulation, along with the overall average for the full duration. We use the pedestrian space and pedestrian interaction, and apply the novel PLOS model to determine the minute-by-minute PLOS and the overall PLOS. This approach provides a detailed understanding of walking conditions and how modifications to the design layouts in the study area can influence the walking patterns and experience of pedestrians, as well as the overall PLOS of a sidewalk (City of London, 2010; Kim et al., 2014).

6.1.1 Base Scenario

Figure 6.1. presents the results for the Base Scenario. It includes pedestrian space, pedestrian interaction, and PLOS on a minute-by-minute basis, as well as the overall average PLOS.

Figure 6.1a. illustrates pedestrian space for each minute of the 15-minute microsimulation period, together with the overall average. Pedestrian space fluctuates over time and responds to changes in pedestrian volume because the microsimulation model is stochastic. Pedestrian space varies throughout the microsimulation. Minute 1 records the lowest value at 1.52 m^2/ped. Minute 15

records the highest value at 3.82 m²/ped. The average pedestrian space over the full 15-minute period is 2.70 m²/ped. This value falls within the PLOS C range. As discussed in **Section 5.2**, PLOS C conditions were selected for the Base Scenario and Alternative Scenarios to provide a consistent reference point for evaluating the proposed model. The average value of 2.70 m²/ped is consistent with the randomly generated range defined in **Section 5.2.2**.

Figure 6.1b. shows pedestrian interaction for each minute and the overall average. Pedestrian interaction varies over time due to changes in the number and strength of pedestrian pair interactions. It is not constant across the 15-minute microsimulation period. Minute 2 records the lowest pedestrian interaction value at 134.90 m/s². Minute 10 records the highest values at 257.22 m/s². The low value in minute 2 reflects fewer pedestrian pair interactions and fewer path adjustments. The high value in minute 10 indicates more frequent interactions and greater movement adjustments. Minutes 6 and 11 show noticeable reductions following the peak values. This suggests sharp decreases in pedestrian interaction intensity rather than sustained changes in walking conditions. The average pedestrian interaction for the Base Scenario is 184.05 m/s². This value will serve as the reference for comparison with Alternative Scenarios 1 to 5 in the subsequent sections.

Figure 6.1c. presents the minute-by-minute PLOS classification and the overall average PLOS for the 15-minute microsimulation period. In minute 1, pedestrian space is 1.52 m²/ped as shown in **Figure 6.1a**. and pedestrian interaction is 172.00 m/s² as shown in **Figure 6.1b**. This corresponds to PLOS D+ according to the PLOS model shown in **Figure 4.14.** In minutes 2 and 3, pedestrian space increases to 3.41 and 3.18 m²/ped while pedestrian interaction decreases to 134.90 and 154.31 m/s², with minute 2 being the lowest pedestrian interaction value. These conditions correspond to PLOS C0. From minutes 2 to 14, the sidewalk generally operates within PLOS C.

The PLOS shifts between C0 and C- as pedestrian interaction changes. The highest pedestrian interaction values of 257.22 in minute 10 correspond to C-. Lower pedestrian interaction values with similar pedestrian space correspond to C0. In minute 15, pedestrian space reaches 3.82 m^2/ped, and pedestrian interaction is 178.88 m/s^2. This results in PLOS B-. The overall average PLOS for the Base Scenario is C0. However, this average does not reflect the variation observed at the minute level. Conditions range from D+ in minute 1 to B- in minute 15 during the simulation period. Under the traditional HCM method using **Table 2.2**, the 15 minutes would be represented by a single PLOS C value (HCM, 2000; HCM, 2016; TRB, 2020). The minute-level changes observed in this analysis would not be reflected. In addition, the minimum and maximum values for the two indicators, pedestrian space and pedestrian interaction, are observed at different times throughout the simulation period. This shows that changes in pedestrian space do not necessarily correspond to changes in pedestrian interaction at the same time.

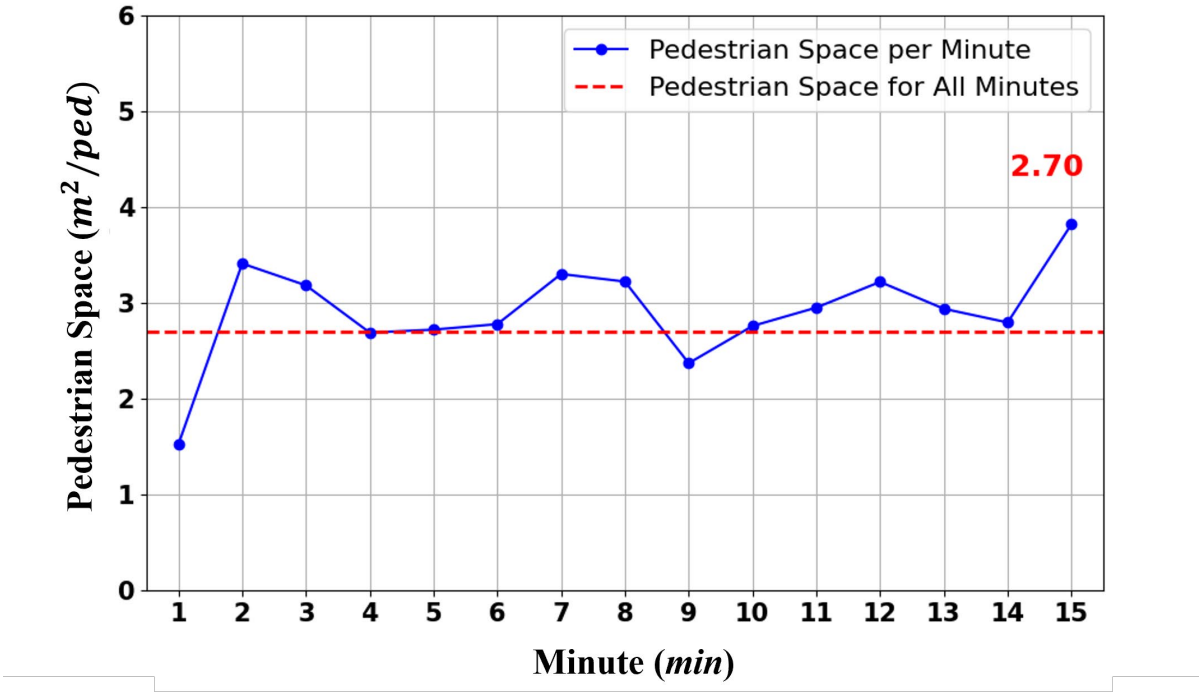

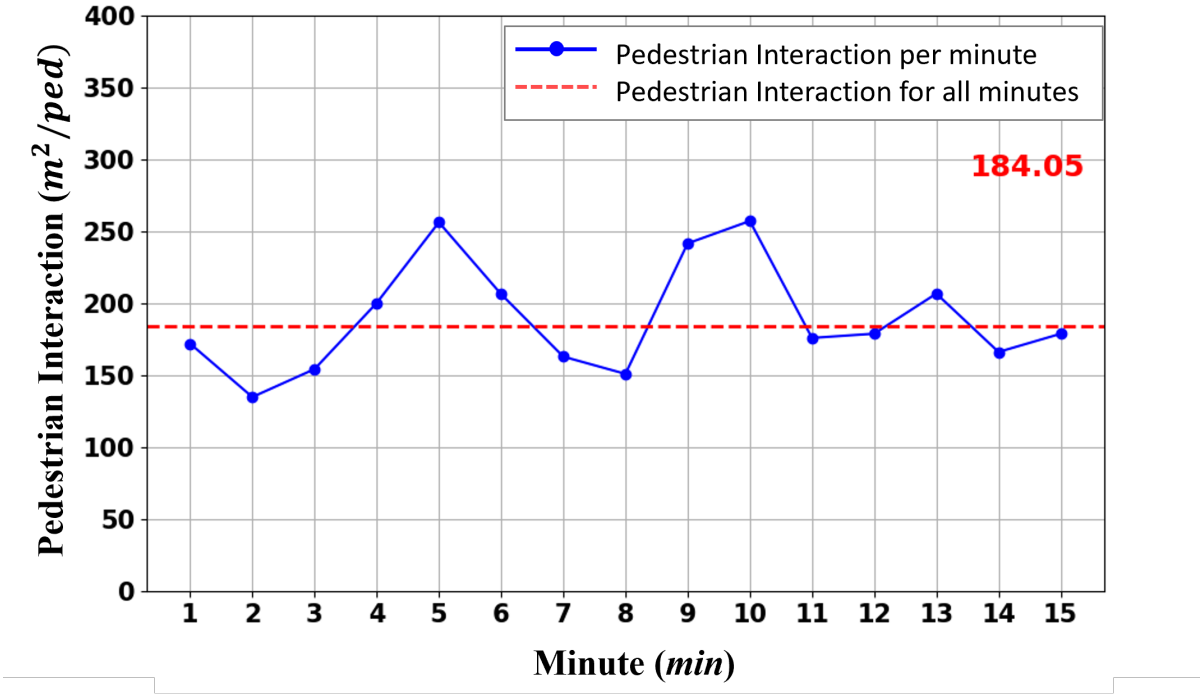

a) Pedestrian Space for Base Scenario

b) Pedestrian Interaction for Base Scenario

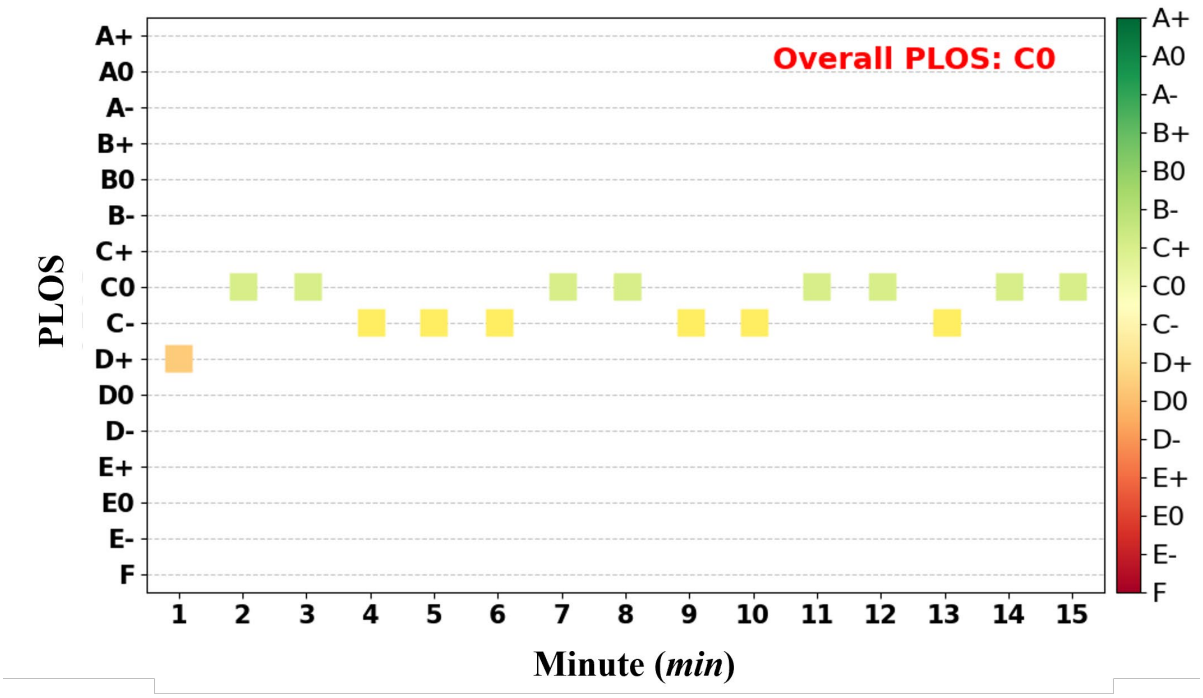

c) Overall PLOS for Base Scenario

Figure 6.1. Results for Base Scenario

6.1.2 Alternative Scenario 1: Addition of Advertisements

Figure 6.2. presents the results for Alternative Scenario 1, where advertisements are introduced in between the seating areas on the right side of the sidewalk.

Figure 6.2a. shows pedestrian space for each minute and the overall average. Pedestrian space fluctuates throughout the period, reflecting the stochastic nature of the microsimulation and variations in pedestrian interaction. Minute 1 records the lowest value at 1.56 m^2/ped, while minute 2 records the highest value at 3.29 m^2/ped. For the remaining minutes, pedestrian space generally remains within the PLOS C range, with moderate variation but no extreme deviations. The average pedestrian space is 2.7 m^2/ped. This value is identical to the Base Scenario and remains within PLOS C. Maintaining the same average pedestrian space ensures that any changes in overall operating conditions is due to the differences in pedestrian interaction rather than available space.

Figure 6.2b. presents pedestrian interaction for each minute and the overall average. Pedestrian interaction varies across the simulation in response to pedestrian pair interactions and local adjustments in walking paths. Minute 1 records the lowest values at 148.22 m/s^2, while minute 6 records the highest value at 276.20 m/s^2. Elevated values are also observed between minutes 5 and 8 and again in minutes 10 and 11, indicating repeated periods of increased pedestrian pair interactions. Compared with the Base Scenario, both the minimum and maximum pedestrian interaction values are higher. The average pedestrian interaction for Alternative Scenario 1 is 203.00 m/s^2, representing an increase of approximately 9% relative to the Base Scenario value of 184.05 m/s^2. This increase suggests that the presence of advertisements introduces localized disruptions in pedestrian walking experience. Pedestrians who pause or slow down near the

advertisements may require others to adjust their trajectories, leading to more frequent path modifications even though the overall pedestrian space remains unchanged.

Figure 6.2c. illustrates the minute-by-minute PLOS and the overall average. In minute 1, pedestrian space is 1.56 m^2/ped and pedestrian interaction is 148.22 m/s^2. This corresponds to PLOS D+ when using the proposed model from **Figure 4.14.** From minutes 2 to 4, higher pedestrian space combined with moderate pedestrian interaction results in C0 conditions. Between minutes 5 and 8, pedestrian interaction increases while pedestrian space remains within the PLOS C range, producing PLOS C-. A similar pattern occurs in minutes 10 and 11. In minute 12, pedestrian interaction decreases, and conditions temporarily improve to C0 before returning to C- toward the end of the period. The overall average PLOS for Alternative Scenario 1 is C-, representing a downgrade from the Base Scenario average of C0 despite identical average pedestrian space due to the noticeable increase in pedestrian interaction after adding advertisements.

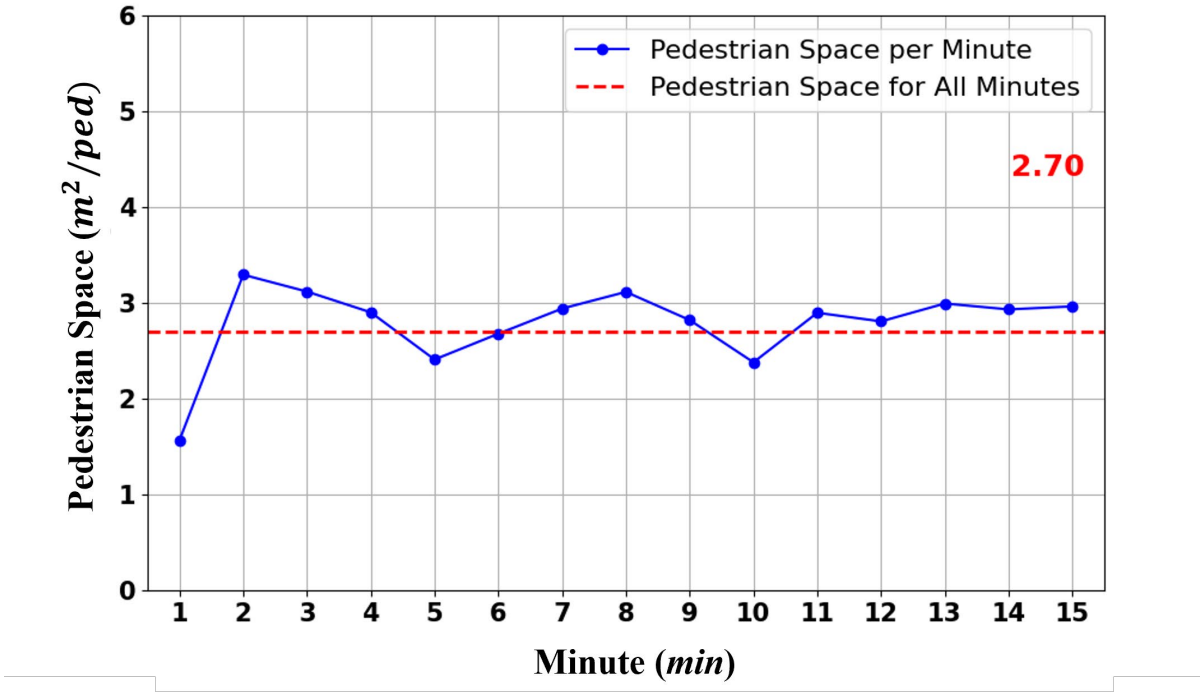

a) Pedestrian Space for Alternative Scenario 1

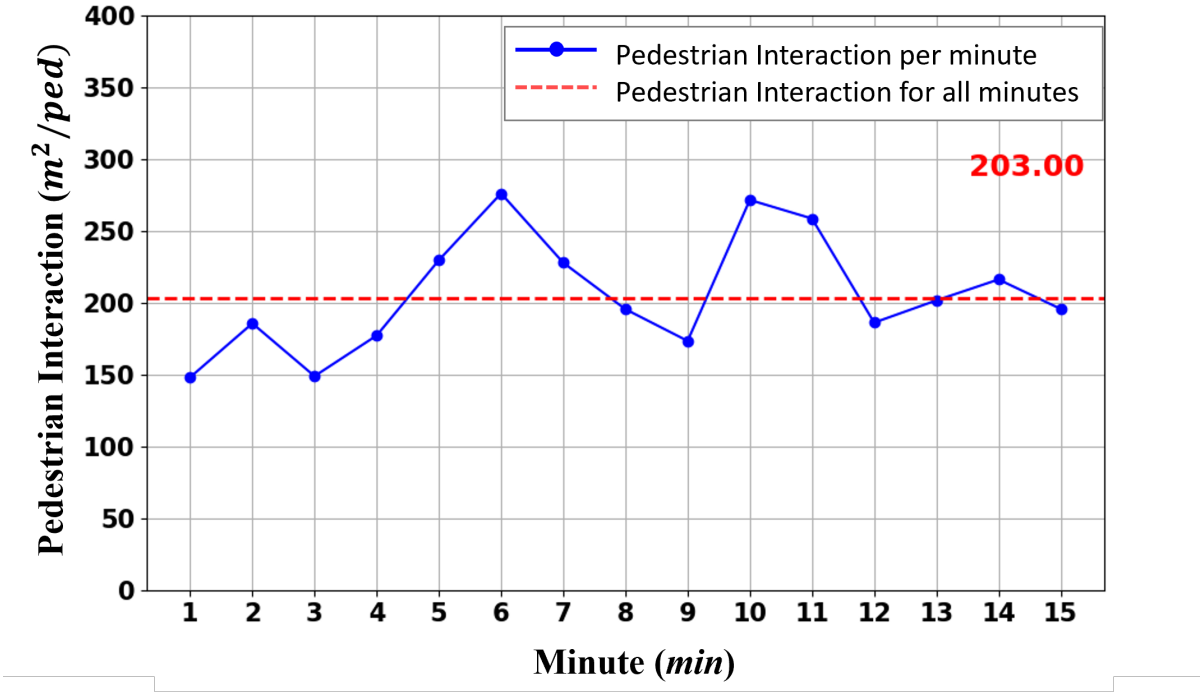

b) Pedestrian Interaction for Alternative Scenario 1

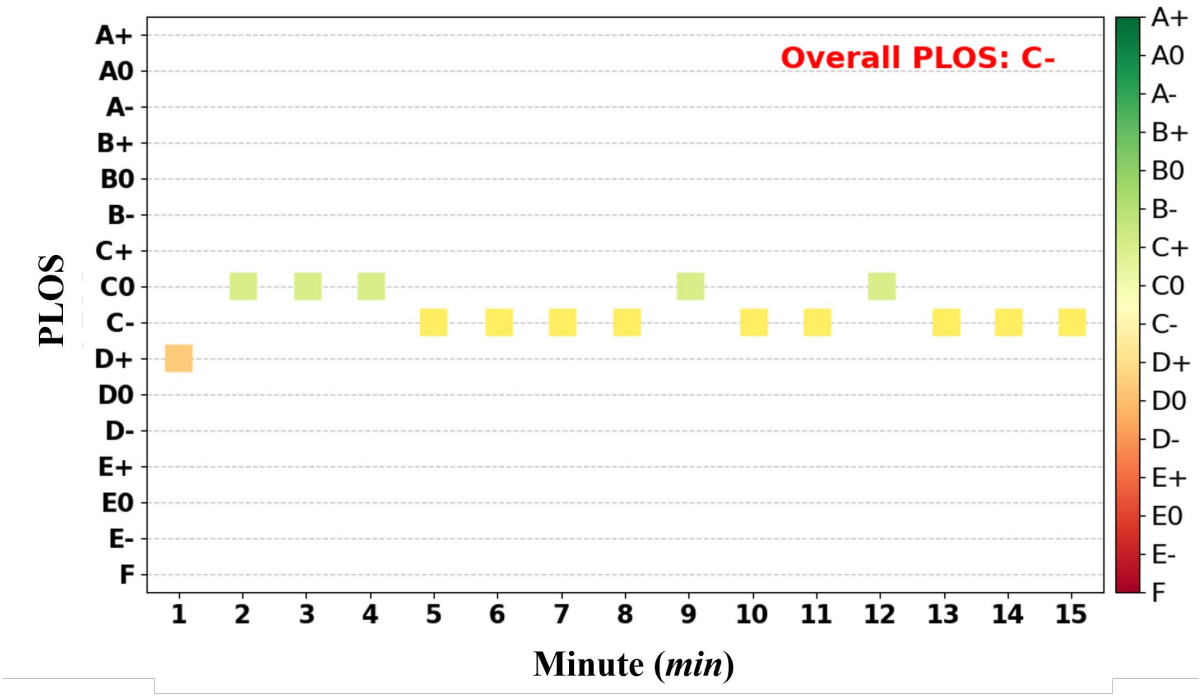

c) Overall PLOS for Alternative Scenario 1

Figure 6.2. Results for Addition of Advertisements (Alternative Scenario 1)

6.1.3 Alternative Scenario 2: Removal of Seats

Figure 6.3. presents the results for Alternative Scenario 2, where seating areas are removed from the sidewalk on the right side of the sidewalk.

Figure 6.3a. shows pedestrian space for each minute together with the overall average. Pedestrian space fluctuates throughout the 15-minute microsimulation period. Minute 1 records the lowest value at 1.61 m²/ped, while minute 15 records the highest value at 4.22 m²/ped. For most of the period, pedestrian space remains within the PLOS C range. The average pedestrian space is 2.70 m²/ped, which is the same as the Base Scenario.

Figure 6.3b. presents pedestrian interaction for each minute and the overall average. Pedestrian interaction varies over time in response to pedestrian pair interactions. Minute 2 records the lowest value at 115.68 m/s², while minute 9 records the highest value at 224.12 m/s². Compared with the Base Scenario, both the minimum and maximum pedestrian interaction values are lower. The average pedestrian interaction for Alternative Scenario 2 is 155.26 m/s², representing a decrease of approximately 15% relative to the Base Scenario value of 184.05 m/s². This is the largest reduction among all Alternative Scenarios. The removal of seating areas increases unobstructed walking space and reduces the frequency of pedestrian interactions and associated path adjustments.

Figure 6.3c. illustrates the minute-by-minute PLOS classification and the overall average. In minute 1, pedestrian space is 1.61 m²/ped and pedestrian interaction is 150.48 m/s². This corresponds to PLOS D+ according to the proposed model in **Figure 4.14**. In minute 2, pedestrian space increases to 3.04 m²/ped and pedestrian interaction decreases to 115.68 m/s², producing PLOS C+. From minutes 3 to 8, pedestrian space remains within the PLOS C range while pedestrian interaction fluctuates between 126.26 and 205.51 m/s². During this period, operating conditions are primarily C0, with brief shifts to C- in minutes 4 and 5. In minute 9, pedestrian interaction reaches 224.12 m/s² and conditions shift to C-. From minutes 10 to 13, pedestrian interaction stabilizes between 145.49 and 167.77 m/s², resulting in consistent C0 conditions. In minutes 14 and 15, pedestrian space increases to 3.77 and 4.22 m²/ped, while pedestrian interaction remains moderate, producing PLOS B-. The overall average PLOS for Alternative Scenario 2 is C0, which is the same as the Base Scenario. Although the average PLOS classification does not change, the decrease in pedestrian interaction indicates improved pedestrian operating conditions throughout much of the simulation period after removing the seats.

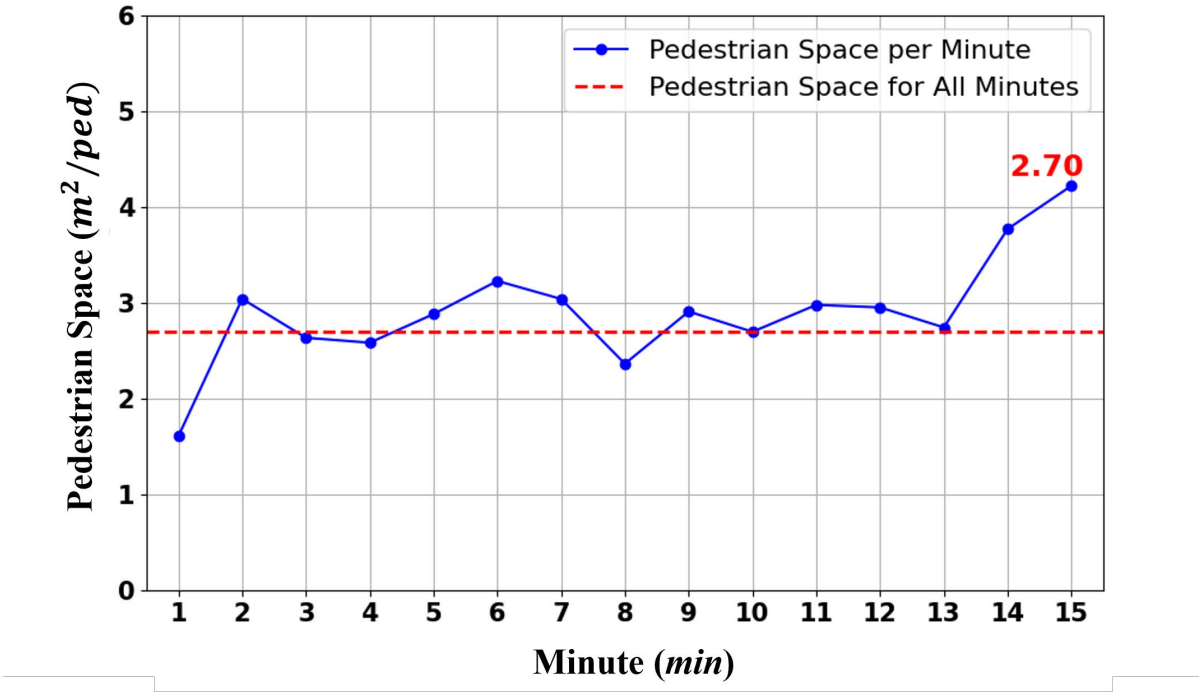

a) Pedestrian Space for Alternative Scenario 2

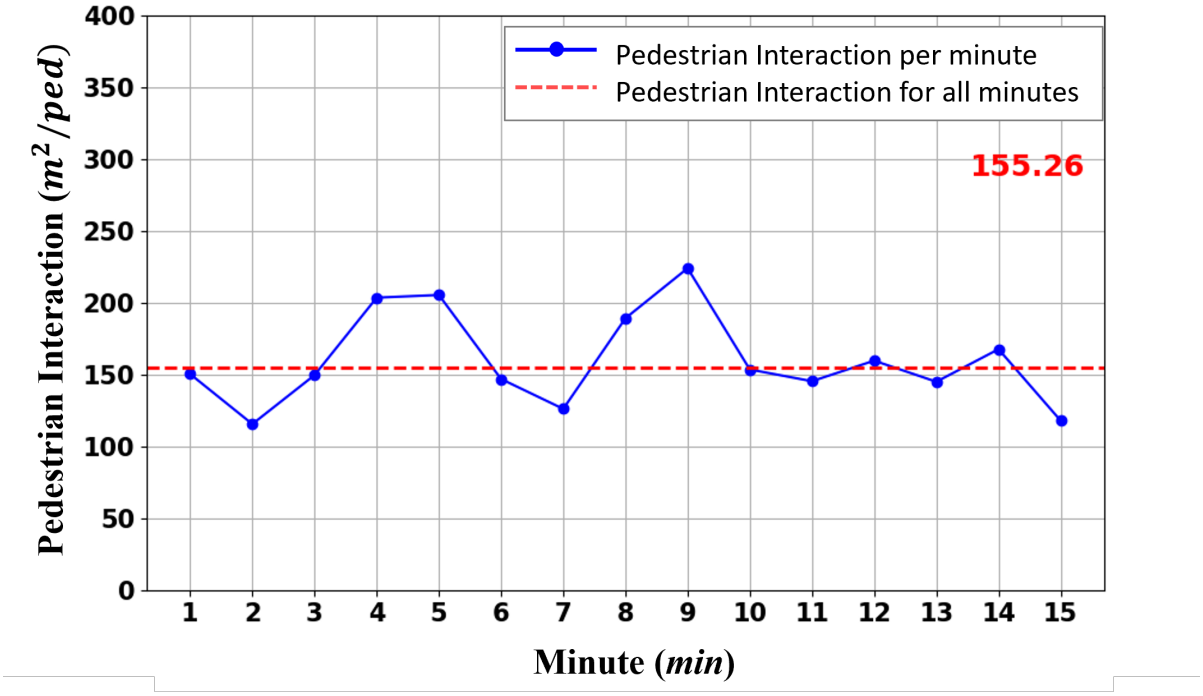

b) Pedestrian Interaction for Alternative Scenario 2

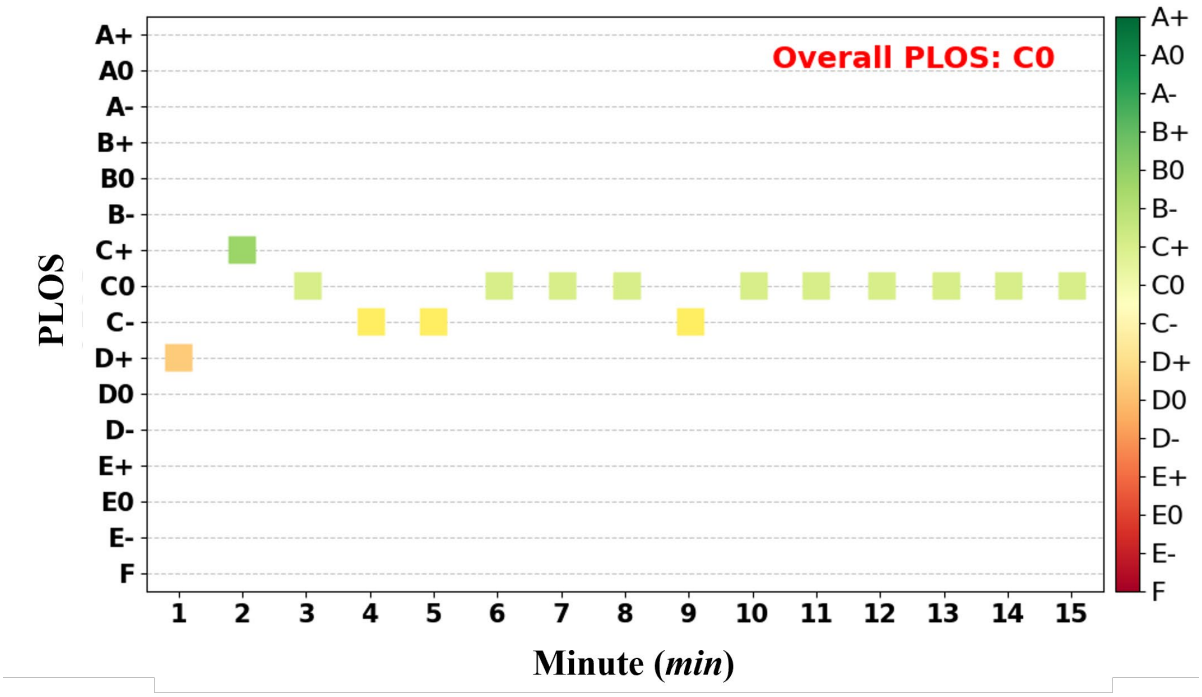

c) Overall PLOS for Alternative Scenario 2

Figure 6.3. Results for Removal of Seats (Alternative Scenario 2)

6.1.4 Alternative Scenario 3: Removal of stairs

Figure 6.4. presents the results for Alternative Scenario 3, where stair areas are removed from the sidewalk.

Figure 6.4a. shows pedestrian space for each minute and the overall average. Minute 1 records the lowest value at 1.58 m²/ped, while minute 15 records the highest value at 4.51 m²/ped. For most of the period, pedestrian space remains within the PLOS C range. The average pedestrian space is 2.70 m²/ped, which is the same as the Base Scenario.

Figure 6.4b. presents pedestrian interaction for each minute and the overall average. Pedestrian interaction varies over time in response to pedestrian pair interactions. Minute 15 records the

lowest value at 130.22 m/s², while minute 9 records the highest value at 269.72 m/s². Compared with the Base Scenario, the minimum pedestrian interaction is slightly lower, while the maximum pedestrian interaction is higher. The average pedestrian interaction for Alternative Scenario 3 is 176.22 m/s², representing a decrease of approximately 5% relative to the Base Scenario value of 184.05. Although the overall average decreases, short periods of elevated pedestrian pair interactions remain, particularly at minute 9. The removal of stair areas increases usable walking space and reduces overall interaction frequency, but localized peaks in pedestrian interaction still occur during specific minutes.

Figure 6.4c. illustrates the minute-by-minute PLOS classification and the overall average. In minute 1, pedestrian space is 1.58 m²/ped and pedestrian interaction is 165.04 m/s², corresponding to PLOS D+ according to the proposed model in **Figure 4.14.** In minutes 2 and 3, pedestrian space increases to 3.01 and 2.78 m²/ped while pedestrian interaction remains moderate, resulting in PLOS C0 conditions. In minutes 4 and 5, pedestrian interaction increases to 210.33 and 231.82 m/s², producing temporary C- conditions. Minutes 6 and 7 return to C0 as pedestrian interaction decreases and pedestrian space increases. In minute 9, pedestrian interaction reaches 269.72 m/s² and conditions shift to C-. From minutes 10 to 14, pedestrian interaction moderates and operating conditions are primarily C0. In minute 15, pedestrian space reaches 4.51 m²/ped and pedestrian interaction decreases to 130.22 m/s², producing PLOS B-. The overall average PLOS for Alternative Scenario 3 is C0, which is the same as the Base Scenario. Although the average PLOS classification does not change, the reduction in average pedestrian interaction indicates modest improvement in overall sidewalk conditions after removing the stairs.

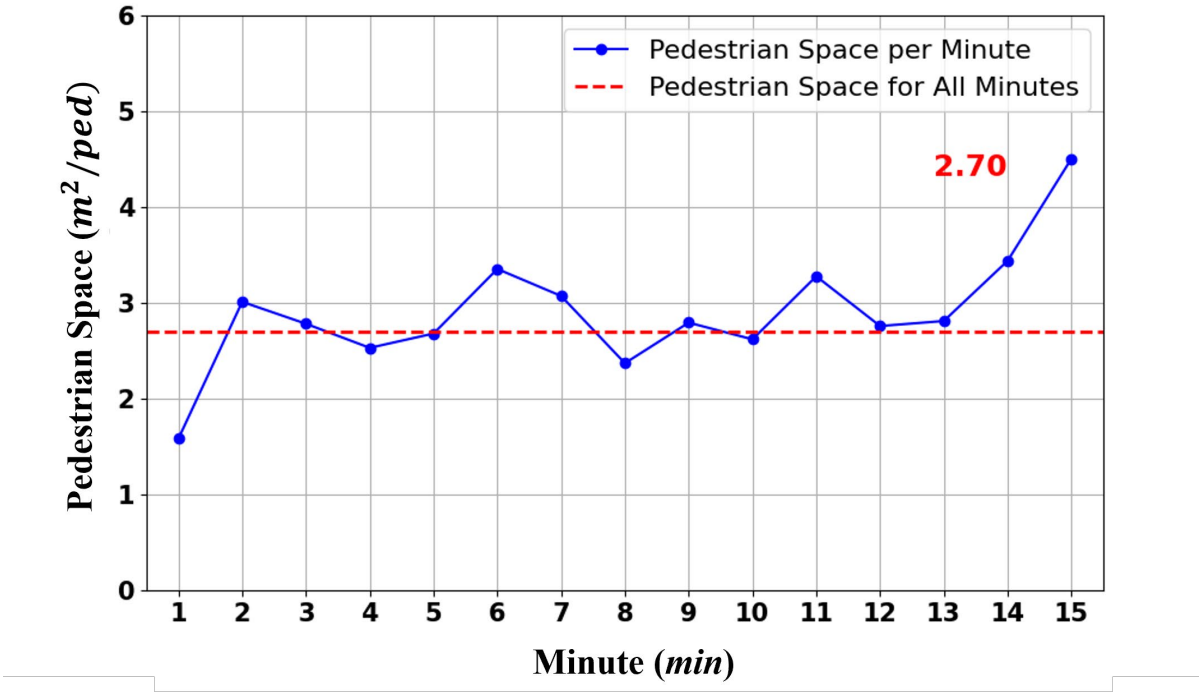

a) Pedestrian Space for Alternative Scenario 3

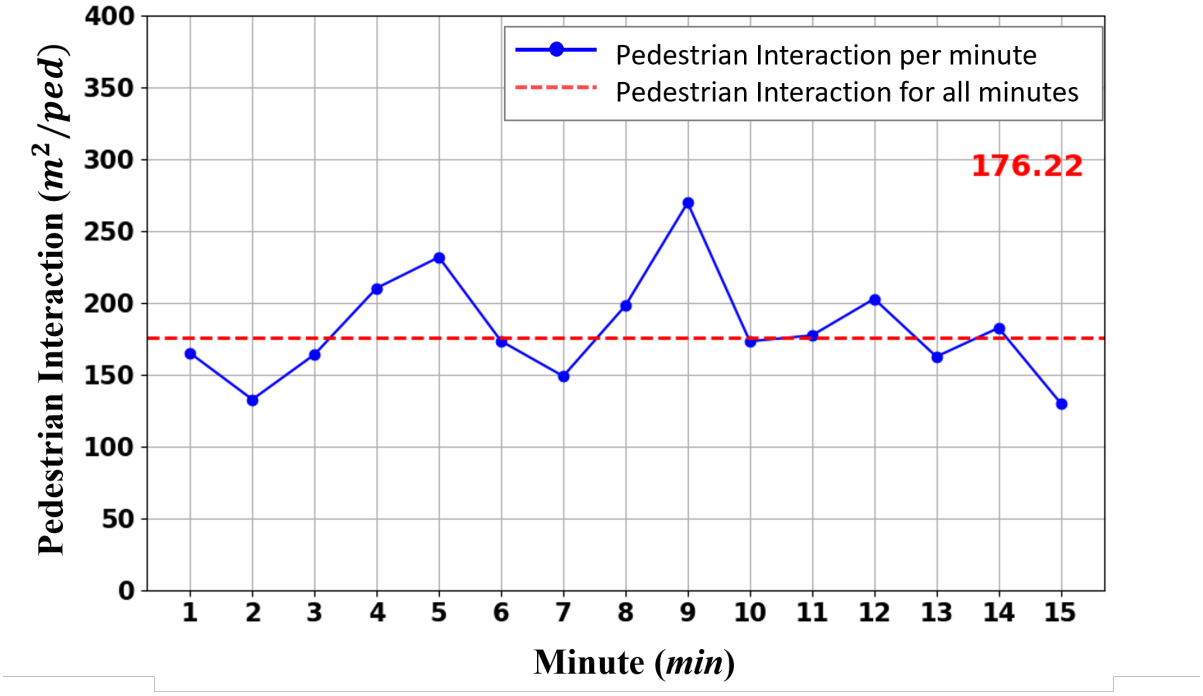

b) Pedestrian Interaction for Alternative Scenario 3

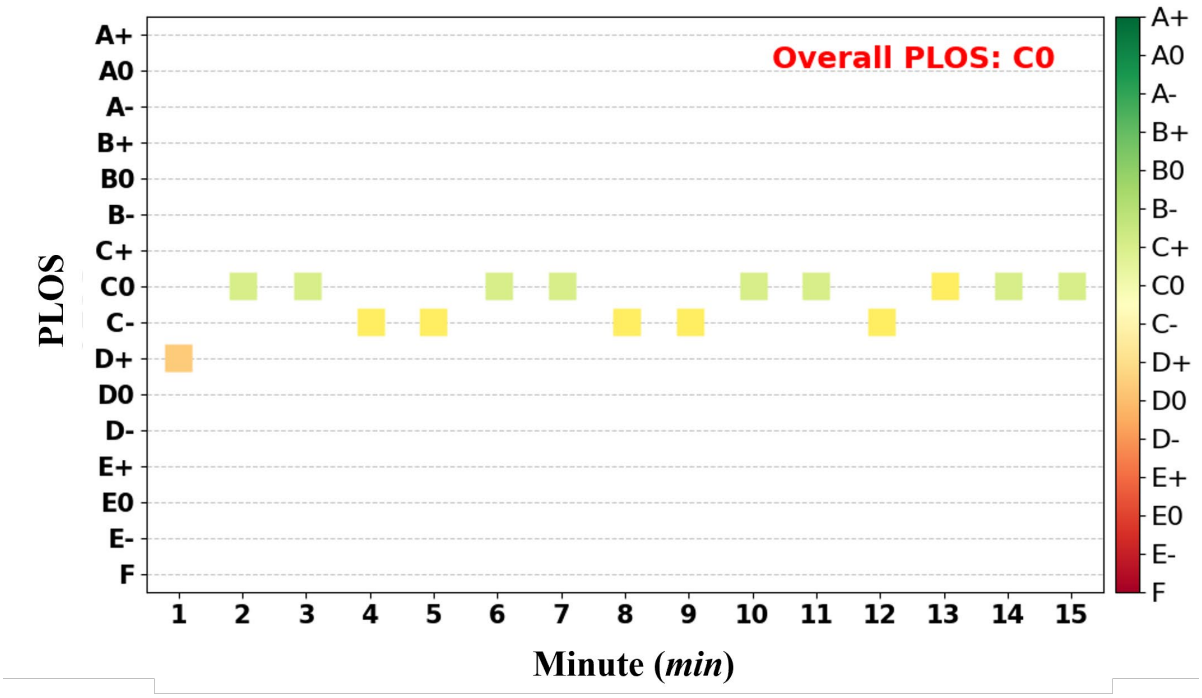

c) Overall PLOS for Alternative Scenario 3

Figure 6.4. Results for Removal of Stairs (Alternative Scenario 3)

6.1.5 Alternative Scenario 4: Addition of Construction Zone

Figure 6.5. presents the results for Alternative Scenario 4, where a construction zone is introduced that blocks a portion of the available walking space.

Figure 6.5a. shows pedestrian space for each minute and the overall average. Pedestrian space fluctuates throughout the 15-minute microsimulation period. Minute 1 records the lowest value at 1.51 m² per person, while minute 2 records the highest value at 3.48 m²/ped. For most of the period, pedestrian space remains within the PLOS C range. The average pedestrian space is 2.70 m²/ped, which is the same as the Base Scenario. Maintaining the same average pedestrian space allows direct comparison of pedestrian interaction effects.

Figure 6.5b. presents pedestrian interaction for each minute and the overall average. Pedestrian interaction varies across the simulation period. Minute 3 records the lowest value at 167.09 m/s², while minute 10 records the highest value at 313.99 m/s². Compared with the Base Scenario, both the minimum and maximum pedestrian interaction values are higher. The average pedestrian interaction for Alternative Scenario 4 is 217.29 m/s², representing an increase of approximately 18% relative to the Base Scenario value of 184.05 m/s². This is the largest increase among all Alternative Scenarios. The range of pedestrian interaction is also greater, indicating more pronounced fluctuations throughout the simulation period. The presence of the construction zone reduces effective walking width in a localized area, which leads to more frequent pedestrian interactions and greater movement adjustments.

Figure 6.5c. illustrates the minute-by-minute PLOS classification and the overall average. In minute 1, pedestrian space is 1.51 m²/ped and pedestrian interaction is 190.65 m/s², corresponding to PLOS D+ according to **Figure 4.14**. In minute 2, pedestrian space increases to 3.48 m²/ped; however, pedestrian interaction also remains elevated at 170.16 m/s², resulting in PLOS C0. From minutes 3 to 5, pedestrian interaction increases from 167.09 to 288.90 m/s² while pedestrian space remains within the PLOS C range. Conditions shift from C0 in minute 3 to C- in minutes 4 and 5. Between minutes 6 and 9, pedestrian interaction remains consistently high and conditions are predominantly C-, with only a brief return to C0 in minute 8. In minute 10, pedestrian interaction reaches its peak at 313.99 m/s², producing PLOS C- conditions. From minutes 11 to 15, pedestrian space remains near 3.00 m²/ped, yet pedestrian interaction remains elevated between 202.50 and 233.94 m/s². As a result, PLOS C- is observed through the remainder of the simulation period. The overall average PLOS for Alternative Scenario 4 is C-, representing a downgrade from the Base Scenario average of C0. Although the average pedestrian space remains unchanged, the sustained

increase in pedestrian interaction results in poorer operating conditions for the sidewalk across the majority of the microsimulation period. This shows that introducing a localized obstruction has a measurable impact on pedestrian interactions and overall sidewalk performance.

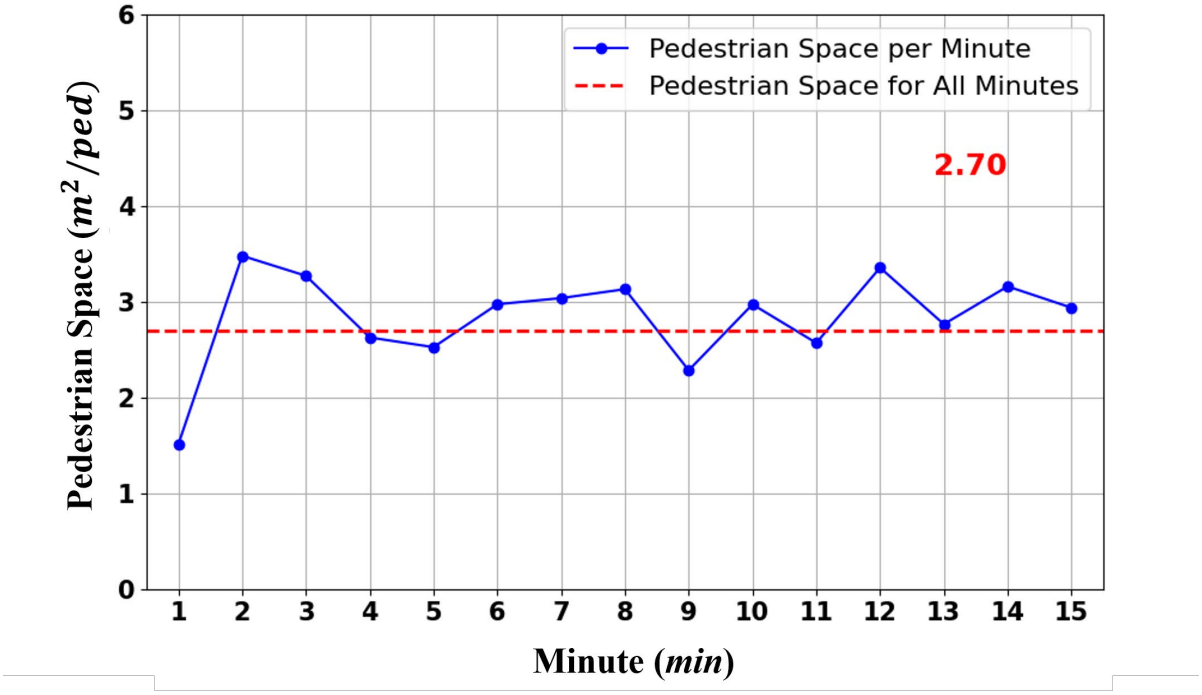

a) Pedestrian Space for Alternative Scenario 4

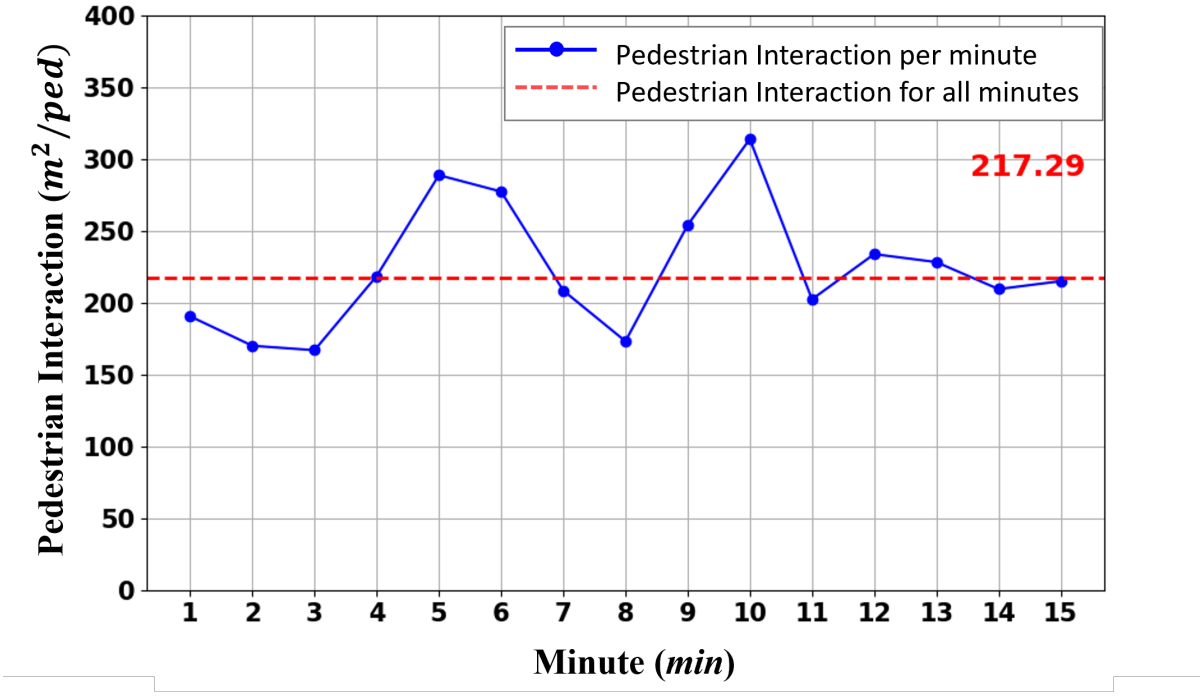

b) Pedestrian Interaction for Alternative Scenario 4

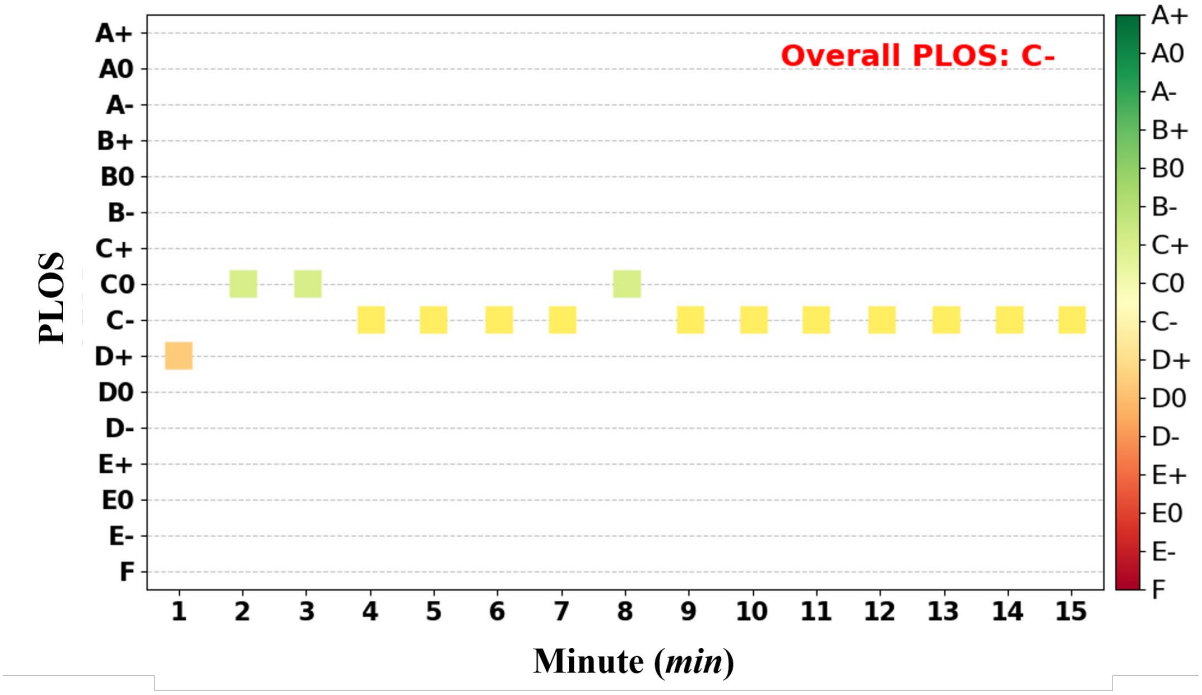

c) Overall PLOS for Alternative Scenario 4

Figure 6.5. Results for Addition of Construction Zone (Alternative Scenario 4)

6.1.6 Alternative Scenario 5: Addition of Hazard Tape

Figure 6.6. presents the results for Alternative Scenario 5, where hazard tape barriers block a portion of the sidewalk along its full length.

Figure 6.6a. shows pedestrian space for each minute together with the overall average. Minute 1 records the lowest value at 1.56 m²/ped, while minute 15 records the highest value at 4.31 m²/ped. For most of the period, pedestrian space remains within the PLOS C range. The average pedestrian space is 2.70 m²/ped, which is consistent with the Base Scenario.

Figure 6.6b. presents pedestrian interaction for each minute and the overall average. Minute 2 records the lowest value at 154.99 m/s², while minute 9 records the highest value at 310.25 m/s². Compared with the Base Scenario, both the minimum and maximum pedestrian interaction values are higher. The average pedestrian interaction for Alternative Scenario 5 is 206.76 m/s², representing an increase of approximately 12% relative to the Base Scenario value of 184.05 m/s². Elevated values are observed across several consecutive minutes, indicating sustained increases in pedestrian interactions. Although the hazard tape reduces only a portion of the sidewalk width, the restriction extends along the full sidewalk length. This continuous narrowing contributes to more frequent path adjustments and higher overall interaction intensity.

Figure 6.6c. illustrates the minute-by-minute PLOS classification and the overall average. In minute 1, pedestrian space is 1.56 m²/ped and pedestrian interaction is 193.20 m/s², corresponding to PLOS D+ according to **Figure 4.14**. In minutes 2 and 3, pedestrian space increases to approximately 2.96 m²/ped while pedestrian interaction decreases, producing PLOS C0. From minutes 4 to 6, pedestrian interaction rises, reaching 285.63 m/s² in minute 5, and operating conditions shift to C-. In minute 7, pedestrian interaction decreases briefly and conditions return

to C0. From minutes 8 to 14, pedestrian interaction remains elevated between 205.65 and 310.25 m/s² while pedestrian space remains within the PLOS C range. In minute 15, pedestrian space reaches 4.31 m² /ped and pedestrian interaction decreases, producing PLOS B-. As a result, the overall average PLOS is C-. Although the average pedestrian space remains unchanged, the increase in pedestrian interaction results in a poorer pedestrian experience. This shows that adding a hazard tape on a section of the sidewalk along its full length affects the amount of pedestrian pair interactions and overall sidewalk performance.

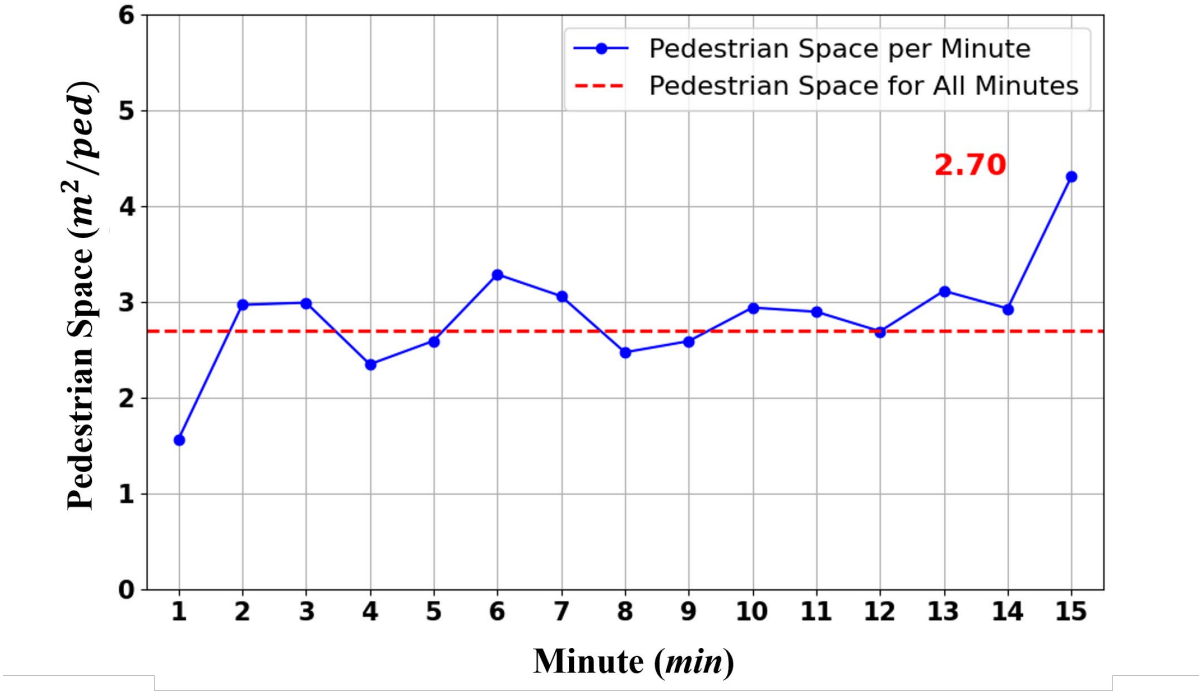

a) Pedestrian Space for Alternative Scenario 5

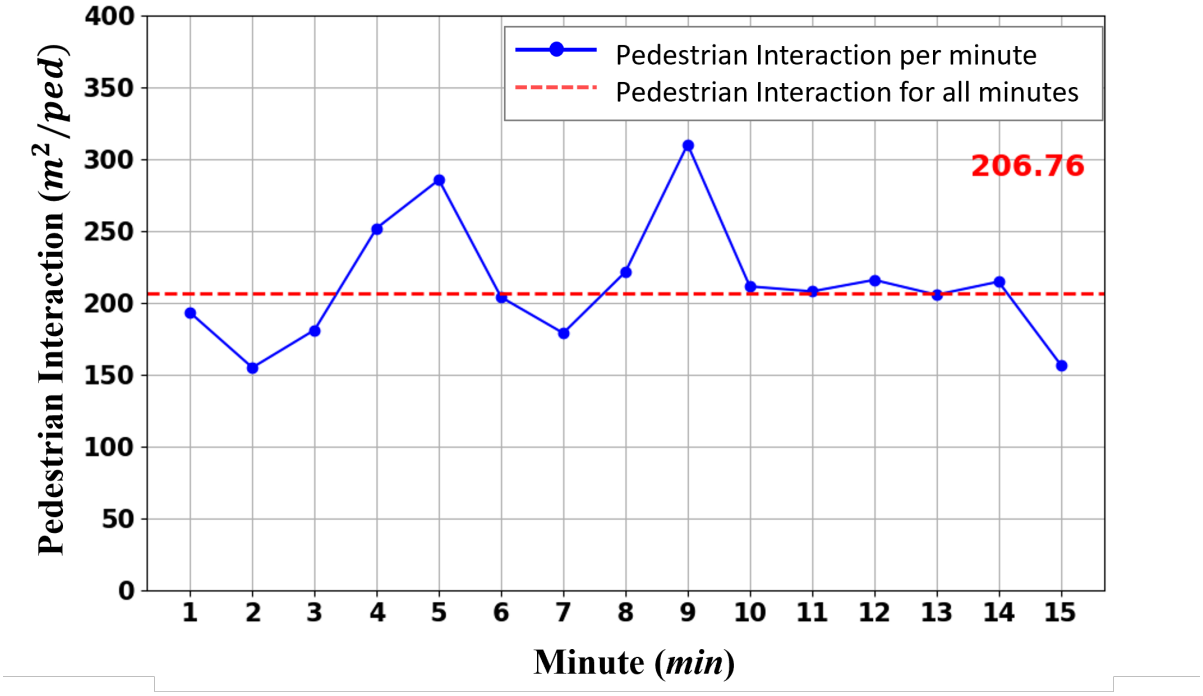

b) Pedestrian Interaction for Alternative Scenario 5

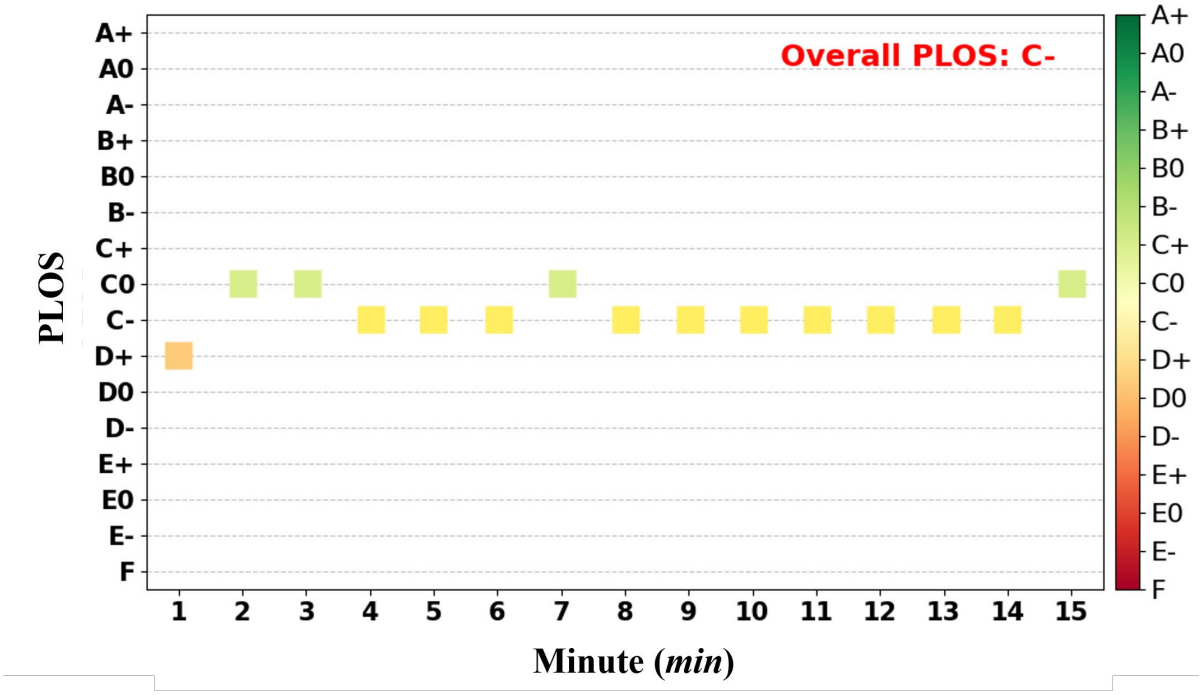

c) Overall PLOS for Alternative Scenario 5

Figure 6.6. Results for Addition of Hazard Tape (Alternative Scenario 5)

6.2 Heat Map Results

This section presents heat maps that illustrate the spatial pattern of pedestrian interaction intensity observed throughout the sidewalk. The purpose of this additional visualization is to show how pedestrian interaction and PLOS is affected by modifying design features or surface elements. We describe the results for the Base Scenario and Alternative Scenarios 1 to 5. Each comparison examines how the introduction of a new design element or layout changes the pedestrian interaction heat map and subsequently PLOS over the same 15-minute simulation period. The heat maps use colour gradients to show how pedestrian interaction varies along the sidewalk. Cooler colours, ranging from blue to green, indicate lower levels of pedestrian interaction, while warmer colours, ranging from yellow to red, indicate higher levels of pedestrian interaction. These colours help distinguish areas with more frequent pedestrian pair interactions, such as shoulder brushing, collision avoidance, or path adjustments, from areas with fewer interactions.

The colour scale shown beside each heat map is based on normalized pedestrian interaction values. After calculating pedestrian interaction across the sidewalk, the values are normalized to a scale between 0 and 1 using the minimum and maximum pedestrian interaction observed in the microsimulation. A value of 0 represents the lowest observed pedestrian interaction intensity (blue), while a value of 1 represents the highest observed intensity (red). Intermediate values, such as 0.25, 0.50, and 0.75, represent proportional increases in pedestrian interaction intensity between the lowest and highest observed values. Therefore, the y-axis labels on the colour bar do not represent raw pedestrian interaction values, but normalized intensity levels used to compare low, moderate, high, and highest pedestrian interaction areas visually.

6.2.1 Base Scenario versus Alternative Scenario 1

The average pedestrian interaction increased from 184.05 m/s² in the Base Scenario to 203.00 m/s² in Alternative Scenario 1. To understand the impact better, we provide **Figure 6.7a and Figure 6.7b** which show the pedestrian interaction heat maps for the Base scenario and Alternative Scenario 1. where advertisement posters were added along the walls of the sidewalk.

If we look at **Figure 5.2**, we observe that the stairs are located on the left side of the sidewalk and seats are located on the right side of the sidewalk and are also exactly in front of each other. The advertisement posters are also positioned on the wall behind the seat. Therefore, this creates a significantly narrow sidewalk for pedestrians, which acts as hotspots since there is less walking space available for pedestrians to walk in. Therefore, we expect to see a significantly higher pedestrian interaction intensity in those hotspots, where the advertisements are due to the increase in the number of shoulder brushing and collisions and the number of times pedestrians need to alter their walking direction to avoid other people.

The Base Scenario in **Figure 6.7a.** shows that the intensity of the heatmap in front of the stairs and seats is high (i.e., shown in red colour). Adding advertisements throughout the sidewalk in Alternative Scenario 1 adversely worsens the conditions of the sidewalk and increases the intensity of the heatmap in those hotspots, as seen in **Figure 6.7b.** This is also apparent as we highlight in the findings in **Section 6.1.2**. Therefore, decision makers should not only avoid adding advertisements in constrained areas where pedestrians typically stay or frequently move within but also try to relocate the stairs or seats in the Base Scenario to improve the design layout of the sidewalk.

Additionally, the Base Scenario in **Figure 6.7a.** shows that the colour pattern of the heat map is mostly consistent through the middle of the sidewalk, even with the highest pedestrian interaction being focused throughout the middle area of the sidewalk width. This can be because the walking trajectory of pedestrians typically follows a straighter line in comparison to Alternative Scenario 1. On the other hand, Alternative Scenario 1 in **Figure 6.7b.** illustrate that the red areas become more visible and concentrated near the advertisements that were added along the sidewalk. These are the areas where pedestrians may stop in the middle of the sidewalk to observe the advertisement posters. The more clustered hotspots on the heatmap of Alternative Scenario 1, in comparison to the Base Scenario, show areas with higher pedestrian interaction where pedestrians need to slow down or adjust their paths to look at the advertisements or walk around others who have stopped and are highlighted by the more intense red colours.

Overall, the addition of advertisements along the sidewalk causes brief interruptions in the movements of pedestrians that are enough to worsen the sidewalk conditions and PLOS, as shown in **Figure 6.7b**. The heat maps for Alternative Scenario 1 support the findings from **Section 6.1.2** and show that pedestrian interaction can capture small behavioural changes within pedestrians, like stopping or shifting paths, that pedestrian space alone might not show.

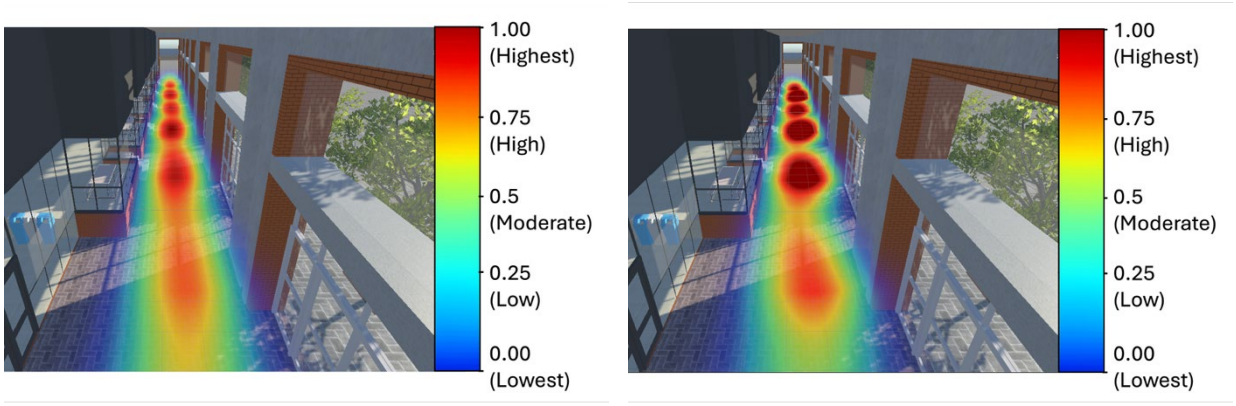

a) Base Scenario b) Alternative Scenario 1

Figure 6.7. Heat Map for Base Scenario versus Alternative Scenario 1

6.2.2 Base Scenario versus Alternative Scenario 2

The average pedestrian interaction decreased from 184.05 m/s² in the Base Scenario to 155.26 m/s² in Alternative Scenario 2. To understand the impact better, we provide **Figure 6.8a and Figure 6.8b** that show the pedestrian interaction heat map for the Base Scenario and Alternative Scenario 2 when the seats are removed throughout the sidewalk.

By looking at **Figure 5.1.**, we observe that the seats are located on the right side of the sidewalk and the stairs are located directly opposite to it on the left. Therefore, by removing the seats and as shown in **Figure 5.3.**, we expect to see a lower pedestrian interaction intensity since more walking space is available for pedestrians in comparison to the Base Scenario. This is largely due to the decrease in the number of times pedestrians need to adjust their walking path to avoid other people, and also the lower number of shoulder brushing and collisions we observe during the microsimulation.

The Base Scenario **Figure 6.8a.** shows that the heatmap intensity in front of the stairs turned from a red colour to a yellow colour in Alternative Scenario 2, as shown in **Figure 6.8b.** Alternative Scenario 2 improves the conditions of the sidewalk, and this is shown in the reduced intensity of the heatmap. Although the PLOS of Alternative Scenario 2 and Base Scenario is the same at PLOS C0, the heat map still highlights the decrease in the pedestrian interaction, which improves the sidewalk. This is because removing multiple seats along the sidewalk creates more walking space for pedestrians and also creates a consistent walking area that was not available before. The Base Scenario has a narrower sidewalk that is constrained by the seats and stairs on each side, which limits the available walking space. This results in more pedestrian interactions for pedestrians, which is highlighted by the more intense red colour in the Base scenario. By removing seats in Alternative Scenario 2, the heatmap intensity decreased and turned to a yellow colour. Although there is an improvement, pedestrians still experience a minimal amount of pedestrian interaction due to the presence of the stairs on the left side of the sidewalk. Therefore, decision makers must consider the overall design layout of the sidewalk when making changes to its layout, especially where we expect more pedestrians to walk by or pass through, to maximize improving the sidewalk.

Additionally, the heatmap for Alternative Scenario 2 in **Figure 6.8a** shows that the colour pattern of the heat map appears more evenly distributed across the sidewalk, with the red areas eliminated in comparison to the Base Scenario. This is because removing stairs increases the available walking space providing pedestrians with more room to move and walk in. The absence of the red areas illustrates the findings from **Section 6.1.3.** that there is a significant decrease in the pedestrian interaction, given that they can move more consistently with minimal interruptions to their walking trajectory to avoid shoulder brushing or collisions with other pedestrians.

Overall, the heat maps for Alternative Scenario 2 support the findings from **Section 6.1.3.** It shows that the removal of the seats along the sidewalk helps minimize changes to the pedestrian's original behaviour that is sufficient to improve the PLOS and sidewalk conditions.

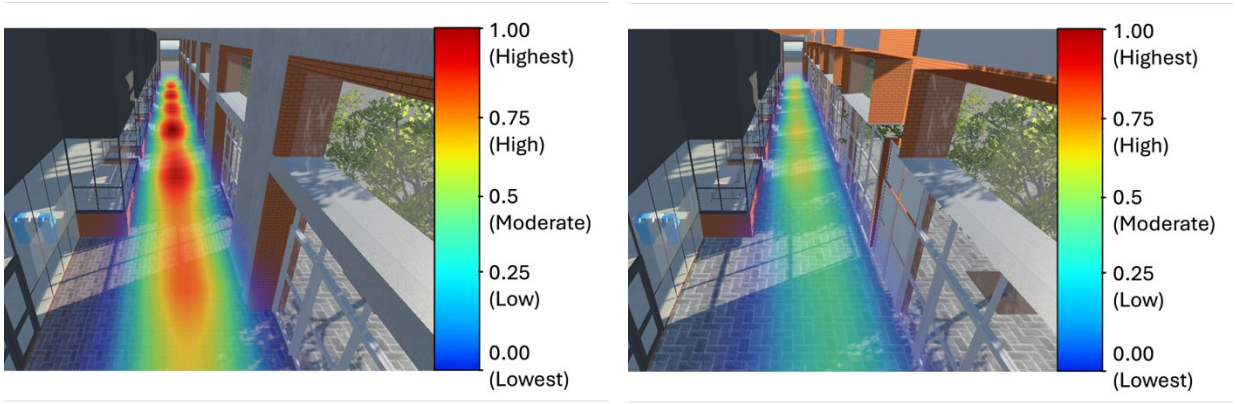

a) Base Scenario b) Alternative Scenario 2

Figure 6.8. Heat Map for Base Scenario versus Alternative Scenario 2

6.2.3 Base Scenario versus Alternative Scenario 3

The average pedestrian interaction decreased from 184.05 m/s² in the Base Scenario to 176.22 m/s² in Alternative Scenario 3. To understand the impact better, we provide **Figure 6.9a. and Figure 6.9b.** that shows the pedestrian interaction heat map for the Base Scenario and Alternative Scenario 3 when the stairs are removed throughout the sidewalk.

By looking at **Figure 5.1.**, we observe that the stairs are located on the left side of the sidewalk and the stairs are located directly opposite to it on the left. Therefore, by removing the stairs and as shown in **Figure 5.4.**, we expect to see a slightly lower pedestrian interaction intensity since there is more available walking space for pedestrians in comparison to the Base Scenario. We

observe this due to the lower number of interruptions where pedestrians need to alter their walking trajectory to avoid shoulder brushing and collisions with other people.

The Base Scenario in **Figure 6.9a.** shows that the heatmap intensity in front of the seats turned from a red colour to a mix of yellow and red colour in Alternative Scenario 3, as shown in **Figure 6.9b.** Alternative Scenario 3 still improves the conditions of the sidewalk, and this is shown in the reduced intensity of the yellow and red colours in the heatmap. Although the PLOS of Alternative Scenario 3 and Base Scenario is the same at PLOS C0, the heat map still highlights the decrease in the pedestrian interaction, showing improvements to the sidewalk operations. Eliminating multiple stairs along the sidewalk allows pedestrians to have more space to walk on and also allows for a more direct walking path since we remove intermittent constrained areas. The Base Scenario has a narrower sidewalk that is constrained by the seats and stairs on each side, which limits the available walking space. This results in more pedestrian interactions for pedestrians, which is highlighted by the intense red colour in the Base scenario. Removing the stairs on the left side in Alternative Scenario 3 decreases the intensity of the heatmap and frequency of high pedestrian interaction. However, we note that there are still areas with some red colour that are less intense, so this illustrates the moderate amount of high pedestrian interaction that pedestrians experience due to the presence of the seats on the right side of the sidewalk.

Additionally, the heatmap for Alternative Scenario 3 in **Figure 6.9b.** shows that although the colour pattern of the heat map appears more evenly distributed across the sidewalk in comparison to the Base Scenario, there are still red colours in the heat map. We observe the less intense red colours in front of the seats throughout the sidewalk because although we removed the stairs, which added more walking space, the seats on the right side still provide enough constraint to pedestrians, leading to areas with some high pedestrian interaction as discussed in **Section 6.1.4.**

Overall, the heat maps for Alternative Scenario 3 support the findings from **Section 6.1.4.** The removal of the stairs along the sidewalk provides enough additional walking space to reduce the pedestrian interaction pedestrians experience as they walk through the sidewalk.

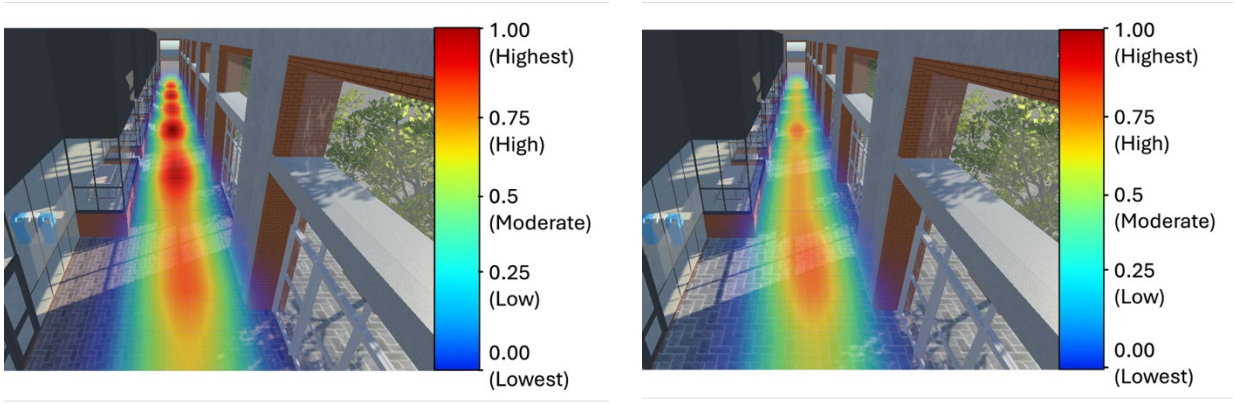

a) Base Scenario b) Alternative Scenario 3

Figure 6.9. Heat Map for Base Scenario versus Alternative Scenario 3

6.2.4 Base Scenario versus Alternative Scenario 4

The average pedestrian interaction increased from 184.05 m/s² in the Base Scenario to 217.29 m/s² in Alternative Scenario 4. To understand the impact better, we provide **Figure 6.10a.** and **Figure 6.10b.** that shows the pedestrian interaction heat map for the Base Scenario and Alternative Scenario 4 when a construction zone is added to a specific area of the sidewalk.

We observe in **Figure 5.1.** that the seats remain on the right side of the sidewalk and the stairs are located directly opposite to it on the left, and a garbage bin is located on the left side close to the south entrance of the sidewalk. In addition to this, Alternative Scenario 4 is shown in **Figure 5.5.** where we add a construction zone on a specific area close to the south entrance of the sidewalk. By adding the construction zone in its particular location on the sidewalk, we expect to see higher

pedestrian interaction and higher intensity of colours on the heat map. This is because the walking space is significantly reduced and constrained for a portion of the sidewalk.

The Base Scenario in **Figure 6.10a.** shows that the heatmap intensity in front of the construction zone and its directly adjacent area turns from a faint red colour to an intense deep red colour in Alternative Scenario 4, as shown in **Figure 6.10b.** We also observe that there is a significantly larger area where the red colour is apparent, and that the areas of the blue, green, and yellow colours are also wider, and it is closer to the edge of the sidewalks and closer to the doors within the area of the construction zone in Alternative Scenario 4. On the contrary, the outside border of the heatmap (in blue) for the Base Scenario outlines the typical walking path that pedestrians take, and it is noticeably straighter in comparison to Alternative Scenario 4. This also shows that pedestrians use other areas of the sidewalk to walk on that they might typically not use to maximize the limited walking space available on the sidewalk due to the constraint from the construction zone. Alternative Scenario 4 worsens the conditions of the sidewalk, and this is shown in the increased areas with red colours and the high intensity of the colours of the heatmap and is also highlighted in **Section 6.1.5.** where the PLOS changes from C0 to C- from the Base Scenario to Alternative Scenario 4. A simple addition that can block the walking area of pedestrians clearly impacts the conditions of a sidewalk so decision-makers should be mindful of the design layout of the sidewalk and consider avoiding adding an item that acts as a physical obstacle.

Additionally, the heatmap for Alternative Scenario 4 in **Figure 6.10b.** shows that the colour pattern is more intense, which means that pedestrian pair interactions are experiencing high pedestrian interactions frequently, especially where the construction zone is located. In comparison to the Base Scenario, although we can see in **Figure 6.10a.** that there are still areas with blue, green, yellow and red colours, it is less intense since pedestrians have a consistent walking space available

throughout the sidewalk. This confirms pedestrians experience a much higher level of pedestrian interaction throughout most of the corridor due to the addition of an object in one location in the sidewalk. This means that there are more shoulder brushes, collisions, and more frequent path adjustments among pedestrians to avoid each other and the construction zone area. The concentrated red area near the construction zone also indicates that movement becomes more constrained, possibly as pedestrians shift or slow down in response to nearby obstacles or a tighter walking space.

Overall, the heat maps for Alternative Scenario 4 support the findings from **Section 6.1.5**. Alternative Scenario 4 visually confirms how significantly higher the pedestrian interaction is for this scenario compared to the Base Scenario. The heat map shows that even small design changes that reduce available space or redirect pedestrian movement can significantly increase pedestrian interaction and lower overall PLOS.

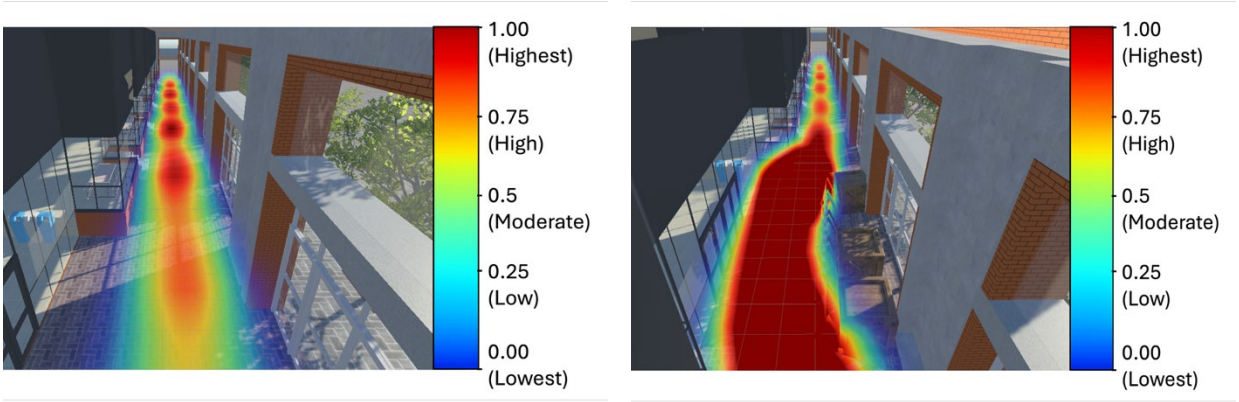

a) Base Scenario b) Alternative Scenario 4

Figure 6.10. Heat Map for Base Scenario versus Alternative Scenario 4

6.2.5 Base Scenario versus Alternative Scenario 5

The average pedestrian interaction increased from 184.05 m/s² in the Base Scenario to 206.76 m/s² in Alternative Scenario 5. To understand the impact better, we provide **Figure 6.11a.** and **Figure 6.11b.** that shows the pedestrian interaction heat map for the Base Scenario and Alternative Scenario 5 when we add a hazard tape on the sidewalk that spans its full length.

By looking at **Figure 5.1.**, we observe that the seats remain on the right side of the sidewalk and the stairs are located directly opposite to it on the left, and a garbage bin is on the left side close to the south entrance of the sidewalk. In addition to this, Alternative Scenario 5 is shown in **Figure 5.6.** where we add a hazard tape along a designated section of the sidewalk on the right side that fully spans its entire length. Adding the hazard tape creates a complete barrier to pedestrian movement within that section and forces pedestrians to avoid the restricted area, limiting their walking space throughout the sidewalk. We expect to see that the entire sidewalk will have a higher number of shoulder brushing and collisions due to the decrease in the available walking space throughout.

The Base Scenario in **Figure 6.11a.** shows that the colours in the heatmap for the entire sidewalk are more intense in Alternative Scenario 5, as shown in **Figure 6.11b.** We also observe that the colour pattern of the heatmaps and where the blue, green, yellow, and red colours for the Base Scenario and Alternative Scenario 5 are identical to each other, with minor differences. One important thing we note is that the heatmap for Alternative Scenario 5 also shows a stronger red colour overall that highlights that the PLOS and sidewalk conditions worsen in comparison to the Base Scenario as described in **Section 6.1.6**. where PLOS downgrades from C0 to C-. Minor changes to the sidewalk, such as restricting a small section that takes up the entire sidewalk affects

how the sidewalk functions and decision-makers should understand and consider these before implementing changes.

Additionally, the heatmap for Alternative Scenario 5 in **Figure 6.11b.** shows that the more intense red colour is also slightly more continuous and uniformly spread along the sidewalk rather than appearing as separate clusters between seating and stairs areas in the Base Scenario. This suggests that pedestrians are moving in a more consistent pattern, even though overall pedestrian interaction is slightly higher than in the Base Scenario, given that the seated section is removed due to the addition of the hazard tape. The highest amount of pedestrian pair interaction remains focused through the center of the sidewalk, and the intensity of the areas with blue, green, and yellow colours closer to the edge of the sidewalk near by the stairs on the left side and the seats on the right side, remains identical in Alternative Scenario 5 and the Base Scenario. This can be attributed to the fact that pedestrians experience similar amounts of pedestrian interaction in these areas for both scenarios, and that the main change occurs in the middle of the sidewalk when adding a hazard tape on the right side.

Overall, the heatmap for Alternative Scenario 5 supports the findings from **Section 6.1.6**. It shows how restricting a small portion of the sidewalk can still affect the pedestrian interaction and lower the overall PLOS by reducing the amount of walking space available, which restricts pedestrians.

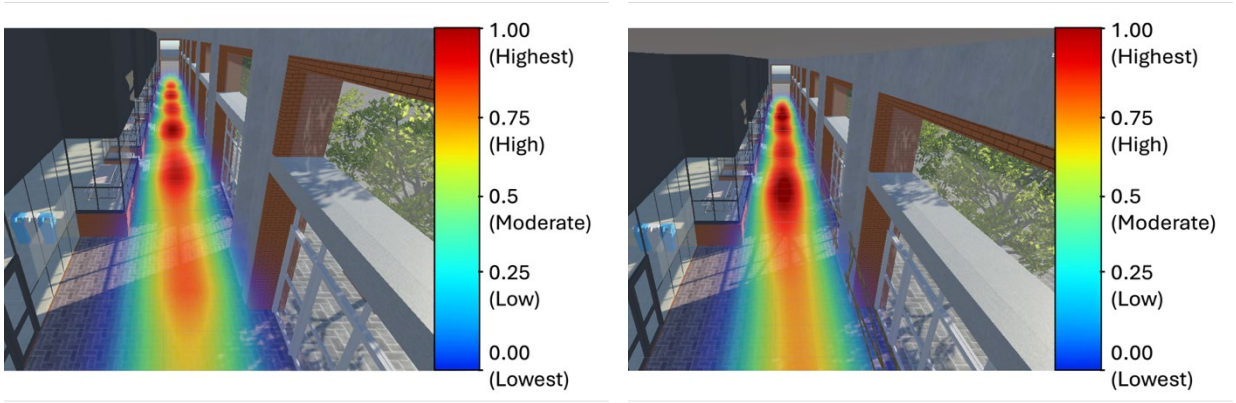

a) Base Scenario b) Alternative Scenario 5

Figure 6.11. Heat Map for Base Scenario versus Alternative Scenario 5

6.3 Discussion of Results

Our proposed novel PLOS framework offers several advantages over the traditional HCM PLOS framework, as shown in **Table 2.2**, particularly from the perspective of a decision maker responsible for evaluating the operations of sidewalks and pedestrians' walking experience (HCM, 2010).

First, our proposed PLOS framework provides a more complete way to measure sidewalk performance by accounting for both pedestrian space and pedestrian interaction as separate indicators in the PLOS model. While the HCM PLOS framework relies primarily on pedestrian space as the single input indicator and reports a single average value over 15 minutes, our proposed novel PLOS framework captures how pedestrian conditions change from minute to minute and overall (HCM, 2000; HCM, 2016; TRB, 2020). This allows decision makers to understand not only the overall PLOS but also when and where on the sidewalk pedestrians experience more constrained walking conditions during the 15-minute microsimulation period.

Second, the addition of pedestrian interaction in our PLOS model introduces an important indicator that is not captured in the HCM PLOS model (HCM, 2000; HCM, 2016). Pedestrian interaction reflects different pedestrian pair interactions by quantifying how pedestrians adjust their movement in response to other people (City of London, 2010; Kim et al., 2014; Huber et al., 2014). These include instances where pedestrians must alter their walking path to avoid shoulder brushing or collisions with other people. The results from analyzing the Alternative Scenarios in comparison to the Base Scenario of the study area shown in the previous section of **Section 6.1,** demonstrate that changes to the design layout of a sidewalk, such as adding or removing surface elements or reducing effective walking width, can meaningfully affect pedestrian interaction even when pedestrian space remains similar. Under the HCM PLOS framework, these changes would not be detected, and the analysis would incorrectly suggest that pedestrian conditions remain the same throughout the entire 15-minute period.

The PLOS results also show why some subcategories appear more frequently than others. For example, PLOS C+ conditions were limited in the results because a PLOS C+ grade requires pedestrian space to remain within the PLOS C range while the pedestrian interaction value falls below the lower threshold for PLOS C. Although the average pedestrian space was approximately 2.70 m^2/ped for all scenarios, pedestrian interaction values were generally within the C0 or C- ranges. As a result, most scenarios did not produce C+ conditions, and no overall scenario received a PLOS C+ grade. The only minute-level PLOS C+ condition was observed in Alternative Scenario 2 during minute 2, where pedestrian interaction decreased to 115.68 m/s^2 after the seating areas were removed. This shows that pedestrian space alone was sufficient to maintain PLOS C conditions, but pedestrian interaction was generally not low enough to produce C+ conditions across the evaluated scenarios. Third, the use of heat maps provides a clear and intuitive way to

visualize how pedestrian interaction is distributed across the sidewalk. From a decision-making standpoint, this visualization helps identify specific locations or hotspots along the sidewalk where walking conditions worsen or improve due to changes to the design layout of the sidewalk. The heat maps reveal patterns that are not apparent from quantitative results alone, such as localized areas of high pedestrian pair interaction or recurring points of congestion that affect the walking experience of pedestrians (Lv and Hu, 2020; Choi et al., 2025). This additional location-based understanding can support more targeted design modifications rather than relying on uniform or typically used design assumptions.

In practice, the proposed PLOS model can support municipalities, consulting firms, transportation engineers, planners, and designers when evaluating existing sidewalk conditions, design alternatives, and temporary sidewalk modifications. The numerical outputs, including pedestrian space, pedestrian interaction, and PLOS, can be used to compare how different layouts affect sidewalk performance. The heat maps can then be used to identify specific locations where pedestrian interaction is concentrated. For example, if a construction zone causes pedestrians to follow curved or constrained walking paths, the heat map can show where pedestrians experience higher levels of movement restriction. This information can help determine whether mitigation measures are needed, such as widening the temporary pedestrian path, adjusting the location of barriers, improving wayfinding, reducing obstructions, or providing an alternative pedestrian route (City of London, 2010).

The PLOS model can also be used to compare construction staging options or design layouts before implementation (Papadimitriou et al., 2018). For example, different temporary sidewalk configurations can be tested in the simulation environment, and the resulting pedestrian space, pedestrian interaction, PLOS, and heat maps can be compared. The preferred option would be the

layout that maintains acceptable pedestrian space while minimizing pedestrian interaction and reducing localized areas of movement constraints. This demonstrates how the proposed PLOS framework can support evidence-based planning and design decisions, rather than relying only on average pedestrian space or general design assumptions (Papadimitriou et al., 2018).

Overall, our proposed novel PLOS framework offers a more sensitive and informative tool for evaluating the effectiveness of a sidewalk. By accounting for pedestrian interaction and pedestrian space, capturing minute-by-minute changes, and visualizing results through heat maps, our PLOS framework provides insights that are not available using the traditional HCM PLOS analysis and better supports sidewalk planning and design.

6.4 Chapter Summary

Chapter 6 presented the results of applying the proposed PLOS model to the Base Scenario and five Alternative Scenarios. For each scenario, pedestrian space, pedestrian interaction, and PLOS were evaluated on a minute-by-minute basis over the 15-minute microsimulation period. The results showed that all scenarios maintained an average pedestrian space of approximately 2.70 m^2/ped, while pedestrian interaction varied depending on the design modification. Alternative Scenarios 2 and 3 reduced average pedestrian interaction compared with the Base Scenario, while Alternative Scenarios 1, 4, and 5 increased pedestrian interaction and resulted in poorer operating conditions.

The chapter also presented heat map results to visualize where pedestrian interaction occurs across the sidewalk. The heat maps used normalized pedestrian interaction values between 0 and 1 to identify areas with lower and higher interaction intensity. The results showed that advertisements, construction zones, and hazard tape increased pedestrian interaction in specific locations or along

larger portions of the sidewalk. In contrast, removing seats or stairs reduced pedestrian interaction in constrained zones. These location-based results supported the numerical findings by showing where pedestrian interactions became more concentrated or less intense under different design layouts.

Overall, **Chapter 6** demonstrated the advantages of the proposed PLOS framework compared with the traditional HCM PLOS approach. While the HCM framework reports a single PLOS value based mainly on pedestrian space, the proposed model incorporates pedestrian interaction and captures minute-by-minute changes in walking conditions. The results showed that scenarios with similar pedestrian space values can still produce different levels of pedestrian interaction and different PLOS outcomes. This chapter therefore shows that combining pedestrian space, pedestrian interaction, and heat map visualization provides a more detailed and practical assessment of sidewalk performance.

Chapter 7. Summary, Conclusion and Recommendations

This study proposed a novel PLOS model to evaluate sidewalk performance more effectively. The research was conducted through three main objectives. The first objective was to identify and develop indicators that better capture pedestrian walking experience. The second objective was to develop a novel PLOS model using these indicators. The third objective was to implement the PLOS model in a real case study area and use visualization outputs to support the interpretation of the results. The 3D visualization was used as a supporting tool to communicate pedestrian movement patterns, the pedestrian interaction indicator, and heat map results, rather than as the primary research contribution (Lv and Hu, 2020; Abu Alatta and Momani, 2021; Choi et al., 2025).

7.1 Summary

The goal of this study was to develop a PLOS framework to evaluate the effectiveness and performance of sidewalks more effectively. The proposed model responds to limitations in traditional PLOS methods, which commonly rely on pedestrian space, density, volume, or flow rate to evaluate pedestrian facilities (Pushkarev and Zupan, 1975; HCM, 2000; HCM, 2016; Nag et al., 2020). While these indicators are useful for describing available walking space and pedestrian demand, they do not fully capture how pedestrians adjust their movement in response to other pedestrians or constrained sidewalk areas. Previous studies and pedestrian comfort guidance have shown that pedestrian interactions, personal space, evasive movement, shoulder brushing, and collisions can affect pedestrian walking conditions beyond space-based measures alone (City of London, 2010; Finch et al., 2010; Kim et al., 2014). This study achieved its three research objectives by developing input indicators, proposing a new PLOS model, and applying

the model to a real sidewalk case study. The results demonstrate the advantages of incorporating both numerical outputs and 3D visualization when evaluating pedestrian operating conditions.

7.1.1 Development of Input Indicators to Capture Pedestrian Space and Pedestrian Interaction

Traditional PLOS frameworks primarily rely on pedestrian space as a single indicator (Pushkarev and Zupan, 1975; HCM, 2000; HCM, 2016; TRB, 2020). This limits their ability to reflect how pedestrians interact while walking. To address this limitation, this study developed pedestrian interaction as a second input indicator. Pedestrian interaction was defined using social force and walking direction (Helbing and Molnar, 1995; Moussaid et al., 2010; Kim et al., 2014; Feliciani and Nishinari, 2018). Social force represents the influence pedestrians exert on one another based on proximity, while walking direction distinguishes between uni-directional and bi-directional movements through passing and meeting events (Helbing and Molnar, 1995; Lam et al., 2003; Lee et al., 2005; Alhajyaseen et al., 2011). The relationship between pedestrian space and pedestrian interaction was quantified through a correlation analysis in **Section 4.1** where a value of -0.28 was observed. This weak negative correlation provides an initial indication that the two indicators capture different aspects of pedestrian behaviour. Pedestrian space reflects the amount of available walking area, while pedestrian interaction reflects how pedestrians adjust their paths, slow down, or change direction in response to others.

Results from **Chapter 6** further demonstrate the distinction between pedestrian space and pedestrian interaction. In the Base Scenario, the average pedestrian space over the 15-minute microsimulation period was 2.70 m²/ped, which falls within the PLOS C range. However, pedestrian interaction varied substantially from minute to minute and produced both PLOS C0 and

C- conditions. This shows that pedestrian space alone does not fully describe the walking conditions experienced by pedestrians. The proposed framework captures these minute-level changes and provides a more detailed representation of sidewalk performance.

7.1.2 Proposal of a New PLOS model Incorporating Pedestrian Space and Pedestrian interaction

Building on the developed input indicators, this study proposed a novel PLOS model that combines pedestrian space and pedestrian interaction. A key contribution of the model is that it does not only assign the traditional letter grades from A to F. It also introduces three secondary categories within each level, represented by "- / 0 / +" . These subcategories use pedestrian interaction as the second indicator and allow the framework to detect changes in walking conditions even when pedestrian space remains within the same PLOS range. The "- / 0 / +" classification structure is adapted from the City of London PLOS model and is not presented as the main contribution of this study (City of London, 2010). Instead, the contribution of this study is the simulation-based implementation of pedestrian interaction within a PLOS framework (City of London, 2010; Finch et al., 2010; Helbing and Molnar, 1995; Kim et al., 2014). Pedestrian interaction was calculated using pedestrian trajectory outputs, pedestrian distance, social force, and walking direction. This allows the model to evaluate pedestrian interaction effects more continuously than manual observation methods and to detect changes in walking conditions even when pedestrian space remains within the same PLOS range.

This study also contributes by automating the calculation of pedestrian interaction, visualizing constraints in pedestrian movement through heat maps, and applying the model to compare a Base Scenario with five Alternative Scenarios. These contributions allow the proposed framework to

support practical evaluation of sidewalk design alternatives and “what-if” scenarios before implementation.

The results from applying the PLOS model to the Base Scenario and Alternative Scenarios discussed in **Chapter 6** show the value of this using both indicators. In Alternative Scenario 1, the addition of advertisements increased average pedestrian interaction from 184.05 m/s² in the Base Scenario to 203.00 m/s², resulting in a downgrade from C0 to C- as discussed in **Sections 6.1.2 and 6.2.1.** In contrast, Alternative Scenario 2 reduced average pedestrian interaction to 155.26 m/s² after seating areas were removed, while average pedestrian space remained approximately 2.70 m²/ped as discussed in **Sections 6.1.3 and 6.2.2**. Although the overall PLOS remained C0, the decrease in pedestrian interaction indicates improved walking conditions that would not be fully captured by a pedestrian-space-only assessment.

Similarly, Alternative Scenarios 4, and 5 showed that changes such as introducing construction zones or adding hazard tape can significantly increase pedestrian interaction, with average pedestrian interaction values reaching as high as 217.29 m/s² in Alternative Scenario 4, as shown in **Sections 6.1.5 and 6.2.4.** Under the traditional HCM PLOS framework, these scenarios would generally remain classified as PLOS C because the average pedestrian space does not change. The novel PLOS model, however, captures the deterioration in walking conditions by accounting for changes in pedestrian interactions and movement adjustments.

7.1.3 Implementation of New PLOS Model and 3D Visualization of Results

The proposed PLOS framework was implemented in the York Lanes study area at York University’s Keele campus. The sidewalk is approximately 72 m long and 3 m wide and was selected due to consistent pedestrian activity and observable interaction patterns. Six scenarios

were evaluated, including the Base Scenario and five Alternative Scenarios. These scenarios represented changes to the sidewalk layout, including adding advertisements, removing seating, removing stairs, introducing a construction zone, and adding hazard tape barriers.

For each scenario, pedestrian space and pedestrian interaction were calculated over the 15-minute microsimulation period, and PLOS was classified on a minute-by-minute basis. The results show that even modest design changes can affect pedestrian operating conditions. For example, the Base Scenario reached both PLOS D+ and B- conditions within the same 15-minute microsimulation period despite an overall average of C0. This confirms that walking conditions fluctuate over short intervals and that a single average PLOS value can mask important variations.

To enhance interpretation, the 2D microsimulation model developed in PTV Viswalk was integrated with a 3D visualization developed in Unity. This integration supported the interpretation of the calculated indicators and provided a visual representation of pedestrian pair interactions as shown in **Section 6.1**. The heat map analysis in **Section 6.2** further illustrated how pedestrian interaction concentrates in specific spatial zones under different design conditions. Together, the quantitative and visual results demonstrate that the proposed framework supports systematic evaluation of alternative sidewalk designs and "what-if" scenarios that offer a more comprehensive assessment of pedestrian performance than traditional single-indicator PLOS methods.

7.2 Future Work and Recommendations

While this study demonstrates the potential of combining pedestrian space and pedestrian interaction in evaluating sidewalk performance, several opportunities exist to extend and refine the proposed PLOS model.

PLOS Model Calibration and Sensitivity Testing of Model Parameters

A limitation of this study is that the weighting or scaling factors used in the walking direction sub-indicator were not calibrated using observed pedestrian trajectory data. The same-direction scaling factor of 1 and the bi-directional scaling factor were determined from the structure of the walking direction equation and the assumption that opposite-direction pedestrian interactions create greater movement constraint than same-direction interactions. These factors were applied consistently across all simulations and scenarios. In addition, the current formulation captures same-direction and opposite-direction movement at the pedestrian-pair level, but it does not evaluate detailed counterflow characteristics such as different directional split percentages, lane formation, or changes in pedestrian capacity under varying bi-directional flow conditions.

Future work should conduct sensitivity testing and calibration using observed pedestrian data to confirm whether these scaling factors are appropriate for different sidewalk environments, pedestrian volumes, and walking conditions. Sensitivity testing is commonly recommended when developing composite indicators or index-based methods because it helps assess how assumptions and weighting choices affect the final results (OECD, 2008; Saisana et al., 2005; Greco et al., 2019).

In this study, Viswalk's Social Force Model serves as the behavior-generation mechanism, whereas the post-processing Social Force calculation serves as a comparative interaction metric applied to the exported trajectories. We agree that using the second Social Force calculation as independent evidence that the Viswalk model is correct would create a circular argument. However, this is not how we use the measure in this study. We used the same Viswalk behavioral settings and the same post-processing parameters (A = 11 and B = 0.77) for every scenario and only changed experimental conditions including pedestrian volume to account for different

pedestrian space and walking direction scenarios, specifically uni-directional (100-0) and bi-directional (50-50) walking movement.

Therefore, differences between scenarios do not result from changes in the Viswalk behavioral parameters or changes in the post-processing formulation. We use the calculated Social Force to compare relative interaction intensity across scenarios rather than to estimate an independently measured physical force. Future work should test the sensitivity of the pedestrian interaction results to different A and B values, evaluate alternative Social Force formulations, and calibrate the pedestrian interaction calculation using observed pedestrian trajectory data (Helbing and Molnar, 1995; Johansson et al., 2007; Kretz et al., 2018).

PLOS Model Calibration and Implementation Across Different Pedestrian Facilities

In our study, the boundary values for pedestrian interaction were calibrated based on the characteristics of the selected study area at York Lanes. As a result, the current thresholds for pedestrian interaction are specific to this sidewalk. If the proposed PLOS framework is implemented at a different sidewalk or pedestrian facility, a calibration phase would be required to determine appropriate pedestrian interaction thresholds that reflect local pedestrian behaviour, walking patterns, and specific facility characteristics.

Future studies should therefore apply the novel PLOS framework to a wider range of real-world pedestrian facilities and collect pedestrian interaction data across different contexts, such as commercial districts, transit station access points, indoor malls, and other high-activity pedestrian environments (Nag et al., 2020; Shu et al., 2021). By aggregating data from multiple locations, it would be possible to develop generalized pedestrian interaction thresholds that are less dependent on a single site. This would enable the PLOS framework to be applied more broadly, without

requiring a full calibration phase for each new location. This improvement will make the PLOS model more practical for planning and design applications.

Future work should also test the proposed PLOS model under a wider range of pedestrian volumes, sidewalk layouts, and movement conditions. In this study, not all PLOS subcategories appeared in the scenario results. For example, PLOS C+ conditions were limited because pedestrian interaction values generally did not fall below the lower threshold for PLOS C under the tested conditions. Although one C+ condition was observed in Alternative Scenario 2 during minute 2, no overall scenario received a PLOS C+ grade. Applying the model to additional sites and a broader range of pedestrian conditions would help confirm whether the full range of PLOS subcategories can be observed and whether the threshold values are transferable to other sidewalk environments.

Expand Scenario Testing Using Real-World Sidewalk Conditions

In this study, all Base and Alternative Scenarios were defined and tested by developing 2D microsimulation models using PTV Viswalk, which is effective for modelling pedestrian behaviour and controlled sidewalk environments. However, simulated environments cannot fully represent the complexity and variability of real-world sidewalk conditions. As a result, future studies should focus on implementing the proposed PLOS framework in real-world locations to complement and validate the microsimulation-based scenarios created. This includes expanding the existing scenarios by incorporating real-world pedestrian trajectory data (e.g., x,y,z coordinates) collected from fixed monitoring cameras such as CCTV systems or motion sensors. Comparing simulated trajectories with observed pedestrian movements would help validate the pedestrian interaction calculation and ensure that the model accurately reflects how pedestrians interact and adjust their movement in practice.

Applying the PLOS framework to real sidewalks with varying design layouts, pedestrian volumes, and walking patterns would also allow the PLOS model to be tested under more diverse and realistic conditions. This would strengthen confidence in the PLOS model and support the development of a more robust and transferable PLOS framework that can be applied beyond controlled simulation environments.

Impact of Pedestrians Intentionally Moving Together

A limitation of this study is the assumption that pedestrians move independently and primarily aim to avoid one another. In real-world environments, pedestrians often intentionally walk together in social groups, such as friends, families, classmates, or colleagues. These group behaviours can influence walking speed, preferred spacing, and pedestrian pair interaction patterns, and may affect both pedestrian space and pedestrian interaction. Recent studies in the computer vision and pedestrian dynamics literature have shown that social groups can be automatically identified using pedestrian trajectory data and video-based analysis. For example, vision-based methods have been developed to detect pedestrians walking together by clustering trajectories and analysing relative positions and movement patterns (Ge et al., 2011; Khan et al., 2015). More recent research also uses machine-learning and graph-based approaches to distinguish group behaviour from individual pedestrian interactions (Nicolas, 2023).

Future work can build on these advances by integrating group-detection algorithms into the proposed PLOS framework (Moussaid et al., 2010; Ge et al., 2011; Khan et al., 2015; Nicolas, 2023). By identifying pedestrians who are intentionally moving together, pedestrian interaction values could be adjusted to distinguish between intentional group interactions and avoidance-based interactions. Incorporating group behaviour would improve the realism of the PLOS model and

allow it to better reflect everyday walking conditions, particularly in environments such as campuses, shopping areas, and transit facilities where group walking is common.

Automate the Calculation and Visualization Processes

This study used a simulated computer-vision environment to prototype the calculation of pedestrian space, pedestrian interaction, PLOS classification, and heat-map visualization. Future work should focus on implementing the proposed PLOS framework in real-world settings using fixed monitoring cameras, such as CCTV systems, to collect pedestrian data directly from operating sidewalks. Automating the full workflow, including data collection, PLOS calculation, and 3D visualization, would allow the framework to be used as a practical decision-support tool for planners and engineers. Such a system could present results through a simple user interface, showing both numerical outputs and heat maps that highlight where pedestrian pair interactions and movement restrictions are concentrated.

From a planning perspective, this would enable practitioners to compare design alternatives, assess temporary conditions, and evaluate proposed sidewalk changes more effectively than traditional HCM PLOS methods, which report only a single average value (HCM, 2016; Papadimitriou et al., 2018). Implementing the framework in real projects would help demonstrate its value in supporting evidence-based sidewalk design and operational decisions. The proposed PLOS model is intended to support planning, design, and management decisions, rather than directly assign penalties. For example, the outputs could help municipalities and consulting firms evaluate temporary construction impacts, compare mitigation measures, and identify design improvements that reduce pedestrian interaction. However, using the model for penalties, enforcement, or regulatory

approval would require additional municipal policy development, validation, and implementation guidance beyond the scope of this study.

Explore Additional Indicators That May Complement Pedestrian Space And Pedestrian Interaction

While pedestrian space and pedestrian interaction capture two key aspects of walking experience, future research can explore whether additional indicators further improve the ability of the PLOS model to reflect real-world conditions. For example, we can examine if lateral movement can better capture how pedestrians shift sideways to avoid others or obstacles, particularly in busy or constrained environments. Other extensions could include more detailed treatment of walking direction beyond uni-directional and bi-directional walking direction, such as weaving behaviour or frequent changes in direction.

Future work can also examine whether vector-based social force formulations can improve the pedestrian interaction calculation. In this study, walking direction is represented as a scalar term that distinguishes between same-direction and opposite-direction pedestrian interactions. While this approach supports a practical PLOS classification structure, it does not fully represent the direction and magnitude of pedestrian movement. A vector-based approach could provide a more detailed representation of pedestrian interaction behaviour and improve the sensitivity of the proposed PLOS model (Helbing and Molnar, 1995; Johansson et al., 2007; Karamouzas et al., 2014).

As discussed in the previous section, incorporating pedestrian group behaviour, where individuals intentionally walk together rather than independently, may also enhance the accuracy of the PLOS model. Evaluating these additional indicators would help determine whether they provide

meaningful improvements to PLOS assessment or whether pedestrian space and pedestrian interaction already capture most of the significant influences on the walking experience of pedestrians within pedestrian facilities.

Chapter 8. References

1. Abu Alatta, R., & Momani, H. (2021). Integrating 3D game engines in enhancing urban perception: a case study of students' visualization of urban space. ACE: architecture, city and environment, 16(47).
2. Adwitiya, R. I., & Sumabrata, R. J. (2022, April). Microscopic Analysis of the Transportation Modes and Movement of Pedestrians in Dukuh Atas Transit-Oriented Development Area Using PTV Viswalk. In IOP Conference Series. Earth and Environmental Science (Vol. 1000, No. 1, p. 012022). IOP Publishing.
3. Akimov, E. V., Kruzhkov, D. M., and Yakimenko, V. A. (2019). Compensation for errors in determining the angle in the flight-navigation complex of the aircraft in case of failure of the satellite navigation system. *INCAS Bulletin*, *11*, 7-16.
4. Alhajyaseen, W. K., Nakamura, H., and Asano, M. (2011). Effects of bi-directional pedestrian flow characteristics upon the capacity of signalized crosswalks. *Procedia-social and behavioral sciences*, *16*, 526-535.
5. Alhassan, H. M., and Mashros, N. (2015). Modelling of pedestrian speed-density and volume-density relationships in outdoor walkways. *Journal Teknologi*, *73*(4).
6. Allirani, H., & Verma, A. (2025). Development of Level of Service Criteria for Pedestrianized Urban Street: A Quantitative and Qualitative Approach. Journal of Transportation Engineering, Part A: Systems, 151(3), 04024124.
7. Anjum, N., and Cavallaro, A. (2008). Multifeature object trajectory clustering for video analysis. *IEEE Transactions on Circuits and Systems for Video Technology*, *18*(11), 1555-1564.
8. Arechavaleta, G., Laumond, J. P., Hicheur, H., and Berthoz, A. (2008). An optimality principle governing human walking. *IEEE Transactions on Robotics*, *24*(1), 5-14.
9. Asadi-Shekari, Z., Moeinaddini, M., & Shah, M. Z. (2014). A pedestrian level of service method for evaluating and promoting walking facilities on campus streets. Land use policy, 38, 175-193.
10. Asadi-Shekari, Z., Moeinaddini, M., and Shah, M. Z. (2013). A pedestrian level of service method for evaluating and promoting walking facilities on campus streets. *Land Use Policy*, 38, 175-193.

11. Asadi-Shekari, Z., Moeinaddini, M., and Shah, M. Z. (2015). Pedestrian safety index for evaluating street facilities in urban areas. *Safety science*, *74*, 1-14.
12. Bensebaa, A., and Larabi, S. (2018). Direction estimation of moving pedestrian groups for intelligent vehicles. *The Visual Computer*, *34*(6), 1109-1118.
13. Bian, J. (2019). *Video trajectory analysis* (Doctoral dissertation).
14. Bian, J., Tian, D., Tang, Y., and Tao, D. (2019). Trajectory data classification: A review. *ACM Transactions on Intelligent Systems and Technology (TIST)*, *10*(4), 1-34.
15. Bisagno, N., Zhang, B., and Conci, N. (2018). Group lstm: Group trajectory prediction in crowded scenarios. In *Proceedings of the European Conference on Computer Vision (ECCV) Workshops* (pp. 0-0).
16. Boltes, M., Seyfried, A., Steffen, B., and Schadschneider, A. (2010). Automatic extraction of pedestrian trajectories from video recordings. In *Pedestrian and evacuation dynamics 2008* (pp. 43-54). Springer, Berlin, Heidelberg.
17. Blue, V. J., Embrechts, M. J., and Adler, J. L. (1997, October). Cellular automata modeling of pedestrian movements. In *1997 IEEE international conference on systems, man, and cybernetics. computational cybernetics and simulation* (Vol. 3, pp. 2320-2323). Ieee.
18. Blue, V. J., and Adler, J. L. (1999). Cellular automata microsimulation of bidirectional pedestrian flows. *Transportation Research Record*, *1678*(1), 135-141.
19. Blue, V. J., and Adler, J. L. (2000). Modeling four-directional pedestrian flows. *Transportation research record*, *1710*(1), 20-27.
20. Blue, V. J., and Adler, J. L. (2001). Cellular automata microsimulation for modeling bi-directional pedestrian walkways. *Transportation Research Part B: Methodological*, *35*(3), 293-312.
21. Caprile, B., and Torre, V. (1990). Using vanishing points for camera calibration. *International journal of computer vision*, *4*(2), 127-139.
22. Campisi, T., Tesoriere, G., Skoufas, A., Zeglis, D., Andronis, C., and Basbas, S. (2022). Perceived pedestrian level of service: the case of Thessaloniki, Greece. *Transportation research procedia*, *60*, 124-131.
23. Cepolina, E. M., Menichini, F., and Rojas, P. G. (2018). Level of service of pedestrian facilities: Modelling human comfort perception in the evaluation of pedestrian behaviour patterns. *Transportation research part F: traffic psychology and behaviour*, *58*, 365-381.

24. City of Brampton (2022). Transportation and Safety Assessment Report for the Environmental Assessment Study for Ken Whillians Drive Extension
25. City of Toronto (2025). Supplementary Report: Summary of Transportation Impacts Related to the Proposed Ontario Place (955 Lake Shore Boulevard West) Redevelopment.
26. Chen, Jinyang, Rangding Wang, Liangxu Liu, and Jiatao Song. "Clustering of trajectories based on Hausdorff distance." In *2011 international conference on electronics, communications and control (icecc)*, pp. 1940-1944. IEEE, 2011.
27. Chen, Y. C. (2017). A tutorial on kernel density estimation and recent advances. Biostatistics & Epidemiology, 1(1), 161-187.
28. Chiarandini (2015). Computer Game Programming AI: Movement in 3D Path Finding. *University of Southern Denmark,* 1-41
29. Choi, C. H., Park, S. W., Park, J., Kim, J. H., Kim, J. S., Yang, H. S., ... & Sim, C. B. (2025). Prediction and prevention of crowd-crush accidents using crowd-density simulation based on unity engine. Discover Applied Sciences, 7(1), 1-25.
30. Christopoulou, P., and Pitsiava-Latinopoulou, M. (2012). Development of a model for the estimation of pedestrian level of service in Greek urban areas. *Procedia-Social and Behavioral Sciences*, *48*, 1691-1701.
31. City of London. (2010). Pedestrian Comfort Guidance for London, Version 2 2019.
32. City of Toronto (2025). Supplementary Report: Summary of Transportation Impacts Related to the Proposed Ontario Place (955 Lake Shore Boulevard West) Redevelopment.
33. Corbetta, A., Meeusen, J., Lee, C. M., and Toschi, F. (2016). Continuous measurements of real-life bidirectional pedestrian flows on a wide walkway. *arXiv preprint arXiv:1607.02897*.
34. Curio, C., Edelbrunner, J., Kalinke, T., Tzomakas, C., and Von Seelen, W. (2000). Walking pedestrian recognition. *IEEE Transactions on intelligent transportation systems*, *1*(3), 155-163.
35. Daamen, W., and Hoogendoorn, S. P. (2003). Experimental research of pedestrian walking behavior. *Transportation research record*, *1828*(1), 20-30.

36. Dabiri, S., and Heaslip, K. (2018). Inferring transportation modes from GPS trajectories using a convolutional neural network. *Transportation research part C: emerging technologies*, *86*, 360-371.
37. Da Silva, T. L. C., Zeitouni, K., and de Macêdo, J. A. (2016, June). Online clustering of trajectory data stream. In *2016 17th IEEE International Conference on Mobile Data Management (MDM)* (Vol. 1, pp. 112-121). IEEE.
38. Dixon, L. B. (1996). Bicycle and pedestrian level-of-service performance measures and standards for congestion management systems. *Transportation research record*, *1538*(1), 1-9.
39. Ehrenfeucht, R., & Loukaitou-Sideris, A. (2010). Planning urban sidewalks: Infrastructure, daily life and destinations. *Journal of Urban Design*, *15*(4), 459-471.
40. El-Didy, M. H., Hassan, G. F., Afifi, S., and Ismail, A. (2024). Crowding between urban planning and environmental psychology: Guidelines for bridging the gap. Open House International, 49(4), 670-695.
41. Engelniederhammer, A., Papastefanou, G., and Xiang, L. (2019). Crowding density in urban environment and its effects on emotional responding of pedestrians: Using wearable device technology with sensors capturing proximity and psychophysiological emotion responses while walking in the street. *Journal of Human Behavior in the Social Environment*, *29*(5), 630-646.
42. Enzweiler, M., and Gavrila, D. M. (2008). Monocular pedestrian detection: Survey and experiments. *IEEE transactions on pattern analysis and machine intelligence*, *31*(12), 2179-2195.
43. Enzweiler, M., and Gavrila, D. M. (2010, June). Integrated pedestrian classification and orientation estimation. In *2010 IEEE Computer Society Conference on Computer Vision and Pattern Recognition* (pp. 982-989). IEEE.
44. Fan, R., Yu, H., Liu, P., & Wang, W. (2013). Using VISSIM simulation model and Surrogate Safety Assessment Model for estimating field measured traffic conflicts at freeway merge areas. *IET Intelligent Transport Systems*, *7*(1), 68-77.
45. Federal Highway Administration (1998). Recommended Procedures: Chapter 13 for Pedestrians. *Highway Capacity Manual*
46. Federal Highway Administration. (2002). *Pedestrian facilities users guide: Providing safety and mobility*. U.S. Department of Transportation, Report No. FHWA-RD-01-102.

47. Federal Highway Administration. (2004). *Guide for the planning, design, and operation of pedestrian facilities*. U.S. Department of Transportation.
48. Feliciani, C., and Nishinari, K. (2016). Empirical analysis of the lane formation process in bidirectional pedestrian flow. *Physical Review E*, *94*(3), 032304.
49. Feliciani, C., and Nishinari, K. (2018). Measurement of congestion and intrinsic risk in pedestrian crowds. *Transportation research part C: emerging technologies*, *91*, 124-155.
50. Ferrer, S., Ruiz, T., and Mars, L. (2015). A qualitative study on the role of the built environment for short walking trips. *Transportation research part F: traffic psychology and behaviour*, *33*, 141-160.
51. Ferrer-Ortiz, C., Marquet, O., Mojica, L., and Vich, G. (2022). Barcelona under the 15-minute city lens: Mapping the accessibility and proximity potential based on pedestrian travel times. *Smart Cities*, *5*(1), 146-161.
52. Finch, E., Iverson, G., Dye, J., 2010. Pedestrian Comfort Guidance for London. In: European Transport Conference, 2010. Glasgow Scotland, United Kingdom Available at: http://content.tfl.gov.uk/pedestrian-comfort-guidance-technical-guide.pdf
53. Fitzpatrick, K., Brewer, M. A., & Turner, S. (2006). Another look at pedestrian walking speed. Transportation research record, 1982(1), 21-29.
54. Fonseca, F., Ribeiro, P. J., Conticelli, E., Jabbari, M., Papageorgiou, G., Tondelli, S., and Ramos, R. A. (2022). Built environment attributes and their influence on walkability. *International Journal of Sustainable Transportation*, *16*(7), 660-679.
55. Fort Collins (2011). Pedestrian Plan. *https://www.fcgov.com/fcmoves/files/ped-plan.pdf*
56. Fu, L., Shi, Q., Qin, H., Zhang, Y., and Shi, Y. (2022). Analysis of movement behavior of pedestrian social groups through a bottleneck. *Physica A: Statistical Mechanics and its Applications*, 128257.
57. Gallup, A. C., Hale, J. J., Sumpter, D. J., Garnier, S., Kacelnik, A., Krebs, J. R., and Couzin, I. D. (2012). Visual attention and the acquisition of information in human crowds. *Proceedings of the National Academy of Sciences*, *109*(19), 7245-7250.
58. Gandhi, T., and Trivedi, M. M. (2008, June). Image based estimation of pedestrian orientation for improving path prediction. In *2008 IEEE Intelligent Vehicles Symposium* (pp. 506-511). IEEE.

59. Gariel, M., Srivastava, A. N., and Feron, E. (2011). Trajectory clustering and an application to airspace monitoring. *IEEE Transactions on Intelligent Transportation Systems*, *12*(4), 1511-1524.
60. Ge, W., Collins, R. T., & Ruback, R. B. (2011). Vision-based analysis of small groups in pedestrian crowds. IEEE Transactions on Pattern Analysis and Machine Intelligence, 34(5), 1003–1016.
61. Gettman, D., Pu, L., Sayed, T., & Shelby, S. G. (2008). *Surrogate safety assessment model and validation* (No. FHWA-HRT-08-051). Turner-Fairbank Highway Research Center.
62. Gorrini, A., Bandini, S., and Sarvi, M. (2014). Group dynamics in pedestrian crowds: Estimating proxemic behavior. Transportation research record, 2421(1), 51-56.
63. Gorrini, A., Presicce, D., Messa, F., and Choubassi, R. (2023). Walkability for children in Bologna: Beyond the 15-minute city framework. Journal of Urban Mobility, 3, 100052.
64. Greco, S., Ishizaka, A., Tasiou, M., & Torrisi, G. (2019). On the methodological framework of composite indices: A review of the issues of weighting, aggregation, and robustness. Social indicators research, 141(1), 61-94.
65. Greenfeld, J. S. (2002, January). Matching GPS observations to locations on a digital map. In *Transportation Research Board 81st Annual Meeting* (Vol. 22).
66. Haas, J. K. (2014). A history of the unity game engine.
67. Hagos, K. G., & Adnan, M. (2020). Effect of sidewalk vendors on pedestrian movement characteristics: A microscopic simulation study of Addis Ababa, Ethiopia. *Cities*, *103*, 102769
68. Helbing, D., and Molnar, P. (1995). Social force model for pedestrian dynamics. *Physical review E*, *51*(5), 4282.
69. Helbing, D., Farkas, I., & Vicsek, T. (2000). Simulating dynamical features of escape panic. *Nature*, *407*(6803), 487-490.
70. Helbing, D., Farkas, I. J., Molnar, P., and Vicsek, T. (2002). Simulation of pedestrian crowds in normal and evacuation situations. *Pedestrian and evacuation dynamics*, *21*(2), 21-58.
71. Helbing, D., Johansson, A., and Al-Abideen, H. Z. (2007). Dynamics of crowd disasters: An empirical study. *Physical review E*, *75*(4), 046109.
72. Helbing, D., and Johansson, A. (2013). Pedestrian, crowd, and evacuation dynamics. *arXiv preprint arXiv:1309.1609*.

73. Higham, D. J., & Higham, N. J. (2016). *MATLAB guide*. Society for Industrial and Applied Mathematics.
74. Highway Capacity Manual (HCM). (2000). Pedestrian Level of Service. Washington, D.C. *Transportation Research Board*
75. Highway Capacity Manual (HCM). (2016). Washington, D.C. *Transportation Research Board*
76. Holmes, S., Huynh, R., & Millard-Ball, A. (2018). Pedestrian planning on college campuses. *Planning for Higher Education*, *46*(2), 65-80.
77. Hong Kong Transportation Department. (2023). The Transport Planning and Design Manual. *https://www.td.gov.hk/filemanager/en/content_5055/V2_12_2023.pdf*
78. Hoogendoorn, S. P., Daamen, W., and Bovy, P. H. (2003, January). Extracting microscopic pedestrian characteristics from video data. In *Transportation Research Board Annual Meeting* (pp. 1-15). National Academy Press.
79. Hoogendoorn, S., and Daamen, W. (2005). Self-organization in pedestrian flow. In *Traffic and Granular Flow'03* (pp. 373-382). Springer, Berlin, Heidelberg.
80. Huang, S., Ying, X., Rong, J., Shang, Z., and Zha, H. (2016). Camera calibration from periodic motion of a pedestrian. In *Proceedings of the IEEE conference on computer vision and pattern recognition* (pp. 3025-3033)
81. Huber, M., Su, Y. H., Krüger, M., Faschian, K., Glasauer, S., & Hermsdörfer, J. (2014). Adjustments of speed and path when avoiding collisions with another pedestrian. PloS one, 9(2), e89589.
82. Jafari, A., & Liu, Y. C. (2024). Pedestrians' safety using projected time-to-collision to electric scooters. *Nature communications*, *15*(1), 5701.
83. Jaskiewicz, F. (2000). Pedestrian level of service based on trip quality. *Transportation Research Circular, TRB*.
84. Jia, X., Feliciani, C., Murakami, H., Nagahama, A., Yanagisawa, D., and Nishinari, K. (2022). Revisiting the level-of-service framework for pedestrian comfortability: velocity depicts more accurate perceived congestion than local density. *Transportation research part F: traffic psychology and behaviour*, *87*, 403-425.
85. Johansson, A., Helbing, D., & Shukla, P. K. (2007). Specification of the social force pedestrian model by evolutionary adjustment to video tracking data. *Advances in Complex Systems, 10*(supp02), 271–288.

86. Johansson, A., Helbing, D., Al-Abideen, H. Z., and Al-Bosta, S. (2008). From crowd dynamics to crowd safety: a video-based analysis. *Advances in Complex Systems*, *11*(04), 497-527.
87. Kadali, B. R., and Vedagiri, P. (2016). Evaluation of pedestrian crosswalk level of service (LOS) under mixed traffic conditions. *Transportation Research Part A: Policy and Practice*, 89, 124-137.
88. Karamouzas, I., Skinner, B., & Guy, S. J. (2014). Universal power law governing pedestrian interactions. *Physical review letters*, *113*(23), 238701.
89. Kilambi, P., Ribnick, E., Joshi, A. J., Masoud, O., and Papanikolopoulos, N. (2008). Estimating pedestrian counts in groups. *Computer Vision and Image Understanding*, *110*(1), 43-59.
90. Kim, S., Choi, J., Kim, S., and Tay, R. (2014). Personal space, evasive movement and pedestrian level of service. *Journal of advanced transportation*, *48*(6), 673-684.
91. Kim, S., Park, S., & Lee, J. S. (2014). Meso-or micro-scale? Environmental factors influencing pedestrian satisfaction. *Transportation Research Part D: Transport and Environment*, *30*, 10-20.
92. Khan, S. D. (2013). Estimating Speeds and Directions of Pedestrians in Real-Time Videos: A solution to Road-Safety Problem. In *Ageingai@ ai* ia*.
93. Khan, S. D., Vizzari, G., Bandini, S., & Basalamah, S. (2015). Detection of social groups in pedestrian crowds using computer vision. Advances in Visual Computing, 653–662.
94. Kong, S., Huang, Z., Scott, N., Zhang, Z. A., & Shen, Z. (2019). Web advertisement effectiveness evaluation: Attention and memory. *Journal of Vacation Marketing*, *25*(1), 130-146.
95. Konovalova, A., & Petrova, T. (2023). Pun processing in advertising posters: evidence from eye tracking. *Journal of Eye Movement Research*, *16*(3), 10-16910.
96. Kretz, T., Hengst, S., & Vortisch, P. (2008). Pedestrian flow at bottlenecks-validation and calibration of vissim's social force model of pedestrian traffic and its empirical foundations. *arXiv preprint arXiv:0805.1788*.
97. Kretz, T. (2011). A level of service scheme for microscopic simulation of pedestrians that integrates queuing, uni-and multi-directional flow situations. *European Transport Research Review*, *3*(4), 211-220.
98. Kretz, T., Lohmiller, J., & Sukennik, P. (2018). Some indications on how to calibrate the Social Force Model of pedestrian dynamics. *Transportation Research Record, 2672*(20), 228–238.

99. Kuang, H., Li, X., Song, T., and Dai, S. (2008). Analysis of pedestrian dynamics in counter flow via an extended lattice gas model. *Physical Review E*, *78*(6), 066117.

100. Lakoba, T. I., Kaup, D. J., & Finkelstein, N. M. (2005). Modifications of the Helbing-Molnar-Farkas-Vicsek social force model for pedestrian evolution. *Simulation*, *81*(5), 339-352.

101. Lallemand, J., Ronge, A., Szczot, M., and Ilic, S. (2014, September). Pedestrian orientation estimation. In *German Conference on Pattern Recognition* (pp. 476-487). Springer, Cham.

102. Lam, W. H., Lee, J. Y., Chan, K. S., & Goh, P. K. (2003). A generalised function for modeling bi-directional flow effects on indoor walkways in Hong Kong. *Transportation Research Part A: Policy and Practice*, *37*(9), 789-810.

103. Landis, B. W., Vattikuti, V. R., Ottenberg, R. M., McLeod, D. S., & Guttenplan, M. (2001). Modeling the roadside walking environment: pedestrian level of service. Transportation research record, 1773(1), 82-88.

104. Lam, W. H., Lee, J. Y., Chan, K. S., and Goh, P. K. (2003). A generalised function for modeling bi-directional flow effects on indoor walkways in Hong Kong. *Transportation Research Part A: Policy and Practice*, *37*(9), 789-810.

105. Lee, J. Y. (2016). Development and analysis of pedestrian comfort indicators using a pedestrian traffic flow simulation model. *Journal of Korean Society of Transportation, 34*(6), 499–509.

106. Lee, J. Y., Goh, P. K., and Lam, W. H. (2005). New level-of-service standard for signalized crosswalks with bi-directional pedestrian flows. *Journal of transportation engineering*, *131*(12), 957-960.

107. Lee, J. G., Han, J., and Whang, K. Y. (2007, June). Trajectory clustering: a partition-and-group framework. In *Proceedings of the 2007 ACM SIGMOD international conference on Management of data* (pp. 593-604).

108. Li, T., Xu, B., Lu, W., Chen, Z., Zhang, S., & Xia, F. (2024). The parameter calibration of social force model for pedestrian flow simulation based on YOLOv5. *Sensors*, *24*(15), 5011.

109. Li, Z., Lee, J. G., Li, X., and Han, J. (2010, April). Incremental clustering for trajectories. In *International conference on database systems for advanced applications* (pp. 32-46). Springer, Berlin, Heidelberg.

110. Lian, L., Mai, X., Song, W., Richard, Y. K. K., Wei, X., and Ma, J. (2015). An experimental study on four-directional intersecting pedestrian flows. *Journal of Statistical Mechanics: Theory and Experiment*, *2015*(8), P08024.

111. Liu, M. W., Wang, S. M., Oeda, Y., and Sumi, T. N. (2019). Simulating uni-and bi-directional pedestrian movement on stairs by considering specifications of personal space. *Accident Analysis and Prevention*, *122*, 350-364.

112. Lv, Fengjun, Tao Zhao, and Ramakant Nevatia. "Camera calibration from video of a walking human." *IEEE transactions on pattern analysis and machine intelligence* 28, no. 9 (2006): 1513-1518.

113. Lv, F., & Hu, C. A. (2020, November). Research on simulation of pedestrian flow Unity 3D through multiple exit architecture. In *2020 International Conference on Computer Engineering and Intelligent Control (ICCEIC)* (pp. 51-54). IEEE.

114. Ma, J., Song, W. G., Zhang, J., Lo, S. M., and Liao, G. X. (2010). k-Nearest-Neighbor interaction induced self-organized pedestrian counter flow. *Physica A: Statistical Mechanics and its Applications*, *389*(10), 2101-2117.

115. Ma, J., Song, W. G., Lo, S. M., and Fang, Z. M. (2013). New insights into turbulent pedestrian movement pattern in crowd-quakes. *Journal of Statistical Mechanics: Theory and Experiment*, *2013*(02), P02028.

116. Minegishi, Y., Ohmiya, Y., Sano, T., and Tange, M. (2022). Analysis and Modeling of Pedestrian Flow in a Confined Corridor Focusing on the Headway Distance and Velocity of Pedestrians. *Fire Technology*, *58*(2), 709-735.

117. Mishra, B., & Chowdhury, A. (2023). Applying Eye Tracking Technique to Evaluate Poster Design: A Study on World Peace Poster. In *Communication Design and Branding: A Multidisciplinary Approach* (pp. 175-183). Cham: Springer Nature Switzerland.

118. Mohammadi, A., Chowdhury, M. T. U., Yang, S., & Park, P. Y. (2021). Developing levels of pedestrian physical distancing during a pandemic. *Safety science*, *134*, 105066.

119. Mōri, M., and Tsukaguchi, H. (1987). A new method for evaluation of level of service in pedestrian facilities. *Transportation Research Part A: General*, *21*(3), 223-234.

120. Moussaid, M., Perozo, N., Garnier, S., Helbing, D., and Theraulaz, G. (2010). The walking behaviour of pedestrian social groups and its impact on crowd dynamics. *PloS one*, *5*(4), e10047.

121. Muraleetharan, T., ADACHI, T., UCHIDA, K. E., HAGIWARA, T., & KAGAYA, S. (2004). A study on evaluation of pedestrian level of service along sidewalks and at crosswalks using conjoint analysis. Infrastructure planning review, 21, 727-735.

122. National Association of City Transportation Officials. (2013). Urban street design guide. NACTO

123. Nag, D., Goswami, A. K., Gupta, A., and Sen, J. (2020). Assessing urban sidewalk networks based on three constructs: a synstudy of pedestrian level of service literature. *Transport reviews*, *40*(2), 204-240.

124. New York City (2006). New York City Pedestrian Level of Service Study Phase I.

125. New York City (2008). Pedestrian Level of Service Study, Phase 1. *Chapter 2: Current HCM Methodology,*

126. Nicolas, A. (2023). Social groups in pedestrian crowds: A review of their impact on dynamics. Journal of Urban Mobility, 3, 100045.

127. OECD (2008). *Handbook on Constructing Composite Indicators: Methodology and User Guide.* Organisation for Economic Co-operation and Development, Paris.

128. Oliver-Solà, J., Josa, A., Rieradevall, J., & Gabarrell, X. (2009). Environmental optimization of concrete sidewalks in urban areas. *The International Journal of Life Cycle Assessment*, *14*(4), 302-312.

129. Ontario Traffic Council (2022). Multi-Modal Level-of-Service Guidelines. *20-3587.*

130. Pelekis, N., Andrienko, G., Andrienko, N., Kopanakis, I., Marketos, G., and Theodoridis, Y. (2012). Visually exploring movement data via similarity-based analysis. *Journal of Intelligent Information Systems*, *38*(2), 343-391.

131. Papadimitriou, D., Kaplanidou, K., & Apostolopoulou, A. (2018). Destination image components and word-of-mouth intentions in urban tourism: A multigroup approach. Journal of Hospitality & Tourism Research, 42(4), 503-527.

132. Petritsch, T. A., Landis, B. W., McLeod, P. S., Huang, H. F., Challa, S., Skaggs, C. L., ... and Vattikuti, V. (2006). Pedestrian level-of-service model for urban arterial facilities with sidewalks. *Transportation Research Record*, *1982*(1), 84-89.

133. Piciarelli, C., and Foresti, G. L. (2006). On-line trajectory clustering for anomalous events detection. *Pattern Recognition Letters*, *27*(15), 1835-1842.

134. Piciarelli, C., Foresti, G. L., and Snidaro, L. (2005, September). Trajectory clustering and its applications for video surveillance. In *IEEE Conference on Advanced Video and Signal Based Surveillance, 2005.* (pp. 40-45). Ieee.

135. Polus, A., Schofer, J. L., & Ushpiz, A. (1983). Pedestrian flow and level of service. Journal of transportation engineering, 109(1), 46-56.

136. Pushkarev, B. & Zupan, J. (1975). Urban Space for Pedestrians, *Regional Plan Association*

137. Rahayuningsih, T., Pranoto, Nindyawati, Umniati, B. S., and Mardhika, M. A. S. (2017, September). Mapping of pedestrian characteristics and level of service for facilities at Universitas Negeri Malang using geographic information system. In *AIP Conference Proceedings* (Vol. 1887, No. 1, p. 020057). AIP Publishing LLC.

138. Raj, J., and Vedagiri, P. (2022). Modeling Level of Service of Urban Roads Based on Travelers' Perceptions. *European Transport-Trasporti Europei*.

139. Raman, R., Sa, P. K., Majhi, B., and Bakshi, S. (2016). Direction estimation for pedestrian monitoring system in smart cities: An HMM based approach. *IEEE Access*, *4*, 5788-5808.

140. Ribeiro, A. I., and Hoffimann, E. (2018). Development of a neighbourhood walkability index for Porto metropolitan area. How strongly is walkability associated with walking for transport?. *International journal of environmental research and public health*, *15*(12), 2767.

141. Rodriguez-Valencia, A., Vallejo-Borda, J. A., Barrero, G. A., and Ortiz-Ramirez, H. A. (2022). Towards an enriched framework of service evaluation for pedestrian and bicyclist infrastructure: acknowledging the power of users' perceptions. *Transportation*, *49*(3), 791-814.

142. Saisana, M., Saltelli, A., & Tarantola, S. (2005). Uncertainty and sensitivity analysis techniques as tools for the quality assessment of composite indicators

143. Saltarin-Molino, M. A., Moros-Daza, A., & Camacho-Sanchez, C. (2023). Taking steps forward: Innovative evaluation of pedestrian infrastructure through a multivariate analysis. *Case studies on transport policy*, *14*, 101091.

144. Sawas, A., Abuolaim, A., Afifi, M., and Papagelis, M. (2018, June). Tensor methods for group pattern discovery of pedestrian trajectories. In *2018 19th IEEE International Conference on Mobile Data Management (MDM)* (pp. 76-85). IEEE

145. Sharifi, A., and Khavarian-Garmsir, A. R. (2020). The COVID-19 pandemic: Impacts on cities and major lessons for urban planning, design, and management. *Science of the total environment*, *749*, 142391.

146. Sharifi, M. S., Christensen, K., Chen, A., and Song, Z. (2019). Exploring effects of environment density on heterogeneous populations' level of service perceptions. *Transportation Research Part A: Policy and Practice*, *124*, 115-127.

147. Schadschneider, A., Chowdhury, D., and Nishinari, K. (2010). *Stochastic transport in complex systems: from molecules to vehicles*. Elsevier.

148. Seer, S., Brändle, N., and Ratti, C. (2014). Kinects and human kinetics: A new approach for studying pedestrian behavior. *Transportation research part C: emerging technologies*, *48*, 212-228.

149. Shimizu, H., and Poggio, T. (2004, June). Direction estimation of pedestrian from multiple still images. In *IEEE Intelligent Vehicles Symposium, 2004* (pp. 596-600). IEEE.

150. Shu, S., Bian, Y., Zhao, L., Rong, J., & Liu, X. (2021). Modelling pedestrian level of service on sidewalks with multi-factors based on different pedestrian flow rates. Transport, 36(6), 486-498.

151. Siddharth, S. M. P., & Perumal, V. (2024). Development of the social force model considering pedestrian characteristics and behavior. *Transportation research record*, *2678*(5), 436-450.

152. Song, X., Han, D., Sun, J., and Zhang, Z. (2018). A data-driven neural network approach to simulate pedestrian movement. *Physica A: Statistical Mechanics and its Applications*, *509*, 827-844.

153. Steffen, B., and Seyfried, A. (2010). Methods for measuring pedestrian density, flow, speed and direction with minimal scatter. *Physica A: Statistical mechanics and its applications*, *389*(9), 1902-1910.

154. Tajima, Y., Takimoto, K., and Nagatani, T. (2002). Pattern formation and jamming transition in pedestrian counter flow. *Physica A: Statistical Mechanics and its Applications*, *313*(3-4), 709-723.

155. Takimoto, K., Tajima, Y., and Nagatani, T. (2002). Effect of partition line on jamming transition in pedestrian counter flow. *Physica A: Statistical Mechanics and Its Applications*, *308*(1-4), 460-470.

156. Tanaboriboon, Y., & Guyano, J. A. (1989). Level-of-service standards for pedestrian facilities in Bangkok: A case study. ITE journal, 59(11), 39-41.

157. Transport Canada. (2010). *Pedestrian crossing control guide*. Morr Transportation Consulting

158. Transportation Association of Canada. (2018). *Pedestrian crossing control guide* (3rd ed.).

159. Transportation Research Board (TRB), Highway Capacity Manual (2020). A Guide for Multimodal Mobility Analysis, 6th Edition.

160. Ulhaq, D., Basfian, M. F., Ayuningtyas, N. V., & Brilianti, D. F. (2024). Analysis of Sidewalk Comfort Level Based on Width, Cleanliness, Surface Condition, Lighting, and Availability of Signage and Directional Indicators on Sudibyo Street Sidewalks in Tegal City. *Journal of Scientific Research, Education, and Technology (JSRET)*, *3*(4), 1611-1621.

161. Vallejo-Borda, J. A., Cantillo, V., and Rodriguez-Valencia, A. (2020). A perception-based cognitive map of the pedestrian perceived quality of service on urban sidewalks. *Transportation research part F: traffic psychology and behaviour*, *73*, 107-118.

162. Wachowicz, M., Ong, R., Renso, C., and Nanni, M. (2011). Finding moving flock patterns among pedestrians through collective coherence. *International Journal of Geographical Information Science*, *25*(11), 1849-1864

163. Wang, Q. L., Chen, Y., Dong, H. R., Zhou, M., and Ning, B. (2015). A new collision avoidance model for pedestrian dynamics. *Chinese Physics B*, *24*(3), 038901.

164. Wang, Z., Ma, J., Zhao, H., Qin, Y., and Jia, L. (2012). Effect of prediction on the self-organization of pedestrian counter flow. *Journal of Physics A: Mathematical and Theoretical*, *45*(30), 305004.

165. Węglarczyk, S. (2018). Kernel density estimation and its application. In *ITM web of conferences* (Vol. 23, p. 00037). EDP Science

166. Won, J. I., Kim, S. W., Baek, J. H., and Lee, J. (2009, March). Trajectory clustering in road network environment. In *2009 IEEE Symposium on Computational Intelligence and Data Mining* (pp. 299-305). IEEE.

167. Xiao, Y., Gao, Z., Qu, Y., and Li, X. (2016). A pedestrian flow model considering the impact of local density: Voronoi diagram based heuristics approach. *Transportation research part C: emerging technologies*, *68*, 566-580.

168. Yang, S., Chowdhury, T. U., Mohammadi, A., & Park, P. Y. (2022). Development of a Method for Evaluating Social Distancing Situations on Urban Streets during a Pandemic. *Sustainability*, *14*(14), 8741.

169. Yang, S., Claudio, P., Ahmad, A., Park, P., & Sohn, G. (2019). Development of a computer-vision based on real-time pedestrian comfort estimation system (poster). In *Transportation association of Canada and ITS Canada 2019 joint conference and exhibition*.

170. Yoon, T., Choi, M., & Lee, S. (2025). Pedestrian Perceived Risk of Construction Obstructions and Barriers Identified via Image Segmentation. *Applied Sciences*, *15*(10), 5261.

171. Yu, J., Chung, H. I., and Hahn, H. (2009, August). Walking assistance system for sight impaired people based on a multimodal information transformation technique. In *2009 ICCAS-SICE* (pp. 1639-1643). IEEE.

172. Zannat, K. E., Raja, D. R., and Adnan, M. S. G. (2019). Pedestrian facilities and perceived pedestrian level of service (plos): A case study of chittagong metropolitan area, Bangladesh. *Transportation in developing economies*, *5*(2), 9

173. Zhang, J., Klingsch, W., Schadschneider, A., and Seyfried, A. (2012). Ordering in bidirectional pedestrian flows and its influence on the fundamental diagram. *Journal of Statistical Mechanics: Theory and Experiment*, *2012*(02), P02002.

174. Zhao, G., Takafumi, M., Shoji, K., and Kenji, M. (2012). Video based estimation of pedestrian walking direction for pedestrian protection system. *Journal of Electronics (China)*, *29*(1), 72-81